REVIEWS OF MODERN PHYSICS VOLUME 41, NUMBER 4, PART I OCTOBER 1969

Pair Production by Photons*

J. W. MOTZ
National Bureau of Standards, Washington, D.C. 20234

HAAKON A. OLSEN
University of Trondheim (NLHT), Trondheim, Norway

H. W. KOCH
American Institute of Physics, New York, New York 10017

This paper reviews, analyzes, and integrates the various quantitative results that have been obtained for the process of pair production by photons. Included in this summary is a detailed review of total and differential cross sections for pair production in an atomic and in an electron field, with a critical evaluation of the conditions of validity and the accuracy of the results. In addition, a summary is given of the important kinematic relations, theoretical considerations, and the polarization effects that occur in pair production. The paper does not include a treatment of radiative corrections to pair production, thick-target pair production, or pair production by electrons in the field of a nucleus (trident production). Otherwise, the review is intended to include results on pair production available up to January 1969.

CONTENTS

I. INTRODUCTION

The radiation process which occurs when an electron collides with an atomic nucleus, the bremsstrahlung process, was recognized and studied as early as 1923 (Kramers, 1923). On the other hand, the pair-production process, which on a theoretical basis is closely related to the bremsstrahlung process, was discovered much later.

The Dirac equation which was discovered in 1928 (Dirac, 1928) predicted states of particles of negative energy. These negative-energy states were subsequently interpreted by Dirac (1930) by his hole theory as giving rise to real physical particles with charges opposite to those of the electrons. Actually, Dirac assumed in his paper that these particles were protons. It was only later that Oppenheimer and Dirac made the bold assumption that the holes might describe new particles, antielectrons, with the same mass as the electron, but with positive charge. The theory was, however, not readily accepted, as indicated in the following translated quotation by Pauli (1933):

> "Dirac has therefore recently made an attempt, which has already been discussed by Oppenheimer, to identify the holes with antielectrons, particles with charge $+e$ and the same mass as the electron. There should then likewise exist antiprotons besides the protons. The obvious lack of such particles is then traced back to a special initial condition for which only one kind of particle is present. This seems to be unsatisfactory already, because the laws of nature in this theory regarding electrons and antielectrons is exactly symmetric. It follows that (in order to satisfy momentum and energy conservation at least two) γ-ray photons might spontaneously convert into an electron and an antielectron. Thus, we do not believe that the attempt can be taken seriously."

Shortly after Pauli's article was written, the matter was settled when the antielectron, the positron, was discovered experimentally by Anderson "with due reserve in interpretation in view of the importance and striking nature of the announcement" (Anderson, 1932). The experimental findings were confirmed in later

* This report is the third in a series on Coulomb processes for electrons and photons, which includes a review on bremsstrahlung (Koch and Motz, 1959) and on electron scattering (Motz, Olsen, and Koch, 1964).

experiments (Anderson, 1933) and the existence of the positron was established.

The first calculations pertaining to the pair-production process in the field of a nucleus appeared shortly after Anderson's discovery, by Nishina and Tomonaga (1933), Oppenheimer and Plesset (1933), and Heitler and Sauter (1933). Later, relativistic calculations for the production of electron–positron pairs by photons and for the related process of bremsstrahlung (Koch and Motz, 1959) were carried out by Bethe and Heitler (1934). Although the Bethe–Heitler theory depends on the Born approximation, it has proved to be remarkably successful in predicting the important features of these processes. Meanwhile, more accurate and detailed calculations and experimental studies of these processes have become available (Bethe and Ashkin, 1953; Heitler, 1954; Olsen, 1968).

The present paper reviews, analyzes, and integrates the various quantitative results that have been obtained for the process of pair production by photons. This summary includes a detailed review of total and differential pair cross sections with a critical evaluation of the conditions of validity and the accuracy of the results. In addition, a summary is given of the important kinematic relations, theoretical considerations, and the polarization effects that occur in pair production.

This paper does not include a treatment of radiative corrections to pair production (Olsen, 1968), thick-target pair production, or pair production by electrons in the field of a nucleus (trident production). Otherwise, the review is intended to include results on pair production available up to January 1969.

Section II defines the symbols, notation, constants, and energy–momentum relations used in this report. Section III gives the important kinematic relations for pair production in the field of a nucleus and in the field of an electron. Section IV discusses the type of calculations and approximations that have been used for this process. Section V summarizes the polarization effects in the pair process, which may involve linearly or circularly polarized photons or longitudinally or transversely polarized electrons or positrons, and gives the important relations for using this process to determine the polarization of a photon beam or to produce polarized electron or positron beams. Sections VI and VII give the available cross-section formulas for pair production in an atomic and an electron field, respectively. Finally, Sec. VIII compares and evaluates the various cross-section results.

II. DEFINITIONS

The following definitions and relationships are given for the symbols and constants used in this review. The constants are given with three significant figures although more accurate values are available.

$d\Omega_+$, $d\Omega_-$, $d\Omega_r = \sin\theta_+ d\theta_+ d\Phi_+$, $\sin\theta_- d\theta_- d\Phi_-$, $\sin\theta_r d\theta_r d\Phi_r$
= element of solid angle in the direction of $\mathbf{p}_+$, $\mathbf{p}_-$, or $\mathbf{q}$, respectively, relative to $\mathbf{k}$.

$d\Omega = \sin\theta d\theta d\Phi$ = element of solid angle in the direction of $\mathbf{p}_+$ relative to $\mathbf{p}_-$.

$\frac{d\sigma}{dE_+}$ = Pair cross-section differential with respect to the positron energy. The polarization effects for this cross section are specified by the functional dependence on the various combinations of the polarization variables which are shown in Table 6.03.

$\frac{d^2\sigma}{dE_+ d\Omega_+}$ = Pair cross-section differential with respect to the positron energy and the solid angle in the direction of $\mathbf{p}_+$ relative to $\mathbf{k}$. The polarization effects are specified by the functional dependence on the various combinations of the polarization variables which are shown in Table 6.03.

$\frac{d^2\sigma}{dE_+ dw}$ = Pair cross-section differential with respect to the positron energy and the angle θ between $\mathbf{p}_+$ and $\mathbf{p}_-$, where $\theta = (k/E_+E_-)w$.

$\frac{d^3\sigma}{dE_+ d\Omega_+ d\Omega_-}$ = Pair cross-section differential with respect to the positron energy and the solid angles in the direction of $\mathbf{p}_+$ and $\mathbf{p}_-$ relative to $\mathbf{k}$. The polarization effects are specified by the functional dependence on the various combinations of the polarization variables which are shown in Table 6.03.

$\frac{d\sigma}{d\Omega_r}$ = Pair cross-section differential with respect to the solid angle for the recoiling target particle in the direction of $\mathbf{q}$ relative to $\mathbf{k}$.

$\frac{d\sigma}{dP_p}$ = Pair cross-section differential with respect to the resultant pair momentum P_p acquired by the electron and positron.

$\frac{d\sigma}{dq}$ = Pair cross-section differential with respect to the momentum transfer q to the target particle.

E_+, E_- = Total energy of the positron or electron, respectively, for pair production in the laboratory system,* in m_0c^2 units.

E_0, E_r = Initial and final (recoil) total energy, respectively, of the target particle for pair production in the laboratory system,* in m_0c^2 units with $E_0=m_r/m_0$.

$\mathbf{e}$, $\mathbf{e}^*$ = Complex unit vectors for photon polarization such that $\mathbf{e}\cdot\mathbf{e}^*=1$, $\mathbf{e}\cdot\mathbf{k}=0$, and that $\mathbf{e}\exp[i(\mathbf{k}\cdot\mathbf{r}-kt)]$ is proportional to the electromagnetic-vector potential. These vectors are complex or real when applied to photon beams with *elliptical* or *linear* polarization, respectively.

$\mathbf{e}$ = Unit vector for linear photon polarization such that $\mathbf{e}\cdot\mathbf{e}=1$ and $\mathbf{e}\cdot\mathbf{k}=0$.

$F(q)$, $G_E(q)$ = Atomic- and nuclear-charge form factors, respectively, for static charge density of the atom or nucleus, $\rho(\mathbf{r})$ (per electron or per proton)

$=\int \exp(i\mathbf{q}\cdot\mathbf{r})\rho(\mathbf{r})\,d^3r$.

$F_1(\bar{q})$, $F_2(\bar{q})$ = Dirac and Pauli invariant form factors related to $G_E(\bar{q})$ and $G_M(\bar{q})$ by

$$G_E=F_1-(\bar{q}^2/4m_r^2)\kappa F_2, \qquad G_M=F_1+\kappa F_2,$$

where κ is the anomalous magnetic moment of the nucleus in units of the Bohr magneton, $e/2m_r$.

$G_M(q)$ = Magnetic nuclear form factor, for static magnetic moment density, $\mu(\mathbf{r})$, of a nucleus

$=\int \exp(i\mathbf{q}\cdot\mathbf{r})\mu(\mathbf{r})\,d^3r$.

$G_E(\bar{q})$, $G_M(\bar{q})$ = Invariant electric and magnetic nuclear form factors.

k, $\mathbf{k}$ = Initial photon energy and momentum, respectively, in m_0c^2 and m_0c units in the laboratory system.*

$\hat{\mathbf{k}}$ = Unit vector for the photon momentum such that $\hat{\mathbf{k}}=\mathbf{k}/|\,\mathbf{k}\,|$.

$\bar{k}$ = Four-component vector $=\{\mathbf{k}, k\}$ such that $\bar{k}^2=\mathbf{k}^2-k^2$.

k_t = Threshold photon energy for pair production in the laboratory system,* in m_0c^2 units.

$\mathbf{n}_+$, $\mathbf{n}_-$ = Unit vector for the positron and electron momentum, such that $\mathbf{p}_+=p_+\mathbf{n}_+$ and $\mathbf{p}_-=p_-\mathbf{n}_-$.

$\mathbf{n}$ = Unit vector perpendicular to the scattering plane $(\mathbf{k}, \mathbf{p}_+)$ or $(\mathbf{k}, \mathbf{p}_-)$ such that $\mathbf{n}=(\mathbf{k}\times\mathbf{p}_+)/|\,\mathbf{k}\times\mathbf{p}_-\,|$, or $\mathbf{n}=(\mathbf{k}\times\mathbf{p}_-)/|\,\mathbf{k}\times\mathbf{p}_-\,|$.

$\mathbf{p}_+$, $\mathbf{p}_-$ = Momentum of the positron or electron, respectively, for pair production in the laboratory system,* in m_0c units.

$\bar{p}_\pm$ = Four-component vector $=\{\mathbf{p}_\pm, E_\pm\}$ such that $\bar{p}_\pm^2=\mathbf{p}_\pm^2-E_\pm^2$.

$\mathbf{p}_0$, $\mathbf{p}_r$ = Initial and final momentum, respectively, of the target particle for pair production in m_0c units. In the laboratory system,* $\mathbf{p}_0=0$ and $\mathbf{p}_r=\mathbf{q}$.

$\bar{p}_0$ = Four-component vector $=\{\mathbf{p}_0, E_0\}$, such that $\bar{p}_0^2=\mathbf{p}_0^2-E_0^2=-(m_r/m_0)^2$.

$\bar{p}_r$ = Four-component vector $=\{\mathbf{p}_r, E_r\}$, such that $\bar{p}_r^2=\mathbf{p}_r^2-E_r^2=-(m_r/m_0)^2$.

$\mathbf{P}_c$ = Vector for the circular polarization of a photon beam. The magnitude of the vector gives the degree of circular polarization for the beam in the direction of the vector $\boldsymbol{\xi}$ such that $\mathbf{P}_c=P_c\boldsymbol{\xi}$.

P_L = Magnitude of the linear polarization of the photon beam.

$\mathbf{P}_p=\mathbf{p}_+-\mathbf{p}_-$ = resultant pair momentum equal to the vector sum of the positron and electron momenta.

$\mathbf{P}_+$, $\mathbf{P}_-$ = Polarization vector for the positron or electron beam, respectively, produced by photons in the pair process. The magnitude of the vector gives the degree of polarization for the beam in the direction of the vector, and is equal to the average expectation value of the spin operator for the beam. Then $\mathbf{P}_\pm\cdot\boldsymbol{\zeta}_\pm$ is the component of $\mathbf{P}_\pm$ along the chosen quantization axes $\boldsymbol{\zeta}_\pm$.

---

* Primed symbols refer to the center-of-momentum system.

$\mathbf{P}_+^L$, $\mathbf{P}_-^L$ = Longitudinal polarization vector for the positron or electron beam in the direction of the positron or electron momentum. The magnitude of the vector gives the degree of polarization for the beam in the direction parallel to the positron or electron momentum such that $\mathbf{P}_+^L \cdot \mathbf{n}_+ = P_+^L$ or $\mathbf{P}_-^L \cdot \mathbf{n}_- = P_-^L$. This vector is a component of the polarization vector $\mathbf{P}_\pm$, such that

$$P_\pm = [(P_\pm^L)^2 + (P_\pm^T)^2]^{1/2}.$$

$\mathbf{P}_+^T$, $\mathbf{P}_-^T$ = Transverse polarization vector for the positron or electron beam in the direction perpendicular to the positron or electron momentum. The magnitude of the vector gives the degree of polarization for the beam in the direction perpendicular to the positron or electron momentum such that $\mathbf{P}_+^T \cdot \mathbf{n}_+ = 0$ or $\mathbf{P}_-^T \cdot \mathbf{n}_- = 0$. This vector is a component of the polarization vector $\mathbf{P}_\pm$ such that

$$P_\pm = [(P_\pm^L)^2 + (P_\pm^T)\ ]^{1/2}.$$

$\mathbf{q}$ = Momentum transfer to the target particle in pair production in the laboratory system,* in m_0c units $= (\mathbf{k} - \mathbf{p}_+ - \mathbf{p}_-) = \mathbf{p}_r$.

$\bar{q}$ = Four-component vector $= \{\mathbf{q}, q_0\}$ such that $\bar{q}^2 = \mathbf{q}^2 - q_0^2$, where $q_0 = k - E_+ - E_- = E_r - (m_r/m_0) = T_r$.

$\mathbf{r}$ = Radius vector from the center of the nucleus in units of $\lambda\!\!\!^{-}_0$.

T_+, T_- = Kinetic energy of the positron or electron, respectively, for pair production in the laboratory system,* in m_0c^2 units.

T_0, T_r = Initial and final kinetic energy, respectively, of the target particle for pair production in the laboratory system,* in m_0c^2 units such that $T_0 = 0$.

$\mathbf{u}$ = Component of $\mathbf{p}_+$ perpendicular to $\mathbf{k}$, such that $\mathbf{p}_+ = \mathbf{u} + (\mathbf{p}_+ \cdot \hat{\mathbf{k}})\,\hat{\mathbf{k}}$.

$u = p_+ \sin\theta_+ \approx E_+\theta_+$ (for extreme-relativistic energies and small angles).

$\mathbf{v}$ = Component of $\mathbf{p}_-$ perpendicular to $\mathbf{k}$, such that $\mathbf{p}_- = \mathbf{v} + (\mathbf{p}_- - \mathbf{k})\,\hat{\mathbf{k}}$.

$v = p_- \sin\theta_- \approx E_-\theta_-$ (for extreme-relativistic energies and small angles).

$w = (E_+E_-/k)\theta$.

Z = Atomic number of the target atom.

$Ze\rho(r)$ = Charge density for the atom or nucleus, with normalization such that $\int \rho(r)\ d^3r = 1$.

A. Greek Symbols

β_+, β_- = Ratio of the positron or electron velocity, respectively, to the velocity of light.

β_{CM} = Ratio of center-of-momentum velocity in pair production to the velocity of light.

β = Exponential screening constant $= 111Z^{-1/3}$.

$\boldsymbol{\zeta}_+$, $\boldsymbol{\zeta}_-$ = Unit polarization vector for the positron or electron, respectively, produced by photons in the pair process. These vectors are defined as the expectation values, $\boldsymbol{\zeta}_+ = u_+^*\boldsymbol{\sigma}u_+$ and $\boldsymbol{\zeta}_- = u_-^*\boldsymbol{\sigma}u_-$, where u_+ and u_- are eigenstates for $\boldsymbol{\zeta}_+ \cdot \boldsymbol{\sigma}$ and $\boldsymbol{\zeta}_- \cdot \boldsymbol{\sigma}$, respectively, such that $\boldsymbol{\zeta}_+ \cdot \boldsymbol{\sigma}u_+ = u_+$ and $\boldsymbol{\zeta}_- \cdot \boldsymbol{\sigma}u_- = u_-$, where $\boldsymbol{\sigma}$ is the Pauli spin operator. The unit vectors $\boldsymbol{\zeta}_+$ and $\boldsymbol{\zeta}_+$ may be chosen to have arbitrary directions which can be specified in terms of the coordinate system given by the unit orthogonal vectors $\mathbf{n}$, $\mathbf{n}_+$, $\mathbf{n}_+ \times \mathbf{n}$, or $\mathbf{n}$, $\mathbf{n}_-$, $\mathbf{n}_- \times \mathbf{n}$.

θ_+, θ_-, θ_r, θ_p = Angle between $\mathbf{k}$ and $\mathbf{p}_+$, $\mathbf{p}_-$, $\mathbf{q}$, and $\mathbf{P}_p$, respectively.

θ = Angle between $\mathbf{p}_+$ and $\mathbf{p}_-$.

$\mu(r)$ = Nuclear magnetic moment density, such that $\int \mu(r)\ d^3r$ is equal to the ratio of the nuclear magnetic moment μ to the Bohr magneton $(e/2m_r)$.

$\boldsymbol{\xi} = i(\mathbf{e} \times \mathbf{e}^*)$ = Unit vector for *circular* photon polarization with a direction that is parallel or anti-parallel to $\mathbf{k}$ for right-handed or left-handed polarization, respectively.

σ = Total cross section for pair production by photons.

---

* See footnote on page 583.

Φ_+, Φ_-, Φ_r = Azimuthal angle for the positron, electron, or recoil target particle, respectively, measured in a plane orthogonal to **k** from a reference line originating from the point of emission, as shown in Fig. 3.01(a).

Φ = Azimuthal angle equal to $\pi-(\Phi_--\Phi_+)$. For linearly polarized photons discussed in Sec. V, Φ is also defined as the azimuthal angle between the polarization vector **e** and the fixed direction $\mathbf{e}^{(1)}$ which are both orthogonal to **k**.

$\varphi=\pi-\Phi=\Phi_+-\Phi_-$ = dihedral angle which is equal to the difference in the azimuthal angles of the positron and electron.

B. Useful Relations

$$\beta_\pm=p_\pm/E_\pm, \qquad k=E_++E_-+T_r,$$
$$E_\pm^2=p_\pm^2+1, \qquad p_\pm=[T_\pm(T_\pm+2)]^{1/2},$$
$$E_\pm=T_\pm+1, \qquad p_\pm=\beta_\pm/(1-\beta_\pm^2)^{1/2}.$$
$$E_\pm=1/(1-\beta_\pm^2)^{1/2},$$

C. Constants

$a_0=\hbar^2/m_0e^2=137\lambda\!\!\!^{-}_0=(137)^2r_0=0.530\times10^{-8}$ cm (Bohr radius of hydrogen atom).

$A=Z+N$ (number of neutrons)$\approx 2.6Z$ for high Z, $2Z$ for low Z (mass number of nucleus).

$\alpha=e^2/\hbar c=1/137.$

$c=3.00\times10^{10}$ cm/sec (speed of light in vacuum).

$e=1.6\times10^{-19}$ C (electron charge).

$e^2=1.44\times10^{-13}$ MeV·cm.

$\hbar=6.58\times10^{-22}$ MeV·sec $=1.05\times10^{-27}$ erg·sec.

$hc=12.4$ keV·Å.

$\hbar c=1.97\times10^{-11}$ MeV·cm.

$\lambda\!\!\!^{-}_0=\hbar/m_0c=3.86\times10^{-11}$ (Compton wavelength).

$m_0=9.11\times10^{-28}$ g (electron rest mass).

$m_0c^2=0.511$ MeV.

$m_r\approx A\times1.66\times10^{-24}$ g (rest mass of the atomic nucleus).

$m_0/m_r=5.5A^{-1}\times10^{-4}.$

$r_0=e^2/m_0c^2=\lambda\!\!\!^{-}_0/137=2.82\times10^{-13}$ cm (classical electron radius).

$R_{TF}=0.885a_0Z^{-1/3}$ (radius of the Thomas–Fermi atom).

III. KINEMATICS

The following subsections give some of the important kinematic relationships for the pair-production process. These results are based on a relativistic treatment (Borsellino, 1947) of the conservation laws for energy and momentum. A schematic representation of the momentum vectors in the laboratory (unprimed) and the center-of-momentum (primed) systems is given in Figs. 3.01(a) and (b), respectively. These vectors include the electron and positron momenta $\mathbf{p}_+$ and $\mathbf{p}_-$, the photon momentum **k**, and the recoil momentum **q** of the target particle (nucleus, atom, or electron). The recoil momentum **q** is required in order to conserve energy and momentum and is a key parameter in the pair-production process.

A. Energy and Momentum Relations in the Laboratory System

The energy conservation equation in terms of the photon, positron, electron, and recoil-target-particle energies, k, T_+, T_-, and T_r, respectively, is given as

$$k=(T_++1)+(T_-+1)+T_r, \qquad (3.01)$$

where it is assumed that the target particle is initially at rest in the laboratory system such that $T_0=0$.

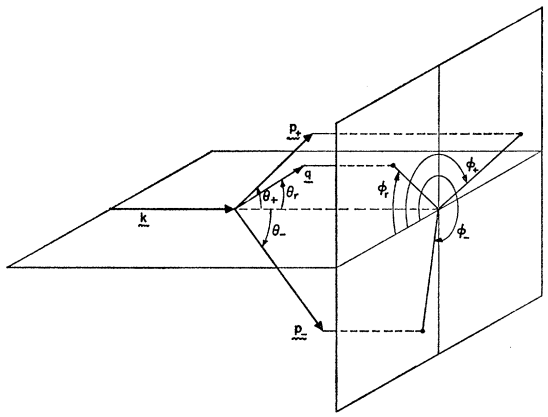

FIG. 3.01. Schematic representation of the momentum vectors for pair production in (a) the laboratory system and (b) the center-of-momentum system. The symbols in the diagrams for the momentum and emission angle of each particle are defined in Sec. II.

The momentum conservation equation in terms of the momenta vectors is given as

$$\mathbf{k}=\mathbf{p}_+ +\mathbf{p}_- +\mathbf{q}. \tag{3.02}$$

From Fig. 3.01(a) and Eq. (3.02)

$$q^2=k^2+p_+^2+p_-^2 +2p_+p_-[\cos\theta_+\cos\theta_- +\sin\theta_+\sin\theta_-\cos(\Phi_+-\Phi_-)] -2p_+k\cos\theta_+ -2p_-k\cos\theta_-, \tag{3.03}$$

where the angles θ_+, θ_-, Φ_+, and Φ_- are defined in Sec. II and shown in Fig. 3.01(a). Another expression for q which involves the recoil angle θ_r, defined in Sec. II and shown in Fig. 3.01(a), is given as

$$q\sin\theta_r=[p_+^2\sin^2\theta_+ +p_-^2\sin^2\theta_- +2p_+p_-\sin\theta_+\sin\theta_-\cos(\Phi_+-\Phi_-)]^{1/2}. \tag{3.04}$$

Some of the above equations can be simplified by introducing the resultant pair-momentum vector $\mathbf{P}_p$ and its corresponding angle θ_p measured with respect to k. This vector is defined as

$$\mathbf{P}_p=\mathbf{p}_+ +\mathbf{p}_-. \tag{3.05}$$

In terms of P_p and θ_p, the expression for q can be written as

$$q\cos\theta_r=k-P_p\cos\theta_p \tag{3.06}$$

and

$$q\sin\theta_r=P_p\sin\theta_p. \tag{3.07}$$

The energy T_r and momentum q of the recoiling particle are related by

$$T_r=[(m_r/m_0)^2+q^2]^{1/2}-(m_r/m_0). \tag{3.08}$$

For small values of q ($q\ll m_r/m_0$), T_r is given by the approximation

$$T_r\approx(m_0/m_r)\tfrac{1}{2}q^2. \tag{3.09}$$

B. Energy and Momentum Relations in the Center-of-Momentum System

The energy and momentum conservation equations in the center-of-momentum system shown in Fig. 3.01(b) are given as

$$k'+T_0'=(T_+'+1)+(T_-'+1)+T_r', \tag{3.10}$$

$$\mathbf{k}'+\mathbf{p}_0'=0, \tag{3.11}$$

and

$$\mathbf{p}_+'+\mathbf{p}_-'+\mathbf{p}_r'=0, \tag{3.12}$$

where T_0', $\mathbf{p}_0'$ and T_r', $\mathbf{p}_r'$ are the kinetic energy and momentum of the target particle before and after the interaction, respectively.

The relation between the photon energy k' in the center-of-momentum system, and the photon energy k in the laboratory system, which is determined by the center-of-momentum velocity β_{CM} in units of the velocity of light, is given as

$$k'=k[(1-\beta_{CM})/(1+\beta_{CM})]^{1/2}. \tag{3.13}$$

The momentum balance in this system [see Fig. 3.01(b)] requires

$$k'=(m_r/m_0)\beta_{CM}(1-\beta_{CM}^2)^{-1/2}. \tag{3.14}$$

It follows that

$$\beta_{CM}=\frac{k}{k+(m_r/m_0)} \tag{3.15}$$

and

$$k'=\left\{\frac{(m_r/m_0)}{[2k+(m_r/m_0)]}\right\}^{1/2} \tag{3.16a}$$

and conversely

$$k=k'\frac{m_r}{m_0/m_r}\left\{k'+\left[k'^2+\left(\frac{m_r}{m_0}\right)^2\right]^{1/2}\right\}. \tag{3.16b}$$

C. Threshold Photon Energy for Pair Production

The threshold photon energy for pair production is designated as k_t' in the center-of-momentum system and k_t in the laboratory system. In the center-of-momentum system, the energy and momentum conservation laws at threshold become

$$k_t'+(m_r/m_0)[(1-\beta_{CM}^2)^{-1/2}-1]=2 \tag{3.17}$$

and

$$k_t'-(m_r/m_0)\beta_{CM}(1-\beta_{CM}^2)^{-1/2}=0. \tag{3.18}$$

TABLE 3.01. Threshold photon energies[a] (in megaelectron volts) in the laboratory system for pair production.

Target particle \ Pair particle	Electron	Muon	Pion	K Meson	Proton
Lead	1.02	2.12×10^{2}	2.80×10^{2}	9.90×10^{2}	1.89×10^{3}
Copper	1.02	2.12×10^{2}	2.81×10^{2}	9.96×10^{2}	1.90×10^{3}
Carbon	1.02	2.14×10^{2}	3.51×10^{2}	1.03×10^{3}	2.03×10^{3}
Proton	1.02	2.40×10^{2}	4.19×10^{2}	1.48×10^{3}	3.75×10^{3}
Electron	2.04	4.43×10^{4}	7.70×10^{4}	9.56×10^{5}	3.45×10^{6}

[a] These energies were evaluated from Eq. (3.19b).

From Eqs. (3.17) and (3.18), the threshold energy in the center-of-momentum system becomes

$$k_t'=2[(m_0+m_r)/(2m_0+m_r)]. \tag{3.19a}$$

From (3.16b), the threshold energy in the laboratory system is

$$k_t=2(1+m_0/m_r). \tag{3.19b}$$

Values of the threshold energy are given in Table 3.01 for the pair production of various particles with different target particles. These values are obtained from Eq. (3.19b).

D. The Minimum Recoil Momentum

The minimum recoil momentum $q_{\min}$ is obtained when all the momentum vectors are pointing along the photon direction such that $\theta_+=\theta_-=0$. This condition gives

$$q_{\min}=k-p_+-p_-. \tag{3.20}$$

From Eq. (3.20) and the energy-conservation relation

$$k+(m_r/m_0)=E_++E_-+[q_{\min}^2+(m_r/m_0)^2]^{1/2},$$

it is found that the absolute minimum of $q_{\min}$ occurs at $E_+=E_-$. This absolute minimum is given as (Borsellino, 1947)

$$q_{\min}=\frac{k\{(m_r/m_0)[k+(m_r/m_0)]-2\}-[k+(m_r/m_0)]\{[(m_r/m_0)k-2]^2-4(m_r/m_0)^2\}^{1/2}}{(m_r/m_0)[2k+(m_r/m_0)]}. \tag{3.21}$$

It is to be noted that at threshold where $k_t=2[1+(m_r/m_0)]$, according to Eq. (3.19b), q is always given by its minimum value $q_{\min}$:

$$q=q_{\min}=\frac{2[1+(m_r/m_0)]}{1+2(m_r/m_0)}=\frac{k_t}{k_t-1}. \tag{3.22}$$

Explicit expressions for $q_{\min}$ are given below for pair production in the field of (1) a nucleus and (2) an electron:

1. Nuclear-Field Pair Production ($m_r\gg m_0$). For $m_r\gg m_0$ Eq. (3.21) becomes

$$q_{\min}=k-(k^2-4)^{1/2}. \tag{3.23}$$

It is interesting to note that this result is valid for any photon energy (i.e., for $k<m_r/m_0$ as well as for $k>m_r/m_0$). Thus $q_{\min}$ is independent of the mass of the recoiling atom.

(a) For high photon energies where $k\gg1$ and where β_+, $\beta_-\rightarrow1$, the expression for $q_{\min}$ in Eq. (3.23) becomes

$$q_{\min}=2/k. \tag{3.24}$$

(b) For photon energies at threshold where $k=k_t=2$, from Eq. (3.19b) and where $\beta_+=\beta_-=0$, the expression for $q_{\min}$ in Eq. (3.22) becomes

$$q_{\min}=2. \tag{3.25}$$

2. Electron-Field Pair Production (Triplet Production with $m_r=m_0$). For $m_r=m_0$, Eq. (3.21) may be written in the form

$$q_{\min}=4k/\{k(k-1)+(k+1)[k(k-4)]^{1/2}\}. \tag{3.26}$$

(a) For high photon energies where $k\gg1$ and where β_+, $\beta_-\rightarrow1$, $q_{\min}$ is given by $q_{\min}=2/k$.

(b) For photon energies at threshold where $k=k_t=4$ from Eq. (3.19b), the expression for $q_{\min}$ in Eq. (3.22) becomes

$$q_{\min}=\tfrac{4}{3}. \tag{3.27}$$

It should be noted that for triplet production at threshold also the pair particles have the same momenta

$$p_+=p_-=\tfrac{4}{3}$$

as it should be, since recoil and pair electrons are indistinguishable particles.

E. The Maximum Recoil Momentum

The maximum recoil momentum q_{max} is obtained when all of the momentum vectors $\mathbf{P}_p$ (or more specifically $\mathbf{p}_+$ and $\mathbf{p}_-$), $\mathbf{k}$, and $\mathbf{q}$ are colinear,

$$q_{max} = |\mathbf{k}| + |\mathbf{p}_+| + |\mathbf{p}_-|.$$

In a manner similar to the derivation of q_{min} (Borsellino, 1947), the absolute maximum of q_{max} which occurs for $E_+ = E_-$ is given as

$$q_{max} = \frac{k\{(m_r/m_0)[k+(m_r/m_0)]-2\}+[k+(m_r/m_0)]\{[(m_r/m_0)k-2]^2-4(m_r/m_0)^2\}^{1/2}}{(m_r/m_0)[2k+(m_r/m_0)]}. \quad (3.28)$$

The maximum and minimum recoil momenta are related by

$$q_{max} \cdot q_{min} = \frac{4[(m_r/m_0)(k+m_r/m_0)-1]}{(m_r/m_0)(2k+m_r/m_0)}. \quad (3.29)$$

A comparison of Eqs. (3.28) and (3.27) shows that $q_{max} = q_{min}$ at threshold photon energies, in accordance with Eq. (3.22).

Explicit expressions for q_{max} are given below for pair production in the field of (1) a nucleus and (2) an electron.

1. Nuclear-Field Pair Production. For $m_r \gg m_0$, one finds from Eq. (3.28) or from (3.26) and (3.29)

$$q_{max} = \frac{k+(m_r/m_0)}{2k+(m_r/m_0)}[k+(k^2-4)^{1/2}].$$

This formula is valid for all values of k as is the corresponding formula (3.23) for q_{min}. Note that while q_{min} is independent of m_r, q_{max} does, for large values of $k (k \gtrsim m_r/m_0)$, depend on the mass of the recoiling atom.

(a) For high photon energies where $k \gg 1$ and where $\beta_+, \beta_- \rightarrow 1$, the expression for q_{max} becomes

$$q_{max} = \frac{2k[(m_r/m_0)+k]}{2k+(m_r/m_0)}. \quad (3.30)$$

(b) For photon energies at threshold where $\beta_+ = \beta_- = 0$ and where $k = k_t = 2$ from Eq. (3.19b), Eq. (3.29) becomes

$$q_{max} = 2. \quad (3.31)$$

2. Electron-Field Pair Production (Triplet Production). For $m_r = m_0$, Eq. (3.28) becomes

$$q_{max} = \{k(k-1)+(k+1)[k(k-4)]^{1/2}\}/(2k+1). \quad (3.32)$$

(a) For high photon energies where $k \gg 1$ and where $\beta_+, \beta_- \rightarrow 1$, the expression for q_{max} becomes

$$q_{max} = k. \quad (3.33)$$

(b) For photon energies at threshold where $k = k_t = 4$ from Eq. (3.19b), the expression for q_{max} becomes

$$q_{max} = \tfrac{4}{3}. \quad (3.34)$$

F. The Minimum Momentum Transfer for a Given Positron (or Electron) Momentum

The minimum momentum transfer for a given positron (or electron) momentum, $q_{min}(\mathbf{p}_+)$ [or $q_{min}(\mathbf{p}_-)$], is obtained when the electron momentum $\mathbf{p}_-$ (or positron momentum $\mathbf{p}_+$) is in line with $\mathbf{q}$ and in the same plane, as shown in Fig. 3.02. Therefore

$$q_{min}(\mathbf{p}_\pm) = (p_\pm^2+k^2-2p_\pm k\cos\theta_\pm)^{1/2}-[(k-E_\pm)^2-1]^{1/2}. \quad (3.35)$$

This minimum transfer is related to the maximum impact parameter r_{max} (in units of the Compton wavelength λ_0), which is discussed by Heitler (1954) and is used to evaluate screening effects (Koch and Motz, 1959), by the following equation:

$$r_{max} = 1/q_{min}. \quad (3.36)$$

The dependence of r_{max} on E_+ for different values of θ_+, as given by Eq. (3.35), is shown in Fig. 3.03(a) and (b) for values of k equal to 21.57 and 315.11, respectively. The solid lines are obtained for the pair process, and the dashed lines are obtained for the inverse bremsstrahlung process in which the initial electron energy E_1 and the photon energy k are substituted for $-E_+$ and $-k$ in the pair process. It is interesting to note that the values for r_{max} have a maximum value in the pair process and become arbitrarily large as the photon energy approaches zero in the bremsstrahlung process.

G. Maximum Recoil and Emission Angles

In a manner similar to the derivation of q_{max} in Eq. (3.28), it can be shown that

$$\cos\theta_r \geq (2m_0/m_r k)[(m_r/m_0)k+(m_r/m_0)^2-1]^{1/2}. \quad (3.37)$$

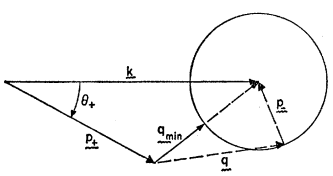

FIG. 3.02. Vector diagram for determination of the momentum transfer $\mathbf{q}$ when $\mathbf{p}_+$ is observed at the angle θ_+. The minimum momentum transfer $\mathbf{q}_{min}$ is obtained when $\mathbf{p}_-$ and $\mathbf{q}$ lie in the same direction and same plane.

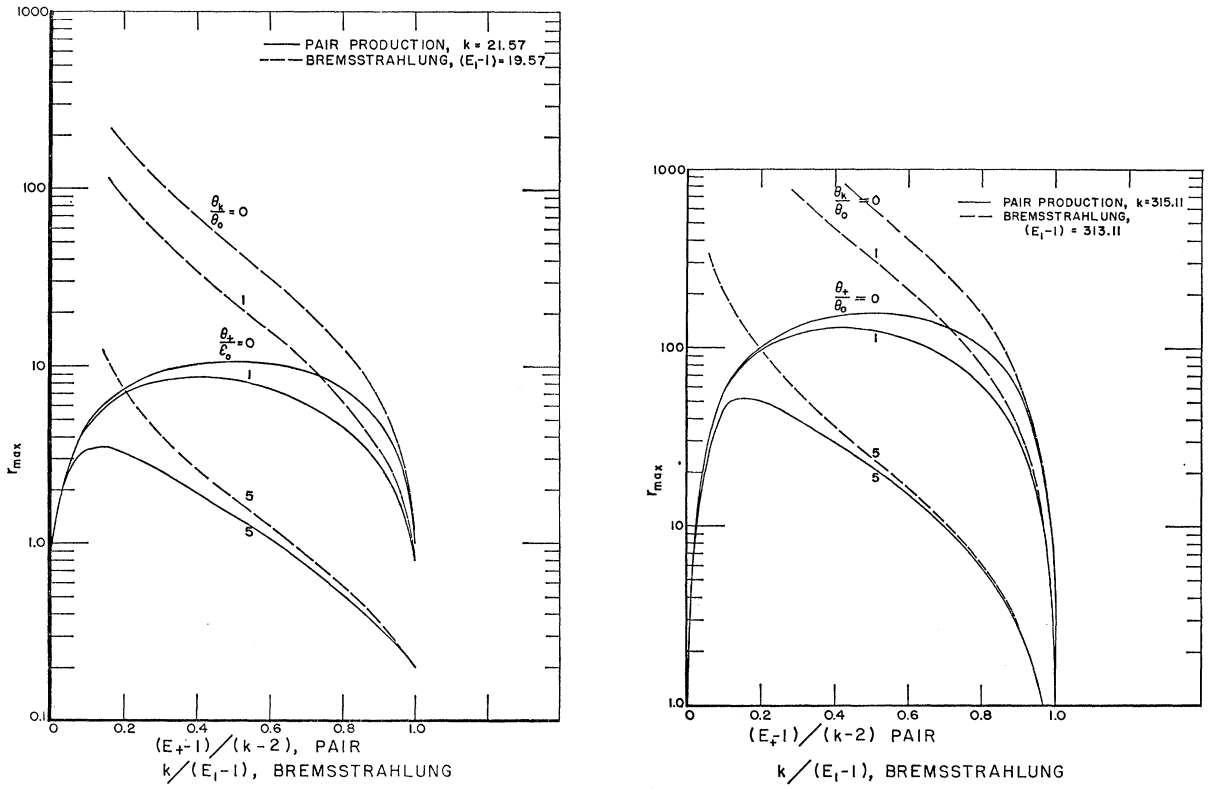

FIG. 3.03. (a) Dependence of the maximum impact parameter r_{max} (in units of $\lambda\!\!\!^{-}_0$) on $(E_+-1)/(k-2)$ for the pair process (solid lines), and on $k/(E_1-1)$ for the bremsstrahlung process (dashed lines). Results are given for k equal to 21.57 in the pair process, and for (E_1-1) equal to 19.57 in the corresponding bremsstrahlung process. The numbers on the curves give the values of the ratio θ_+/θ_0 for the pair process, where θ_0 is equal to $1/k$, and θ_k/θ_0 for the bremsstrahlung process, where θ_k is the photon emission angle and θ_0 is equal to $1/E_1$. (b) Dependence of the maximum impact parameter r_{max} (in units of $\lambda\!\!\!^{-}_0$) on $(E_+-1)/(k-2)$ for the pair process (solid lines), and on $k/(E_1-1)$ for the bremsstrahlung process (dashed lines). Results are given for k equal to 315.1 in the pair process, and for (E_1-1) equal to 313.1 in the corresponding bremsstrahlung process.

Therefore for the case of nuclear-field pair production, the maximum recoil angle $(\theta_r)_{max}$ becomes

$$(\theta_r)_{max}=\cos^{-1}\{(2/k)[1+k(m_0/m_r)]^{1/2}\}, \quad (3.38)$$

and for the case of electron-field pair production (triplet production)

$$(\theta_r)_{max}=\cos^{-1}(2/k^{1/2}). \quad (3.39)$$

The above equations show that at threshold where k is given by Eq. (3.19b), the maximum recoil angle $(\theta_r)_{max}$ is equal to 90°.

Because of the interchangeability of each of the particles in triplet production, the same limit given in Eq. (3.36) for $(\theta_r)_{max}$ applies to the emission angles θ_+ and θ_- as well. Therefore, none of the particles in triplet production can be emitted at angles greater than $(\theta_r)_{max}$ given in Eq. (3.37). On the other hand, for nuclear-field pair production, there is no limitation on the emission angles for the pair particles.

H. Maximum and Minimum Positron Energies for Fixed θ_+

In general, for a recoiling particle of mass m_r, the formulas for the maximum and minimum positron energies are different for the two photon energy regions $k>2m_r/(m_r-m_0)$ and $k<2m_r/(m_r-m_0)$. The formulas are given by the following:

(a) For $k>2m_r/(m_r-m_0)$

$$E_{+max}(\theta_+)=\frac{(m_r/m_0)[k+(m_r/m_0)](k-1)+k\cos\theta_+\{k^2\cos^2\theta_++k[(m_r/m_0)+1][(m_r/m_0)(k-2)-k]\}^{1/2}}{[k+(m_r/m_0)]^2-k^2\cos^2\theta_+}, \quad (3.40)$$

$$E_{+min}=1. \quad (3.41)$$

(b) For $k<2m_r/(m_r-m_0)$

$$E_{+\max,\min}(\theta_+)=\frac{(m_r/m_0)[k+(m_r/m_0)](k-1)\pm k\cos\theta_+\{k^2\cos^2\theta_++k[(m_r/m_0)+1][(m_r/m_0)(k-1)-k]\}^{1/2}}{[k+(m_r/m_0)]^2-k^2\cos^2\theta_+}. \tag{3.42}$$

Explicit expressions for $E_{+\max}$ and $E_{+\min}$ are given below for pair production in the field of (1) a nucleus and (2) an electron:

1. Nuclear-Field Pair Production ($m_r\gg m_0$). For $m_r\gg m_0$ one finds

$$E_{+\max}=\frac{(m_r/m_0)[k+(m_r/m_0)](k-1)+k\cos\theta_+[k^2\cos^2\theta_++(m_r/m_0)^2k(k-2)]^{1/2}}{[k+(m_r/m_0)]^2-k^2\cos^2\theta_+}, \tag{3.43a}$$

$$E_{+\min}=1. \tag{3.43b}$$

From these results it follows that for $k\ll m_r/m_0$

$$E_{+\max}=k-1 \tag{3.44}$$

for all angles, while for $k\gg m_r/m_0$

$$E_{+\max}=\frac{(k-1)}{1+(m_0/m_r)k(1-\cos\theta_+)}, \tag{3.45}$$

giving the maximum value $E_{+\max}=k-1$ only for small angles $\theta_+\ll(2m_r/m_0k)^{1/2}$.

2. Electron-Field Pair Production. For $m_r=m_0$ one finds

$$E_{+\max}=\frac{k^2-1+k\cos\theta_+(k^2\cos^2\theta_+-4k)^{1/2}}{(k+1)^2-k^2\cos^2\theta_+}, \tag{3.46a}$$

$$E_{+\min}=\frac{k^2-1-k\cos\theta_+(k^2\cos^2\theta_+-4k)^{1/2}}{(k+1)^2-k^2\cos^2\theta_+}. \tag{3.46b}$$

IV. THEORY

In the theoretical calculation of the pair-production process,* it is convenient to consider two cases in which the recoil energy T_R of the target particle is (A) negligible and (B) not negligible compared to the photon energy k. The interaction between the created pair and the target particle can be described in Case A by a static potential interaction, and in Case B by the complete relativistic interaction through the matrix element of the target-particle, four-vector current density.

Processes belonging to Class A above include electron or muon pair production in the field of an atom for energies and angles such that

$$T_r=[q^2+(m_r/m_0)^2]^{1/2}-(m_r/m_0)\ll k. \tag{4.01}$$

Since $m_r\gg m_0$, Eq. (4.01) may be written

$$q^2/2m_r\ll k/m_0. \tag{4.02}$$

The potential description of the atomic-field, pair-production process is thus valid, except for high energies and large angles. Class A also includes pair processes in the field of an electron, provided that the photon energy is high and the electron and positron emission angles are small. In such a case, the momentum transfer close to the minimum value, $q_{\min}$ as given by Eq. (3.26), satisfies the condition that

$$q^2/2m_0\ll k/m_0, \tag{4.03}$$

which is equivalent to the condition given by Eq. (4.01).

Processes belonging to Class B include high-energy, large-angle pair production in the field of an atom or an electron such that the condition given by Eq. (4.01) is not fulfilled. In this respect, there is a difference between atomic-field and electron-field pair production at low energies: Atomic-field pair production at low energies may belong to Class A because of the large mass of the nucleus, while triplet production at low energies may be excluded from Class A because the kinetic energy of the recoiling electron, $q^2/2m_0$, may be of the order k/m_0.

A. Pair Production in the Potential Field of the Target Particle

The pair-production cross section for processes belonging to Class A is given by

$$d^3\sigma=[e^2/(2\pi)^4](p_-p_+^2E_+/k)\mid M\mid^2dE_+d\Omega_+d\Omega_-, \tag{4.04}$$

* The theoretical considerations in this section apply to the elastic pair-production process which does not involve atomic-excitation effects. A discussion of the inelastic pair process with atomic excitation is given by Wheeler and Lamb (1939, 1956) and by Knasel (1968).

where the matrix element is given by

$$M=\int \bar{\Psi}_-(\mathbf{r})\,\boldsymbol{\gamma}\Psi_+(\mathbf{r})\cdot\mathbf{e}\,\exp(i\mathbf{k}\cdot\mathbf{r})\,d^3r. \quad (4.05)$$

Here Ψ_- and Ψ_+ are the wave functions of the created electron and positron, respectively, in the field of the target particle, and $\boldsymbol{\gamma}$ and γ_4 are the well-known Dirac matrices (Jauch and Rohrlich, 1955).

It is convenient to distinguish between the following two cases: (1) the Born approximation calculation in which the electrostatic potential of the target particle is included in Ψ_+ and Ψ_- only to the first order, and (2) the exact calculation in which Ψ_+ and Ψ_- are exact wave functions in the electrostatic potential of the target particle.

1. *Born Approximation Calculations*

In the Born approximation calculations, Ψ_+ and Ψ_- are given by the first-order-scattering wave functions

$$\Psi_\pm=u_\pm\exp(\mp i\mathbf{p}_\pm\cdot\mathbf{r})$$
$$+e\int G_\pm(\mathbf{r}-\mathbf{r}')\gamma_4\Phi(\mathbf{r}')u_\pm\exp(\mp i\mathbf{p}_\pm\cdot\mathbf{r}')\,d^3r', \quad (4.06)$$

where u_+ and u_- are the positron and electron free-particle spinors, respectively, $\Phi(\mathbf{r})$ is the potential of the target particle, and where the Green's function $G(\mathbf{r})$ may be written as

$$G_\pm(\mathbf{r})=\frac{1}{(2\pi)^3}\int d^3p\,\frac{i\boldsymbol{\gamma}\cdot\mathbf{p}\mp\gamma_4E_\pm-m_0}{\mathbf{p}^2-\mathbf{p}_\pm^2}\exp(i\mathbf{p}\cdot\mathbf{r}). \quad (4.07)$$

From Eqs. (4.05), (4.06), and (4.07), one obtains the Born approximation matrix element which may be written in the form

$$M=iZe^2\bar{u}_-\left\{\boldsymbol{\gamma}\cdot\mathbf{e}\,\frac{i\gamma\cdot(\bar{p}_--\bar{k})-m_0}{(\bar{p}_--\bar{k})^2+m_0^2}\gamma_4\right.$$
$$\left.+\gamma_4\frac{i\gamma\cdot(\bar{k}-\bar{p}_+)-m_0}{(\bar{p}_+-\bar{k})^2+m_0^2}\,\boldsymbol{\gamma}\cdot\mathbf{e}\right\}u_+\frac{4\pi}{q^2}\rho(\mathbf{q}), \quad (4.08)$$

where we have introduced the charge density $Ze\rho(\mathbf{r})$ of the target particle or atom by means of the potential equation $\nabla^2\Phi(\mathbf{r})=-4\pi Ze\rho(\mathbf{r})$. We have further introduced the Fourier transform of $\rho(\mathbf{r})$, $\rho(\mathbf{q})=\int\exp(i\mathbf{q}\cdot\mathbf{r})\rho(\mathbf{r})\,d^3r$.

All Born approximation calculations are based on Eq. (4.08). This equation together with Eq. (4.04) contain all information concerning the pair-production spectrum, angular distributions, and photon, electron, and positron polarizations.

For a target point particle of charge Ze, $\rho(\mathbf{r})$ is a delta function $\delta(\mathbf{r})$, and we get

$$\rho(\mathbf{q})=1 \qquad \text{(point particle)}. \quad (4.09)$$

For an atom the charge density is given by

$$\rho(\mathbf{r})=\delta(\mathbf{r})-\rho_{el}(\mathbf{r})$$

when the nucleus may be taken to be a point particle. Here $\rho_{el}(\mathbf{r})$ is the average charge density for one atomic electron. In this way the atomic form factor $F(q)$ is introduced through the relation

$$\rho(\mathbf{q})=1-F(\mathbf{q}) \qquad \text{(atomic screening)}, \quad (4.10)$$

with

$$F(\mathbf{q})=\int\exp(i\mathbf{q}\cdot\mathbf{r})\rho_{el}(\mathbf{r})\,d^3r.$$

In general, when the charge distribution of the nucleus also has to be taken into account, the charge density of the atom is given by

$$\rho(\mathbf{r})=\rho_n(\mathbf{r})-\rho_{el}(\mathbf{r}),$$

where $\rho_n(\mathbf{r})$ is the average charge density per proton inside the nucleus. We find

$$\rho(\mathbf{q})=G_E(\mathbf{q})-F(\mathbf{q}), \quad (4.11)$$

where the static electric nuclear form factor is given by

$$G_E(\mathbf{q})=\int\exp(i\mathbf{q}\cdot\mathbf{r})\rho_n(\mathbf{r})\,d^3r.$$

When the momentum transfer q is small, of the order unity or smaller, the extension of the nucleus is unimportant and Eq. (4.10) applies. On the other hand, for much larger values of q [but still small enough so that the condition Eq. (4.01) is fulfilled] the atomic form factor is negligible and the effect of the charge distribution is well described by

$$\rho(\mathbf{q})=G_E(\mathbf{q}) \qquad \text{(extended nucleus)}. \quad (4.12)$$

Equations (4.09), (4.10), and (4.12) give the general effects of the charge distribution. In the case of Eq. (4.12), a term describing the effects of the static magnetic moment distribution of the nucleus may be added, as described, for example, by Olsen (1968, Chap. 5.3).

2. *Exact Calculations*

When the effective expansion parameters $Z\alpha/\beta_\pm$ in the Born expansion of $\Psi_\pm$ are not small, i.e., when the target element is heavy or the velocity of one of the produced particles is small, the Born approximation matrix element [Eq. (4.05)] based on the Born wave functions [Eq. (4.06)] cannot be assumed to give a correct description of the process. In this case, exact scattering-state wave functions should be used in the matrix-element equation (4.05). For high energies and small angles, the Furry–Sommerfeld–Maue wave functions (Furry, 1934; Sommerfeld and Maue, 1935) may be used successfully, as shown by Bethe and Maximon (1954). For lower energies, these wave functions fail to give a correct description, and an expansion of Ψ_+ and Ψ_- in partial waves has to be used. This is the method used by Øverbø, Mork, and Olsen (1968). Also in the exact calculations polarization effects may be taken into account.

B. Pair Production by Relativistic Interaction with the Target Particle

When the kinetic energy of the recoiling particle T_r is not much smaller than the photon energy k, dynamical effects of the target particle have to be included. When we consider the Born approximation, the process to the lowest order in the interaction between the created pair and the target particle, Eqs. (4.04) and (4.08) with certain modifications are still applicable. The present discussion does not include effects due to the direct interaction of the photon with the target particle. [See the discussion by Banerjee (1958).]

The modification in Eq. (4.04) comes about because of the appearance of the energy of the recoil particle in the energy conservation relation which now reads

$$k+m_r/m_0=E_+ +E_+ +E_r.$$

This has the effect that the expression for the cross-section equation (4.04) is replaced by

$$d^3\sigma=\frac{e^2}{(2\pi)^4}\frac{p_-p_+^2E_+}{k}\mid M\mid^2\frac{p_-^2E_r}{E_-(\bar{p}_-\cdot\bar{p}_r)+E_r}dE_+d\Omega_+d\Omega_-, \tag{4.13}$$

where the matrix element M is given by the relativistic generalization of Eq. (4.08) as

$$M=Ze^2\bar{u}_-\left\{\boldsymbol{\gamma}\cdot\mathbf{e}\frac{i\gamma\cdot(\bar{p}_--\bar{k})-m_0}{(\bar{p}_--\bar{k})^2+m_0^2}\gamma_u +\gamma_u\frac{i\gamma\cdot(\bar{k}-\bar{p}_+)-m_0}{(\bar{p}_+-\bar{k})^2+m_0^2}\boldsymbol{\gamma}\cdot\mathbf{e}\right\}u_+\frac{4\pi}{\bar{q}^2}J_u(\bar{p}_0,\bar{p}_r), \tag{4.14}$$

where $ZeJ_u(\bar{p}_0,\bar{p}_r)$ is the four current of the target particle in momentum space, $\bar{q}$ is the four-vector momentum transfer, and $\bar{p}_0$ and $\bar{p}_r$ are the four-vector momenta of the target particle in initial and final states, respectively. The modifications of Eq. (4.08) are that $\mathbf{q}$ in Eq. (4.08) has been replaced by $\bar{q}$ in Eq. (4.14) and that γ_4 multiplied by the fourth component of the (three dimensional) Fourier transform $\rho(\mathbf{q})$ has been replaced by the invariant interaction involving $J_u(\bar{p}_0,\bar{p}_r)$ which is essentially the (four dimensional) Fourier transform of the four-vector current density, such that

$$-i\gamma_uJ_u(\bar{p}_0,\bar{p}_r)=\gamma_4\rho(\bar{p}_0,\bar{p}_r)-i\boldsymbol{\gamma}\cdot\mathbf{J}(\bar{p}_0,\bar{p}_r).$$

The momentum-space current density J_u depends on the spin of the target particle. For instance, for a spin-0 target particle, J_u in the laboratory system is given by

$$J_u(\bar{p}_0,\bar{p}_r)=[1/2(m_rE_r)^{1/2}]G_E(\bar{q})(\bar{p}_0+\bar{p}_r)_u, \tag{4.15}$$

where $G_E(\bar{q})$ is the invariant nuclear electric form factor. In particular, for small values of the recoil momentum $\mathbf{p}_r$, for which $E_r\approx m_r/m_0$, only J_4, of magnitude $J_4\approx iG_E(\mathbf{q})$, will be of importance, and Eq. (4.14) reduces to Eq. (4.08) with $\rho(\mathbf{q})$ given by Eq. (4.12). This exemplifies how the static-potential-limit equation (4.08) is obtained from the relativistic theory as given by Eq. (4.14).

As another example, we consider the case of a spin-$\frac{1}{2}$ target particle. For a point particle one has

$$J_u(\bar{p}_0,\bar{p}_r)=i\bar{u}_2\gamma_uu_1, \tag{4.16}$$

where u_1 and u_2 are the initial- and final-state, free-particle spinors, respectively, for the target particle. Equation (4.14) with J_u given by Eq. (4.16) describes for $Z=1$, for instance, muon pair production in the field of an electron when effects due to the direct interaction of the photon with the target electron are included. For the case of triplet production, Eqs. (4.14) and (4.16) are valid when exchange effects and effects due to the direct interaction of the photon with the target electron are included.

For a spin-$\frac{1}{2}$ particle with internal structure, J_u is given by

$$J_u(\bar{p}_0,\bar{p}_r)=i\bar{u}_2\{F_1(\bar{q})\gamma_u-(\kappa/2m_rZ)F_2(\bar{q})\sigma_{uv}\bar{q}_v\}u_1, \tag{4.17}$$

with κ the anomalous magnetic moment and F_1 and F_2 the Dirac and Pauli invariant form factors, respectively. Again, as for the case of a spin-0 particle, one finds for small values of the recoil momentum $\mathbf{q}$ that J_u is given by $J_u=iG_E(\bar{q})\delta_{u4}$ and Eqs. (4.08) and (4.12) are obtained in this static limit.

As in the analogous Case A above, the equation for the cross section [Eq. (4.13)] and for the matrix element [Eq. (4.14)] contain all information concerning the pair-production process, including polarization effects. Calculations are based on these equations together with appropriate expressions for $J_u(\bar{p}_0,\bar{p}_r)$ as, for example, given by Eqs. (4.15), (4.16), and (4.17).

V. POLARIZATION EFFECTS

A. Fermion Polarization

The polarization of fermions, e.g., electrons, positrons, or muons, is most conveniently described in the rest system of the particle (Motz, Olsen, and Koch, 1964). The fermion polarization vector for complete polarization, $\boldsymbol{\zeta}$, is defined as the expectation value of the Pauli spin matrix vector $\boldsymbol{\sigma}$,

$$\boldsymbol{\zeta}=u^*\boldsymbol{\sigma}u, \tag{5.01}$$

for the state u which is an eigenstate of the component of $\boldsymbol{\sigma}$ along $\boldsymbol{\zeta}$ such that

$$\boldsymbol{\sigma}\cdot\boldsymbol{\zeta}u=u. \tag{5.02}$$

The differential cross section $d\sigma$ for any quantum-electrodynamic process involving polarized fermions is a linear function of the fermion polarization vector $\boldsymbol{\zeta}$, with

$$d\sigma\sim A+\mathbf{B}\cdot\boldsymbol{\zeta}, \tag{5.03}$$

where A and $\mathbf{B}$ are functions of the momenta of the particles taking part in the process and of the polarizations of the particles other than the fermion polarization described by $\boldsymbol{\zeta}$.

The application of Eq. (5.03) depends on whether the fermion is emitted in or initiates the process:

(1) When a fermion beam is emitted in a process, the component of the polarization in the direction $\boldsymbol{\zeta}$ of that beam is given by

$$P(\boldsymbol{\zeta})\equiv\mathbf{P}\cdot\boldsymbol{\zeta}=\frac{\sigma(\boldsymbol{\zeta})-\sigma(-\boldsymbol{\zeta})}{\sigma(\boldsymbol{\zeta})+\sigma(-\boldsymbol{\zeta})}=\frac{\mathbf{B}\cdot\boldsymbol{\zeta}}{A}, \quad (5.04)$$

and the polarization vector of the beam is

$$\mathbf{P}=\mathbf{B}/A, \quad (5.05)$$

where $\mathbf{P}$ may apply either to the positron or electron polarization, $\mathbf{P}_+$ or $\mathbf{P}_-$, respectively, which are discussed in Sec. II.

(2) When a process is initiated by a partially polarized fermion beam with polarization $\mathbf{P}=P\boldsymbol{\zeta}$, the cross section for the process is given by an incoherent superposition of the contributions from the states with $\boldsymbol{\zeta}$ and $-\boldsymbol{\zeta}$ with probabilities w_+ and w_-, respectively,

$$d\sigma(\mathbf{P})=w_+d\sigma(\boldsymbol{\zeta})+w_-d\sigma(-\boldsymbol{\zeta}), \quad (5.06)$$

where $w_++w_-=1$ and $w_+-w_-=P$. From Eq. (5.03) one obtains

$$d\sigma(\mathbf{P})\sim A+P\mathbf{B}\cdot\boldsymbol{\zeta}=A+\mathbf{B}\cdot\mathbf{P}, \quad (5.07)$$

which shows that the partially polarized beam is described by the complete polarization case (5.03), but with $\boldsymbol{\zeta}$ replaced by $\mathbf{P}$.

B. Photon Polarization

Photon polarization is described by means of the photon polarization vector $\mathbf{e}$ which occurs in the vector potential of the radiation

$$\mathbf{A}=\mathbf{e}\exp\left[i(\mathbf{k}\cdot\mathbf{r}-kt)\right]. \quad (5.08)$$

The polarization vector $\mathbf{e}$ is a complex unit vector, $\mathbf{e}\cdot\mathbf{e}^*=1$, perpendicular to $\mathbf{k}$, $\mathbf{e}\cdot\mathbf{k}=0$.

In the cross section for a quantum-electrodynamic radiation process the photon polarization vector $\mathbf{e}$ always occurs bilinearly. The cross section for any process involving an emitted or absorbed photon of polarization specified by $\mathbf{e}$ is of a form proportional to

$$M_{ij}e_ie_j^*=\tfrac{1}{2}\{(M_{ij}+M_{ji})e_ie_j^*-(i/2)(M_{ij}-M_{ji})\delta_{ijk}\xi_k\}, \quad (5.09)$$

where M_{ij} is a function of the momenta of the particles taking part in the process and of the polarizations of the particles other than the photon and where i and j are the indices for summing over the spatial components. In Eq. (5.09) we have introduced the circular polarization vector $\boldsymbol{\xi}$ defined by

$$\boldsymbol{\xi}=i\mathbf{e}\times\mathbf{e}^*, \quad (5.10)$$

and the antisymmetric tensor δ_{ijk} which is defined by

$$\delta_{123}=1 \quad \text{and} \quad \delta_{ijk}=-\delta_{jik}=-\delta_{ikj}. \quad (5.11)$$

Because the cross section is a real quantity, $M_{ij}=M_{ji}^*$ and Eq. (5.09) may be written as

$$d\sigma(\mathbf{e})\sim\tfrac{1}{2}\{2(\mathrm{Re}\,M_{ij})e_ie_j^*+(\mathrm{Im}\,M_{ij})\delta_{ijk}\xi_k\}, \quad (5.12)$$

where Re and Im stands for real and imaginary parts, respectively. The form of the cross-section equation (5.12) holds whether the process is completely differential or when some of the particle momenta or polarizations are not observed. In Eq. (5.12) the linear and circular polarization effects are completely separated in that the first and second terms describe linear and circular photon polarization effects, respectively.

1. Linear polarization

In the case of linear photon polarization the radiation field oscillates in a plane. From Eq. (5.08) it follows that $\mathbf{e}$ for this case is a real vector. The cross section is then, according to Eq. (5.12), proportional to

$$d\sigma(\mathbf{e})\sim(\mathrm{Re}\,M_{ij})e_ie_j. \quad (5.13)$$

In an arbitrary coordinate system with axes $\mathbf{e}^{(1)}$ and $\mathbf{e}^{(2)}$, such that $\mathbf{e}^{(1)}$, $\mathbf{e}^{(2)}$, and $\mathbf{k}$ form a right-handed orthogonal coordinate system, the polarization vector may be written

$$\mathbf{e}=\cos\Phi\mathbf{e}^{(1)}+\sin\Phi\mathbf{e}^{(2)}, \quad (5.14)$$

with Φ the angle between $\mathbf{e}$ and the $\mathbf{e}^{(1)}$ axis. The expression (5.13) may then be written

$$d\sigma(\Phi)\sim M_{11}+M_{22}+(M_{11}-M_{22})\cos 2\Phi+2(\mathrm{Re}\,M_{12})\sin 2\Phi. \quad (5.15)$$

This then gives the influence of the linear polarization on the cross section pertaining to a radiation process. The application of this expression depends on whether the radiation is *emitted* or *absorbed*.

(a) For the case that a photon beam is *emitted*, the observed linear polarization of this photon beam referred to the direction $\mathbf{e}$ is

$$P_L(\mathbf{e})=\frac{d\sigma(\mathbf{e})-d\sigma(\mathbf{e}')}{d\sigma(\mathbf{e})+d\sigma(\mathbf{e}')}, \quad (5.16)$$

where $\mathbf{e}'$ is perpendicular to $\mathbf{e}$; specifically,

$$\mathbf{e}'=-\sin\Phi\mathbf{e}^{(1)}+\cos\Phi\mathbf{e}^{(2)}. \quad (5.17)$$

The polarization may most conveniently be expressed in terms of Φ as

$$P_L(\Phi)=\frac{d\sigma(\Phi)-d\sigma(\Phi+\pi/2)}{d\sigma(\Phi)+d\sigma(\Phi+\pi/2)}. \quad (5.18)$$

By the use of the expression (5.15) one obtains

$$P_L(\Phi)=P_L\cos(2\Phi-2\gamma). \quad (5.19)$$

Here γ is given by

$$\tan 2\gamma = 2 \operatorname{Re} M_{12}/(M_{11}-M_{22}), \tag{5.20}$$

and P_L is the maximum linear polarization

$$P_L = \{(M_{11}-M_{22})^2+4(\operatorname{Re} M_{12})^2\}^{1/2}/(M_{11}+M_{22}). \tag{5.21}$$

The direction of the maximum polarization is, according to Eqs. (5.19) and (5.20), given by $\Phi_m=\gamma$, or

$$\tan 2\Phi_m = 2 \operatorname{Re} M_{12}/(M_{11}-M_{22}). \tag{5.22}$$

Equation (5.21) may also be written in the form

$$P_L = \left\{1-4\left[\frac{M_{11}M_{22}-(\operatorname{Re} M_{12})^2}{(M_{11}+M_{22})^2}\right]\right\}^{1/2} \tag{5.23}$$

which shows that complete linear polarization occurs when

$$(\operatorname{Re} M_{12})^2 = M_{11}M_{22}, \tag{5.24}$$

and that a finite difference between $M_{11}M_{22}$ and $(\operatorname{Re} M_{12})^2$ results in a decrease of linear polarization.

When the coordinate axes $\mathbf{e}^{(1)}$ and $\mathbf{e}^{(2)}$ are oriented so that $\mathbf{e}^{(1)}$ is along $\mathbf{e}$, the linear polarization given by (5.23) becomes

$$P_L = (M_{11}-M_{22})/(M_{11}+M_{22}), \tag{5.25}$$

and complete linear polarization occurs only when one of the functions M_{11} or M_{22} vanish, i.e., when the intensity of the radiation polarized along $\mathbf{e}^{(1)}$ or $\mathbf{e}^{(2)}$ vanishes.

(b) For a process in which a partially linearly polarized photon beam is *absorbed*, the cross section is given as an incoherent superposition of the contributions from the two polarization states described by $\mathbf{e}$ and $\mathbf{e}'$, Eqs. (5.14) and (5.17),

$$d\sigma = w_1 d\sigma(\mathbf{e}) + w_2 d\sigma(\mathbf{e}') \tag{5.26}$$

or

$$d\sigma = w_1 d\sigma(\Phi) + w_2 d\sigma(\Phi+\pi/2), \tag{5.27}$$

where w_1 and w_2 are the probabilities for photon polarizations in the directions given by $\mathbf{e}$ (or Φ) and $\mathbf{e}'$ (or $\Phi+\pi/2$), such that $w_1+w_2=1$ and $w_1-w_2=P_L$, the magnitude of the linear polarization of the initial photon beam. One finds, using the expression (5.15) that

$$d\sigma \sim M_{11}+M_{22}+P_L[(M_{11}-M_{22})\cos 2\Phi + 2(\operatorname{Re} M_{12})\sin 2\Phi]. \tag{5.28}$$

In most cases it is convenient to choose the polarization direction as one of the coordinate axes, e.g., $\mathbf{e}=\mathbf{e}^{(1)}$ (i.e., $\Phi=0$), and thus Eq. (5.27) becomes

$$d\sigma \sim M_{11}+M_{22}+P_L(M_{11}-M_{22}). \tag{5.29}$$

2. *Circular polarization*

For the case of circular polarization, the electric and magnetic field strengths of the radiation rotate with constant amplitudes. From Eq. (5.08) it follows that $\mathbf{e}$ is given by

$$\mathbf{e} = (1/\sqrt{2})\{\mathbf{e}^{(1)}+i\delta\mathbf{e}^{(2)}\}, \tag{5.30}$$

where δ is $+1$ and -1 for right-handed and left-handed circular polarization, respectively. The circular polarization vector $\boldsymbol{\xi}$, Eq. (5.10), is given by

$$\boldsymbol{\xi} = \delta\mathbf{e}^{(1)}\times\mathbf{e}^{(2)} = \delta\hat{\mathbf{k}}, \tag{5.31}$$

where $\hat{\mathbf{k}}=\mathbf{k}/k$. A right-handed-polarized photon is thus characterized by $\boldsymbol{\xi}=\mathbf{k}$ and a left-handed-polarized photon by $\boldsymbol{\xi}=-\mathbf{k}$.

The expression (5.12) proportional to the cross section for this case becomes

$$d\sigma(\boldsymbol{\xi}) \sim M_{11}+M_{22}+(\operatorname{Im} M_{ij})\delta_{ijk}\xi_k = M_{11}+M_{22}+2\delta(\operatorname{Im} M_{12}). \tag{5.32}$$

This expression gives the dependence of the cross section on the circular polarization of the radiation. As for the case of linear polarization the application of (5.32) depends on whether the radiation is emitted or absorbed:

(a) For the case that a photon beam is *emitted* in the process, the component of the circular polarization of the radiation along $\boldsymbol{\xi}$ is given by

$$\mathbf{P}_c\cdot\boldsymbol{\xi} = \frac{d\sigma(\boldsymbol{\xi})-d\sigma(-\boldsymbol{\xi})}{d\sigma(\boldsymbol{\xi})+d\sigma(-\boldsymbol{\xi})}, \tag{5.33}$$

or according to (5.32)

$$\mathbf{P}_c\cdot\boldsymbol{\xi} = [(\operatorname{Im} M_{ij})\delta_{ijk}/(M_{11}+M_{22})]\xi_k, \tag{5.34}$$

so the circular polarization vector of the photon beam is

$$\mathbf{P}_c = [(\operatorname{Im} M_{ij})\delta_{ijk}\hat{k}_k/(M_{11}+M_{22})]\hat{\mathbf{k}} = [2\operatorname{Im} M_{12}/(M_{11}+M_{22})]\hat{\mathbf{k}}. \tag{5.35}$$

(b) For a process in which a partially circularly polarized photon beam is *absorbed*, the cross section is given as an incoherent superposition of the contributions from the two polarization states specified by $\boldsymbol{\xi}$ and $-\boldsymbol{\xi}$,

$$d\sigma = w_1 d\sigma(\boldsymbol{\xi}) + w_2 d\sigma(-\boldsymbol{\xi}), \tag{5.36}$$

where w_1 and w_2 are the probabilities for circular polarizations in the directions $\boldsymbol{\xi}$ and $-\boldsymbol{\xi}$, respectively, such that $w_1+w_2=1$ and such that the circular polarization of the photon beam is

$$\mathbf{P}_c = (w_1-w_2)\boldsymbol{\xi}. \tag{5.37}$$

From (4.32) we find

$$d\sigma \sim M_{11}+M_{22}+(\operatorname{Im} M_{ij})\delta_{ijk}P_k. \tag{5.38}$$

3. *Elliptic polarization*

The general case of elliptic polarization of a photon beam is described by Eq. (5.12). Analogous to the case

of linear polarization in Eq. (5.14), the vector $\mathbf{e}$ may for the case of elliptic polarization be written

$$\mathbf{e}=(a\cos\Phi-i\delta b\sin\Phi)\mathbf{e}^{(1)}+(a\sin\Phi+i\delta b\cos\Phi)\mathbf{e}^{(2)}, \tag{5.39}$$

where the real, positive numbers a and b satisfy

$$a^2+b^2=1 \tag{5.40}$$

and δ is equal to $+1$ and -1 for right-handed and left-handed elliptic polarization, respectively. The ratio a/b is the ratio of the axes of the polarization ellipse, so that $a/b=1$ for circular polarizations and a/b is infinite or zero for linear polarization. The angle Φ is the angle between the $\mathbf{e}^{(1)}$ axis and the ellipse axis represented by a. The special cases of linear and circular polarizations are obtained from (5.39) by setting $ab=0$ and $a=b=1/\sqrt{2}$, respectively.

When this expression for $\mathbf{e}$ is introduced into Eq. (5.12), one obtains

$$d\sigma(\mathbf{e})\sim M_{11}+M_{22}+[(M_{11}-M_{22})\cos 2\Phi +2(\mathrm{Re}\,M_{12})\sin 2\Phi](a^2-b^2)+4\delta ab(\mathrm{Im}\,M_{12}). \tag{5.41}$$

The polarization vector $\mathbf{e}'$ describing the opposite state of elliptic polarization relative to $\mathbf{e}$ in Eq. (5.39) is obtained by interchanging the axes of the polarization ellipse, i.e., interchanging a and b and by reversing the sense of rotation of the radiation field (i.e., changing the sign of δ). One finds

$$\mathbf{e}'=(b\cos\Phi+i\delta a\sin\Phi)\mathbf{e}^{(1)}+(b\sin\Phi-i\delta a\cos\Phi)\mathbf{e}^{(2)}. \tag{5.42}$$

We note that as for the case of linear polarization the polarization vectors corresponding to opposite states of polarization are orthogonal to each other; here $\mathbf{e}\cdot\mathbf{e}'^*=0$.

Corresponding to Eq. (5.41), we find

$$d\sigma(e')=M_{11}+M_{22}-[(M_{11}-M_{22})\cos 2\Phi +2(\mathrm{Re}\,M_{12})\sin 2\Phi](a^2-b^2)-4\delta ab(\mathrm{Im}\,M_{12}). \tag{5.43}$$

From Eqs. (5.41) and (5.43) the special cases of linear and circular polarizations are obtained by setting $ab=0$ and $a=b=1/\sqrt{2}$, respectively [compare Eqs. (5.15) and (5.30)].

(a) For a process in which a photon beam is emitted, the elliptic polarization of the beam is

$$P_e(\mathbf{e})=\frac{d\sigma(\mathbf{e})-d\sigma(\mathbf{e}')}{d\sigma(\mathbf{e})+d\sigma(\mathbf{e}')} \tag{5.44}$$

which according to Eqs. (5.41) and (5.43) becomes

$$P_e(a,b,\delta,\Phi)=\{[(M_{11}-M_{22})\cos 2\Phi+2(\mathrm{Re}\,M_{12})\sin 2\Phi](a^2-b^2)+4\delta ab(\mathrm{Im}\,M_{12})\}/(M_{11}+M_{22}). \tag{5.45}$$

The maximum elliptic polarization, usually called the elliptic polarization of the beam is found to be given by

$$P_e=\{(M_{11}-M_{22})^2+4\,|\,M_{12}\,|^2\}^{1/2}/(M_{11}+M_{22}) \tag{5.46}$$

which, according to Eqs. (5.21) and (5.35), may be written

$$P_e=\{P_L^2+P_c^2\}^{1/2}. \tag{5.47}$$

The elliptic polarization is thus given by the observed linear and circular polarization. The magnitude P_e is determined by Eq. (5.47). The direction of the major axis of the polarization ellipse is determined by the linear polarization (through the angle Φ) and the handedness of the elliptic polarization is determined by the circular polarization (through the quantity δ) as is apparent from Eq. (5.41).

It should be noted that for a completely differential process, where no integrations over angles and no summation over polarization spin states for any of the particles have been performed, then M_{ij} is proportional to the absolute square of the matrix element, so that

$$M_{ij}=M_iM_j^*, \tag{5.48}$$

where M_ie_i is proportional to the matrix element. It then follows immediately that

$$|\,M_{12}\,|^2=M_{11}M_{22}, \tag{5.49}$$

and we find from Eq. (5.46) that

$$P_e=1. \tag{5.50}$$

Photons emitted in a completely differential process are thus completely *elliptically* polarized.

(b) The cross section for a process initiated by the *absorption* of a partially elliptically polarized photon beam is given by

$$d\sigma=w_1d\sigma(\mathbf{e})+w_2d\sigma(\mathbf{e}'), \tag{5.51}$$

where $w_1+w_2=1$ and $w_1-w_2=P_e$. From Eqs. (5.41) and (5.43) we find

$$d\sigma\sim M_{11}+M_{22}+P_e\{[(M_{11}-M_{22})\cos\Phi +2(\mathrm{Re}\,M_{12})\sin 2\Phi](a^2-b^2)+4\delta ab\,\mathrm{Im}\,M_{12}\}, \tag{5.52}$$

where Φ is determined by the directions of the axis of the polarization ellipse, a/b by the ratio of the ellipse axis, and δ by the handedness of the polarization.

C. Dependence of the Pair Cross Sections on the Polarization Variables

The differential cross section for pair production including polarization effects is of the form

$$\frac{d^3\sigma(\mathbf{e},\boldsymbol{\xi},\zeta_+,\zeta_-)}{dE_+d\Omega_+d\Omega_-}=C\{F^0+F^e+\mathbf{F}^\xi\cdot\boldsymbol{\xi}+\mathbf{F}^{\zeta+}\cdot\zeta_++\mathbf{F}^{\zeta-}\cdot\zeta_- +\mathbf{F}^{\zeta+,e}\cdot\zeta_++\mathbf{F}^{\zeta-,e}\cdot\zeta_-+\mathbf{F}^{\zeta+,\xi}\cdot\zeta_++\mathbf{F}^{\zeta-,\xi}\cdot\zeta_- +F_{ij}^{\zeta+,\zeta-}\zeta_{+,i}\zeta_{-,j}+F_{ij}^{\zeta+,\zeta-,e}\zeta_{+,i}\zeta_{-,j}+F_{ij}^{\zeta+,\zeta-,\xi}\zeta_{+,i}\zeta_{-,j}\}, \tag{5.53}$$

TABLE 5.01. Polarization effects in pair production.

		Incident photon beam		
		Unpolarized	With linear polarization, P_L, e	With circular polarization, P_c
$d^3\sigma/dE_+d\Omega_+d\Omega_-$	Exact	$4CF^0$	$4C[F^0+P_LF^e]$	$4C[F^0+\mathbf{P}_c\cdot F^\xi]$
	Born	$4CF^0$	$4C[F^0+P_LF^e]$	$4CF^0$
$\mathbf{P}_+$	Exact	$\mathbf{F}^{\zeta_+}/F^0$	$(\mathbf{F}^{\zeta_+}+P_L\mathbf{F}^{\zeta_+,e})/(F^0+P_LF^e)$	$(\mathbf{F}^{\zeta_+}+P_c\mathbf{F}^{\zeta_+,\xi})/(F^0+\mathbf{P}_c\cdot\mathbf{F}^\xi)$
	Born	0	0	$P_c\mathbf{F}^{\zeta_+,\xi}/F_0$
$d^2\sigma/dE_+d\Omega_+$	Exact	$2\bar{C}\bar{F}^0$	$2\bar{C}[\bar{F}^0+P_L\bar{F}^e\{1-2(\tilde{\mathbf{u}}\cdot\mathbf{e})^2\}]$	$2\bar{C}\bar{F}^0$
	Born	•••	•••	•••
$\mathbf{P}_+$	Exact	$\bar{\mathbf{F}}^{\zeta_+}/\bar{F}^0$	$(\bar{\mathbf{F}}^{\zeta_+}+P_L\bar{\mathbf{F}}^{\zeta_+,e})/(\bar{F}^0+P_L\bar{F}^e)$	$(\bar{\mathbf{F}}^{\zeta_+}+P_c\bar{\mathbf{F}}^{\zeta_+,\xi})/\bar{F}^0$
	Born	0	0	$P_c\bar{\mathbf{F}}^{\zeta_+,\xi}/\bar{F}^0$
$d\sigma/dE_+$	Exact	$2\tilde{C}\tilde{F}^0$	$2\tilde{C}[\tilde{F}^0+P_L\tilde{F}^0]$	$2\tilde{C}\tilde{F}^0$
	Born	•••	•••	•••
$\mathbf{P}_+$	Exact	0	0	$P_c\tilde{\mathbf{F}}^{\zeta_+,\xi}/\tilde{\mathbf{F}}^0$
	Born	0	0	$P\tilde{\mathbf{F}}^{\zeta_+,\xi}/\tilde{F}$

where

$$C=\tfrac{1}{2}[Z^2\alpha r_0^2/(2\pi)^2]\{E_+E_-[1-F(q)]^2/k^3q^4\}$$

and where the F coefficients give the correlations between the various polarizations and momenta of the photon, positron, and electron. These coefficients are given in Table 6.10 for the cross-section formulas with polarization dependence for Born approximation calculations and for high-energy, exact calculations. The coefficients $\mathbf{F}^\xi$, $\mathbf{F}^{\zeta\pm}$, $\mathbf{F}^{\zeta\pm,e}$ and $F_{ij}^{\zeta+,\zeta-,\xi}$ describe polarization–momentum correlations and are accordingly absent in the first-order Born calculation (Olsen, 1968). The rest of the coefficients describing terms in the cross section which contain two of the polarization vectors $\boldsymbol{\zeta}_+$, $\boldsymbol{\zeta}_-$ or $\boldsymbol{\xi}$ are polarization–polarization correlation coefficients. These coefficients have in general finite values also in first-order Born calculations.

The cross-section differential in positron energy and emission angle is obtained by integrating Eq. (5.53) over electron emission angles. The result may be written

$$\frac{d^2\sigma(\mathbf{e},\boldsymbol{\xi},\boldsymbol{\zeta}_+)}{dE_+d\Omega_+}=\bar{C}\{\bar{F}^0+\bar{F}^e(1-2\,|\,\mathbf{u}\cdot\mathbf{e}\,|^2)+\bar{\mathbf{F}}^{\zeta_+}\cdot\boldsymbol{\zeta}_+ +\bar{\mathbf{F}}^{\zeta_+,e}\cdot\boldsymbol{\zeta}_+ +\bar{\mathbf{F}}^{\zeta_+,\xi}\cdot\boldsymbol{\zeta}_+\},\quad(5.54)$$

where

$$\bar{C}=(\alpha Z^2r_0^2/2\pi)\,(E_+/k^3).$$

The unit vectors $\mathbf{e}$ and $\boldsymbol{\zeta}_+$ are defined in Sec. II, $\mathbf{u}$ is defined in Table 6.10A, and the coefficients $\bar{F}^0$, $\bar{F}^e$, etc., which have been calculated, are given in Table 6.09 for Born approximation formulas and for high-energy, exact formulas. It is to be noted that the coefficient $\bar{\mathbf{F}}^\xi$ corresponding to $\mathbf{F}^\xi$ in Eq. (5.53) vanishes, since the only scalar which may be formed of the vectors $\mathbf{k}$, $\mathbf{p}_+$ and the axial vector $\boldsymbol{\xi}$, viz. $\boldsymbol{\xi}\cdot\mathbf{k}\times\mathbf{p}_+$ vanishes, since $\boldsymbol{\xi}$ is parallel to $\mathbf{k}$.

The cross-section differential in the positron energy, obtainable from Eq. (5.54) by integration over positron emission angles, is of the form

$$d\sigma(\boldsymbol{\xi},\boldsymbol{\zeta}_+)/dE_+=\tilde{C}[\tilde{F}^0+\tilde{F}^{\zeta_+}\boldsymbol{\xi}\cdot\boldsymbol{\zeta}_+],\qquad(5.55)$$

where

$$\tilde{C}=\tfrac{1}{4}\alpha Z^2r_0^2k^{-3}.$$

The coefficient $\tilde{F}^0$ gives the spectral dependence of the cross section while $P_c\tilde{F}^{\zeta_+}/\tilde{F}^0$ (Table 5.01) gives the magnitude of the average polarization of the positron beam, a quantity only meaningful for high energies, produced by a photon beam of circular polarization P_c. The coefficients $\tilde{F}^0$ and $\tilde{F}^{\zeta_+}$ are given in Table 6.08.

The more complete expression containing also the correlations between the positron and electron polarization is given for high energies as (Olsen and Maximon, 1959)

$$\frac{d\sigma(\boldsymbol{\xi},\boldsymbol{\zeta}_+,\boldsymbol{\zeta}_-)}{dE_+}=\tilde{C}(\tilde{F}^0+\tilde{F}^{\zeta_+}\boldsymbol{\xi}\cdot\boldsymbol{\zeta}_+ +\tilde{F}^{\zeta_-}\boldsymbol{\xi}\cdot\boldsymbol{\zeta}_- -(E_+^2+E_-^2)\,(\psi_1-\tfrac{2}{3}\psi_2)\,\boldsymbol{\zeta}_+\cdot\hat{\mathbf{k}}\boldsymbol{\zeta}_-\cdot\hat{\mathbf{k}} +2E_+E_-[(\psi_1-\tfrac{1}{3}\psi_2)\,\boldsymbol{\zeta}_+\cdot\boldsymbol{\zeta}_- +\tfrac{1}{3}\psi_2\boldsymbol{\zeta}_+\cdot\hat{\mathbf{k}}\boldsymbol{\zeta}_-\cdot\hat{\mathbf{k}}] -\tfrac{1}{3}k^2\psi_2\{\boldsymbol{\zeta}_+{}^\perp\cdot\boldsymbol{\zeta}_-{}^\perp-2\,\mathrm{Re}\,[\boldsymbol{\zeta}_+\cdot\mathbf{e}\boldsymbol{\zeta}_-\cdot\mathbf{e}^*]\}),\quad(5.56)$$

where $\tilde{F}^{\zeta-}$ is obtained from the Formulas for $\tilde{F}^{\zeta+}$ in Table 6.08 by interchanging E_+ and E_-.

The polarization dependence of the above pair cross sections makes possible the detection of photon polarization and the production of polarized electrons and positrons by the pair process. This dependence is given by the various F coefficients which are introduced in

Eqs. (5.53), (5.54), and (5.55), and which are defined in Tables 6.08, 6.09, and 6.10. As shown in the following sections, D and E, these coefficients have the following significance:

(a) F^e or $\bar{F}^e$ is associated with the detection of linear photon polarization, (b) F^ξ is associated with the detection of circular photon polarization, (c) $F^{\zeta\pm,\xi}$, $\bar{F}^{\zeta\pm,\xi}$, or $\tilde{F}^{\zeta\pm,\xi}$ is associated with the production of polarized electrons and positrons by circularly polarized photons, (d) $F^{\zeta+,\zeta-}$, $\bar{F}^{\zeta+,\zeta-}$, or $\tilde{F}^{\zeta+,\zeta-}$ is associated with the production of correlated polarizations of electrons and positrons by unpolarized photons, and (e) $F^{\zeta\pm}$ is associated with the production of polarized electrons or positrons by unpolarized photons.

Examples of the quantitative effects of polarized and unpolarized photon beams on positron (or electron) polarizations and on cross sections involving positron (or electron) detection with polarization insensitive detectors are given in Table 5.01. A summary of the various cross-section formulas which may be derived from Eqs. (5.53), (5.54), (5.55), and (5.56) is given in Table 6.03. These formulas may be used to determine the polarization of a photon beam as described in Sec. V.D, or to produce polarized electrons or positrons as described in Sec. V.E.

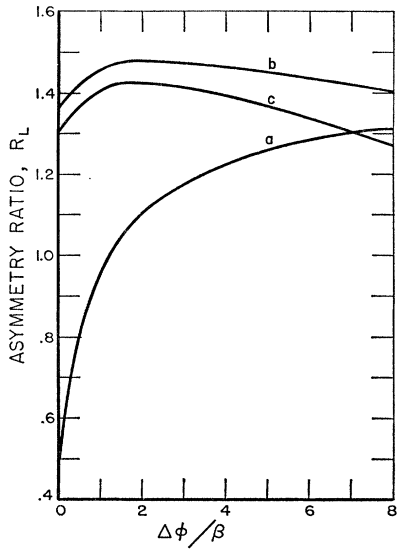

FIG. 5.01. The asymmetry ratio R_L, which is defined in Eq. (5.58) and is calculated by Maximon and Olsen (1962), for the analysis of linear photon polarization. R_L is evaluated for equal energies, $E_+=E_-=k/2$, as a function of $\Delta\Phi/\beta$ for complete screening where $\beta=Z^{1/3}/111$. The azimuthal angle Φ is defined in Fig. 5.02 and it is equal to zero when the pair particles are coplanar. Curve a gives the exact small-angle results valid for $\Delta\Phi\ll1$, with the pair particles observed emergent over angular region $2\Delta\Phi$. Curves b and c give all pair particles observed except those absorbed by a wedge of angular width $2\Delta\Phi\ll1$, with $Z=29$ in curve b and $Z=78$ in curve c.

D. Determination of Photon Polarization by the Pair Process

1. Linear polarization

The linear polarization of a photon beam may be detected by the pair process, as proposed by Yang (1950) and Berlin and Madansky (1950). This method has been discussed in further detail by Wick (1951) and Maximon and Olsen (1962).

The linear polarization P_L of the incident photon beam is determined from measurements of the pair particles emitted in different azimuthal directions with respect to a given photon polarization plane $(\mathbf{e},\mathbf{k})$. The number of particles, N_1 or N_2, which are measured by a detector positioned parallel or perpendicular, respectively, to the polarization plane are given by the equations

$$N_1=A[w_1 d\sigma(\mathbf{e},\Phi_\pm=0)+w_2 d\sigma(\mathbf{e}',\Phi_\pm=0)],$$
$$N_2=A[w_1 d\sigma(\mathbf{e},\Phi_\pm=\tfrac{1}{2}\pi)+w_2 d(\mathbf{e}',\Phi_\pm=\tfrac{1}{2}\pi)], \quad (5.57)$$

where A is a constant that depends on the incident number of photons and the number of atoms per cm^2 in the scattering foil, w_1 and w_2 are the probabilities for photon polarizations in the orthogonal directions $\mathbf{e}$ and $\mathbf{e}'$, respectively, and $\Phi_\pm$ is the azimuthal angle of the pair particle measured with respect to the $(\mathbf{k},\mathbf{e})$ plane. The cross sections $d\sigma$ in Eq. (5.57) have a functional dependence on $\Phi_\pm$ and on the unit vectors $\mathbf{e}$ and $\mathbf{e}'$ for linear photon polarization as given by the coefficients F^e or $\bar{F}^e$ in Tables 6.10 and 6.09. In addition, these cross sections are integrated over the solid angle subtended by the detector, and they may have the form that is differential with respect to the particle energy if the particle detector is a spectrometer.

The linear polarization P_L may be expressed in terms of the measured asymmetry ratio $r_L=N_1/N_2$, and the theoretical asymmetry ratio R_L which is given as

$$R_L=d\sigma(\mathbf{e},\Phi_\pm=0)/d\sigma(\mathbf{e},\Phi_\pm=\tfrac{1}{2}\pi)$$
$$=d\sigma(\mathbf{e}',\Phi_\pm=\tfrac{1}{2}\pi)/d\sigma(\mathbf{e}',\Phi_\pm=0). \quad (5.58)$$

The theoretical ratio R_L is obtained for complete linear polarization ($P_L=1$), and the factor by which it differs from unity may be considered as a figure of merit with which to gauge the sensitivity of the pair process to linearly polarized photon beams. From Eqs. (5.57) and (5.58), the linear polarization is given by the equation

$$P_L=[(R_L+1)/(R_L-1)][(r_L-1)/(r_L+1)]. \quad (5.59)$$

Maximon and Olsen (1962) give quantitative results in which R_L is evaluated for the case of all nearly coplanar pairs and of all except the nearly coplanar pairs. The latter arrangement offers better discrimination for the measurement of linear photon polarization, as shown by the curves for R_L in Fig. 5.01 for the case of equal energy partition ($E_+=E_-=\frac{1}{2}k$), with the pertinent angles defined in Fig. 5.02.

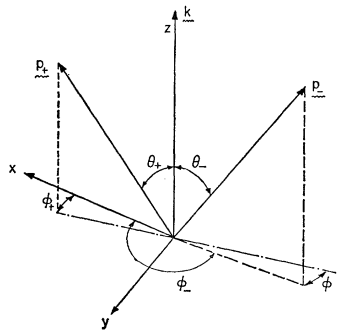

FIG. 5.02. Pair-production angles related to the detection of linear photon polarization. The azimuthal angles Φ_+, and Φ_-, and Φ are measured in the XY plane, such that $\Phi=\pi-(\Phi_--\Phi_+)$. The angular region covered by Φ, from zero to a maximum value of π, is designated as $\Delta\Phi$.

2. *Circular polarization*

The circular polarization of a photon beam may be detected by the pair process, as discussed by Olsen and Maximon (1962) and Kolbenstvedt and Olsen (1965). This method requires azimuthal asymmetry measurements of the electrons emitted with respect to any specified emission plane $(\mathbf{k}, \mathbf{p}_+)$ for the positron. Analogous to the treatment of linear polarization in Sec. V.D.1, the theoretical asymmetry ratio R for circular polarization is given as

$$R_c=d\sigma(\boldsymbol{\xi}, \Phi_-)/d\sigma(\boldsymbol{\xi}, \Phi_-+\pi)$$
$$=d\sigma(-\boldsymbol{\xi}, -\Phi_-)/d\sigma(-\boldsymbol{\xi}, -\Phi_--\pi), \quad (5.60)$$

where the cross sections $d\sigma$ have a functional dependence on the electron azimuthal angle Φ_-, which is measured with respect to the positron emission plane (k, p_+), and on the unit vector $\boldsymbol{\xi}$ for circular photon polarization, as given for example by the coefficient F^{ξ} in Table 6.10. For the specific geometry shown in Fig. 5.03 where $\theta_+=\theta_-$, $E_+=\frac{1}{2}k$, and $\Phi_-=\frac{1}{2}\pi$ such that $\hat{\mathbf{k}}=\mathbf{k}/|k|=\mathbf{u}\times\mathbf{v}/|\mathbf{u}\times\mathbf{v}|$, Kolbenstvedt and Olsen (1965) have evaluated R_c as a function of θ_+ for different photon energies, and their results are given in Fig. 5.04. For the case in which the cross section is integrated over the angles, θ_+, θ_-, and $(\Phi_+-\Phi_-)$ from 0 to π, the Olsen–Maximon calculations (1962) for high energies and complete screening give

$$R_c=(\alpha Z)\frac{(E_+^2+E_-^2)2\pi\ln 2}{(E_+^2+E_-^2+\frac{2}{3}E_+E_-)\ln(183Z^{-1/3})-\frac{1}{9}E_+E_-}. \quad (5.61)$$

With the above available data for R_c, the circular polarization is given by the following equation:

$$\mathbf{P}_c\cdot\boldsymbol{\xi}=[(R_c+1)/(R_c-1)][(r_c-1)/(r_c+1)], \quad (5.62)$$

where r_c is the asymmetry ratio measured in the particular geometry and at the azimuthal angles for which R_c was evaluated.

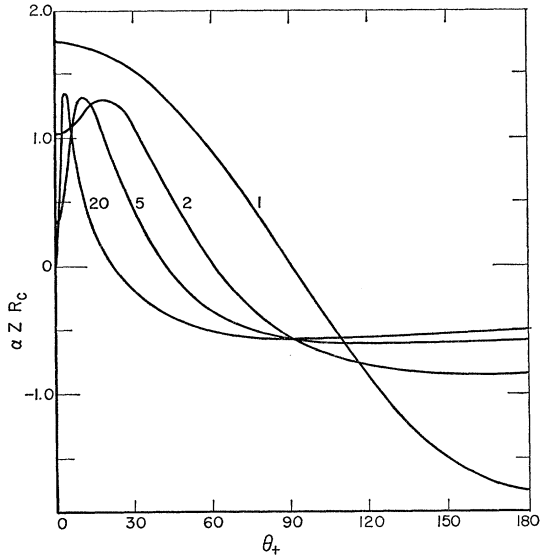

FIG. 5.04. The asymmetry ratio R_c, which is defined in Eq. (5.60) and is calculated by Kolbenstvedt and Olsen (1965), for the analysis of circular photon polarization. The ratio αZR_c is evaluated as a function of the emission angle θ_+ for right-handed circularly polarized photons, with $\theta_+=\theta_-$ and $E_+=E_-=k/2$. The numbers attached to the curves give the photon energies in megaelectron volts.

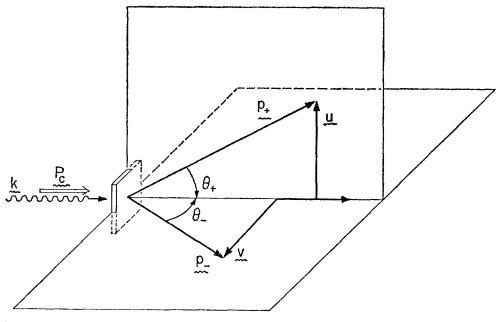

FIG. 5.03. Pair-production angles related to the detection of circular photon polarization. In this geometry, the azimuthal angle Φ in Fig. 5.02 is equal to $\pi/2$, such that the momentum components $\mathbf{u}$ and $\mathbf{v}$ are orthogonal.

E. Production of Polarized Electrons and Positrons by the Pair Process

1. *Polarized electrons and positrons by circularly polarized photons*

The electron or positron beams emitted in certain directions by circularly polarized photons in the pair process may have a certain degree of polarization, as shown, for example, in Table 5.01. For the case where the positron is not observed, the longitudinal and transverse polarizations $\mathbf{P}_-^L$ and $\mathbf{P}_-^T$, respectively, of the electron beam are given by the following equations:

$$\mathbf{P}_-^L=\mathbf{n}_-\frac{d^2\sigma(\mathbf{P}_c, \zeta_-)/dE_-d\Omega_- - d^2\sigma(\mathbf{P}_c, -\zeta_-)/dE_-d\Omega_-}{d^2\sigma(\mathbf{P}_c, \zeta_-)/dE_-d\Omega_- + d^2\sigma(\mathbf{P}_c, -\zeta_-)/dE_-d\Omega_-}, \quad (5.63)$$

with $\hat{\mathbf{p}}_-\cdot\boldsymbol{\zeta}_-=1$ or $\mathbf{n}\cdot\boldsymbol{\zeta}_-=0$ for longitudinal polarization, and

$$\mathbf{P}_-{}^T=\mathbf{n}\frac{d^2\sigma(\mathbf{P}_e,\boldsymbol{\zeta}_-)/dE_-d\Omega_- - d^2\sigma(\mathbf{P}_e,-\boldsymbol{\zeta}_-)/dE_-d\Omega_-}{d^2\sigma(\mathbf{P}_e,\boldsymbol{\zeta}_-)/dE_-d\Omega_- + d^2\sigma(\mathbf{P}_e,-\boldsymbol{\zeta}_-)/dE_-d\Omega_-}, \tag{5.64}$$

with $\hat{\mathbf{p}}_-\cdot\boldsymbol{\zeta}_-=0$ or $\mathbf{n}\cdot\boldsymbol{\zeta}_-=1$ for transverse polarization. These polarizations involve the coefficient $\bar{F}^{\mathfrak{T}-,\xi}$, which is given in Table 6.09. For high energies, Olsen and Maximon (1959) have shown that

$$\mathbf{P}_-{}^L=\mathbf{n}_-P_e\frac{k[(E_-+E_+)(3+2\Gamma)+2E_+(1+4\mu^2\xi^2\Gamma)]}{(E_+^2+E_-^2)(3+2\Gamma)+2E_+E_-(1+4\mu^2\xi^2\Gamma)}, \tag{5.65}$$

where the various quantities are defined in Table 6.09B and in Sec. II. As shown in Fig. 5.05, the transverse polarization is always small while the longitudinal polarization may be large. The mean (integrated over the electron emission angles) longitudinal polarization of the electron beam is shown in Fig. 5.06, and for photon energies greater than approximately 20 MeV this polarization may be written in the simple form (Olsen and Maximon, 1959)

$$\mathbf{P}_-{}^L=(4E_--k)\mathbf{k}/(3k^2-4E_+E_-). \tag{5.66}$$

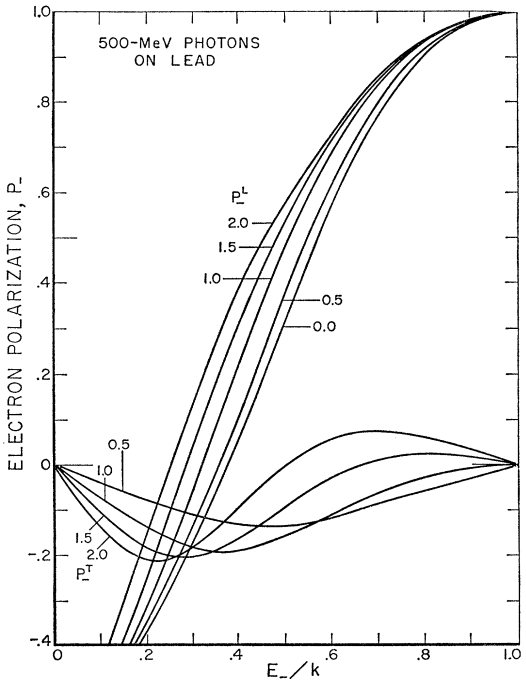

FIG. 5.05. Longitudinal, $\mathbf{P}_-{}^L$, and transverse, $\mathbf{P}_-{}^T$, polarization of electrons produced by 100% circularly polarized 500-MeV photons in lead, as calculated by Olsen and Maximon (1959). The numbers attached to the curves give the values of θ_- in milliradians. [Numerical errors occurring in Figs. 7 and 8 of Olsen and Maximon (1959) have been corrected here.]

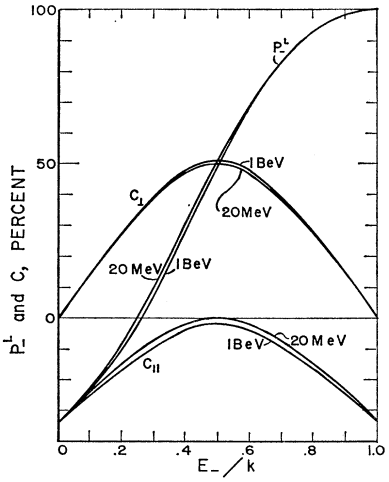

FIG. 5.06. Longitudinal polarization $P_-{}^L$ of electrons produced by 100% circularly polarized photons in lead, as calculated by Olsen and Maximon (1959) with the inclusion of Coulomb and screening effects. Also, results are given for the spin correlation terms defined in Eq. (5.67), $C_\parallel$ and $C_\perp$, for longitudinal and transverse spins, respectively. The results are integrated over the electron emission angles and are shown for incident photon energies of 20 MeV and 1 BeV.

2. *Correlated polarizations of electrons and positrons by unpolarized photons*

If the polarizations of both pair particles are recorded, a correlation C of polarization is obtained:

$$C=\frac{d\sigma(\boldsymbol{\zeta}_+=\boldsymbol{\zeta}_-)-d\sigma(\boldsymbol{\zeta}_+=-\boldsymbol{\zeta}_-)}{d\sigma(\boldsymbol{\zeta}_+=\boldsymbol{\zeta}_-)+d\sigma(\boldsymbol{\zeta}_+=-\boldsymbol{\zeta}_-)}. \tag{5.67}$$

In particular, the average polarization correlation of the electron–positron beam may for energies $k\geq 20$ MeV be written in the simple form

$$C=[4E_-E_+-(\boldsymbol{\zeta}_+\cdot\mathbf{k})^2]/(3k^2-4E_-E_+). \tag{5.68}$$

Curves for $C_\parallel$ (for longitudinal spins, $\boldsymbol{\zeta}_+\cdot\hat{\mathbf{k}}=1$) and for $C_\perp$ (for transversal spins, $\boldsymbol{\zeta}_+\cdot\hat{\mathbf{k}}=0$) are given in Fig. 5.06.

3. *Polarized electrons or positrons by unpolarized photons*

When the momenta of both pair particles are observed in coincidence it is possible to obtain polarized electrons or positrons through momentum–polarization correlations (Olsen and Maximon, 1964) of the form $(\mathbf{p}_+\times\mathbf{p}_-\cdot\boldsymbol{\xi}_\pm)$. It should be pointed out that pair production, through this correlation, is the only electromagnetic process in which strongly polarized high-energy particles are produced from initially unpolarized particles. The longitudinal and transverse polarizations may be considerable as displayed in Fig. 5.07.

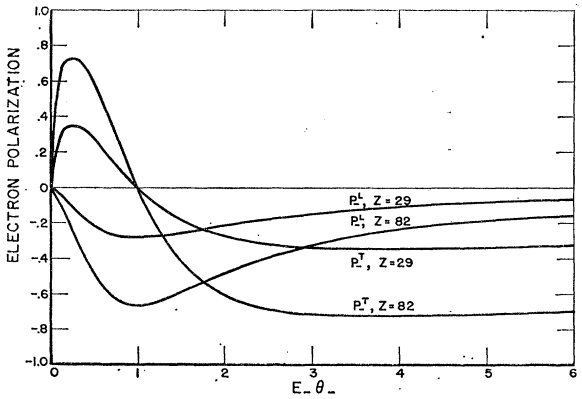

FIG. 5.07. Longitudinal and transverse polarization, P_-^L and P_-^T, respectively, of electrons which are detected in coincidence with the corresponding positron for the case where the emission planes are orthogonal, as given by Olsen and Maximon (1964). The data for P_-^L is given for the case of maximum polarization where $E_-\approx k$, and the data for P_-^T is given also for the optimum case where $E_-=k/\sqrt{2}$. These polarizations are produced by unpolarized photons.

VI. CROSS-SECTION FORMULAS FOR PAIR PRODUCTION IN ATOMIC FIELD

The cross-section formulas for pair production in an atomic field are given for the various differential and integrated forms that have been calculated. The formulas for a particular cross-section form are classified according to the approximation used in the calculation (first Born or exact with relativistic, screening, or nuclear-size approximations as discussed in Sec. IV). A quantitative summary of these approximations is given in Table 6.01, and each formula is accompanied by a list of the conditions of validity which are identified by the letters in Table 6.01.

Each cross-section formula is identified by a label with six elements. The first two elements are a number and a letter which are used to uniquely identify the process under consideration; in this case, the pair-production process as distinguished from other Coulomb processes. With regard to the pair process, the next four elements are digits which serve as convenient indices for locating a particular formula: the first digit gives the number of differential variables in the formula, the second digit gives the number of polarization variables in the formula, the third digit is an index which uniquely specifies a particular combination of the variables given by the first and second digits, and the fourth digit is an index (ranging from 0 to 9) which identifies the 10 types of calculations successively listed by the different columns in Tables 6.02(a) and 6.02(b).

Summaries of the available cross-section formulas for pair production in an atomic field are given in Tables 6.02(a), 6.02(b), and 6.03. Tables 6.02(a) and 6.02(b) give the formulas which are summed over the photon and electron polarization states and therefore which are not dependent on the polarization variables for these particles. Table 6.03 gives the formulas in the forms which show their functional dependence on various combinations of the polarization variables for these particles. The application of the formulas in Table 6.03 for determining the polarization of the particles involved in pair production is discussed in Sec. V. The blank spaces in each table indicate that a formula is not available.

The formulas for the various differential cross sections are given in a form which is differential in the *positron* variables. To obtain corresponding formula differential in the *electron* variables, the following changes should be made in the differential formulas given below:

(a) Replace E_+, E_-, p_+, p_-, and Z, respectively, by E_-, E_+, p_-, p_+, and $-Z$ to convert $d\sigma/dE_+$ to $d\sigma/dE_-$.

(b) Replace E_+, E_-, $\mathbf{p}_+$, $\mathbf{p}_-$, θ_+, and Z, respectively, by E_-, E_+, $\mathbf{p}_-$, $\mathbf{p}_+$, θ_-, and $-Z$ to convert $d^2\sigma/dE_+d\Omega_+$ to $d^2\sigma/dE_-d\Omega_-$. For the polarization-dependent formulas, also replace ζ_+ by ζ_-.

(c) Replace E_+, E_-, and Z, respectively, by E_-, E_+, and $-Z$ to convert $d^2\sigma/dE_+dw$ to $d^2\sigma/dE_-dw$.

For most cases, the nuclear recoil is negligible so that $k=E_++E_-$, and the conversion procedure for the above differential formulas is simple. For these cases of negligible nuclear recoil, the cross sections differential in the positron variables may be interpreted in terms of the cross sections differential in the electron variables by making the simple substitution that $E_+=k-E_-$.

TABLE 6.01. Conditions of validity for pair-cross-section formulas.

A. First Born approximation:

$$\alpha Z/\beta_+,\ \alpha Z/\beta_-\ll 1$$

or

$$\alpha Z/\bar{\beta}_+\ll 1$$

such that $E_+=E_-=k/2$, with $\bar{\beta}_+=\bar{\beta}_-=(1-4/k^2)^{1/2}$

or

$$[\alpha Z/(1-4/k^2)^{1/2}]\ll 1$$

B. No screening: $\alpha Z^{1/3}k\ll 1$

C. Complete screening: $\alpha Z^{1/3}k\gg 1$

D. Extreme-relativistic energies: E_+, E_-, $k\gg 1$

E. Negligible nuclear recoil: $q^2\ll km_r/m_0$

This condition is obtained if $m_0\ll km_r$, i.e., always for small-angle pair production, or if $k\ll m_r$ for large-angle pair production.

F. Small angles: $\theta_+=O(1/E_+)$, $\theta_-=O(1/E_-)$

G. Large angles: $\theta_\pm\gg 1/E_\pm$

H. Exponential screening: $F(q)=[1+(R_{TF}q)^2]^{-1}$

TABLE 6.02. Cross-section formulas for pair production in an atomic field without atomic excitation.[a]

Pair cross section	Formulas[a]								
	First Born					Exact			
	UPN	UPN–ER	SPN	SPN–ER	FN	UPN	UPN–ER	SPN	SPN–ER
σ	3D–0000 Racah	3D–0001 Heitler–Sauter		3D–0003 Bethe–Heitler		3D–0006 Øverbø–Mork–Olsen	3D–0007 Davies–Bethe–Maximon		3D–0009 Davies–Bethe–Maximon
$d\sigma/dE_+$[b]	3D–1000 Bethe–Heitler	3D–1001 Bethe–Heitler		3D–1003 Bethe–Heitler		3D–1006 Øverbø–Mork–Olsen	3D–1007 Davies–Bethe–Maximon		3D–1009 Davies–Bethe–Maximon
$d\sigma/d\Omega_r$	3D–1010 Jost–Luttinger–Slotnick								
$d\sigma/dP_p$	3D–1020 Borsellino								
$d\sigma/dq$			3D–1032 Jost–Luttinger–Slotnick						
$d^2\sigma/dE_+d\Omega_+$[b]	3D–2000 Sauter–Gluckstern–Hull			3D–2003 Schiff			3D–2007 Olsen–Maximon		3D–2009 Olsen Maximon
$d^2\sigma/dE_+dw$[b]		3D–2011 Olsen		3D–2013 Olsen					
$d^3\sigma/dE_+d\Omega_+d\Omega_-$[b]	3D–3000 Bethe–Heitler	3D–3001 Bethe–Heitler			3D–3004 Bjorken–Drell–Frautschi		3D–3007 Bethe–Maximon		3D–3009 Bethe–Maximon

[a] This process is also designated as elastic or coherent pair production. The formulas are classified under the two main categories of First Born or Exact with the following subdivisions: UPN = unscreened point nucleus; FN = finite nucleus; ER = extreme relativistic; SPN = screened point nucleus.

[b] The cross sections which are differential in E_- rather than E_+ may be obtained by the procedure discussed in Sec. VI.

TABLE 6.02(b). Cross-section formulas for pair production in an atomic field with atomic excitation.[a]

Pair cross section	Formulas[a]
σ	3D–0005 Wheeler–Lamb
$d\sigma/dE_+$	3D–1005 Wheeler–Lamb

[a] This process is also designated as inelastic or incoherent pair production. The only formulas available for this process which are given in the above table are calculated with the first Born approximation.

For example, in Figs. 6.04 to 6.08 and in Fig. 6.12, where the differential cross sections are given as functions of the positron energy E_+, the corresponding differential cross sections as functions of the electron energy E_- are obtained by substituting $E_+ = k - E_-$. This substitution procedure is equivalent to reading the abscissa from right to left since $(E_+ - 1)/(k-2) = 1 - (E_- - 1)/(k-2)$.

Pair production in an atomic field may occur without atomic excitation (also designated as "elastic" or "coherent" pair production) and with atomic excitation (also designated as "inelastic" or "incoherent" pair production). These two processes which have different final states are independent of each other, and the cross sections for the two processes are additive. Therefore,

TABLE 6.03. Cross-section formulas with polarization dependence for pair production in an atomic field.

Differential pair cross section	Photon beam with no polarization				Photon beam with linear polarization				Photon beam with circular polarization			
	Polarization variables				Polarization variables				Polarization variables			
	None	ζ_+	ζ_-	ζ_+, ζ_-	e	e, ζ_+	e, ζ_-	e, ζ_+, ζ_-	ξ	ξ, ζ_+	ξ, ζ_-	ξ, ζ_+, ζ_-
$d\sigma/dE_+$[a]	3D-100N	3D-100N	3D-100N	...	3D-100N	3D-100N	3D-100N	...	3D-100N	3D-1229	...	...
$d^2\sigma/dE_+d\Omega_+$[a]	3D-200N	...	...	...	3D-2132 3D-2139	...	...	...	...	3D-2242 3D-2249	...	...
$d^3\sigma/dE_+d\Omega_+d\Omega_-$[a]	3D-300N	3D-3119	...	...	3D-2131 3D-3139	3D-3229	...	...	3D-3149	3D-3249	...	...

[a] N = Integers from 0 to 9, as given in Table 6.02. See discussion in Sec. VI for conversion from E_+ to E_- and ζ_+ to ζ_-. The blanks ... indicate that the formulas are not available.

any given form of the pair cross section, such as σ or $d\sigma/dE_+$, is equal to the sum $[\sigma(\text{elastic})+\sigma(\text{inelastic})]$ {or $[d\sigma/dE_+$ (elastic)$+d\sigma/dE_+$ (inelastic)$]$}. The major contribution to this sum comes from the "elastic" component, and except for low-Z atoms (as shown in Fig. 8.01), the "inelastic" component is negligible. The formulas in Table 6.02(a) apply to pair production without atomic excitation ("elastic" or "coherent"), and the formulas in Table 6.02(b) apply to pair production with atomic excitation ("inelastic" or "incoherent").

Cross-section calculations for pair production with atomic excitation must account for the contributions of the atomic binding, the exchange character of the interaction, and the energy transfer to the recoil electron. The only calculations for pair production with the inclusion of atomic excitation and ionization effects have been made in the first Born approximation by Wheeler and Lamb (1939), and their results are given by Formulas 3D–0005 and 3D–1005 in Table 6.02(b). It is important to note that these formulas apply to the process in which pair production occurs in *an atomic field*. If atomic ionization is involved, an electron is liberated with the production of a triplet. This process of triplet production in an atomic field should not be confused with the triplet production in an electron field which is discussed in Sec. VII.

At extreme-relativistic energies, it is necessary to account for nuclear recoil and size effects for the observation of large-angle pair production. Such calculations are given in the first Born, [finite-nucleus (FN)] column in Table 6.02(a). Otherwise, the formulas in Table 6.02(a) apply to pair production with a negligible energy transfer to the nucleus (negligible nuclear recoil) such that $q^2 \ll km_r/m_0$.

It should be noted that the cross-section formulas in Sec. VI and the kinematic relations in Sec. III may be applied to all processes involving the production by photons of any pair of particles (such as muon pairs), providing the rest mass of the pair particle is substituted for the electron mass m_0. Also, certain bremsstrahlung formulas may be derived from the corresponding pair formulas as follows:

(a) The bremsstrahlung differential cross section $d^2\sigma(\mathbf{k}, \mathbf{p}_1)/dkd\Omega_k$ is obtained from the corresponding pair cross section $d^2\sigma(\mathbf{p}_+, \mathbf{k})/dE_+d\Omega_+$ by substituting $-E_1$, $-\mathbf{p}_1$ for E_+, $\mathbf{p}_+$, k, $\mathbf{k}$ for $-k$, $-\mathbf{k}$, and $dkd\Omega_k$ for $dE_+d\Omega_+$, and by multiplying $d^2\sigma(\mathbf{p}_+, \mathbf{k})/dE_+d\Omega_+$ by the factor k^2/p_1^2. In these expressions, p_1 and E_1 are the initial electron momentum and energy, respectively, in the bremsstrahlung process, and $d\Omega_k$ is the element of solid angle in the direction of $\mathbf{k}$ relative to $\mathbf{p}_1$.

(b) Provided the recoil energy is negligible such that $k=E_++E_-$, $d\sigma(\mathbf{k}, \mathbf{p}_1)/dk$ is directly obtainable from $d\sigma(\mathbf{p}_+, \mathbf{k})/dE_+$ by substituting $-E_1$ for E_+, k for $-k$, dk for dE_+, and by multiplying $d\sigma(\mathbf{p}_+, \mathbf{k})/dE_+$ by k^2/p_1^2.

Formula 3D–0000

[The Racah Formula: Unscreened Point Nucleus]

$$\sigma=\alpha Z^2 r_0^2\left[\frac{692+468\epsilon+76\epsilon^2+108\epsilon^3}{27(1+\epsilon)^3}K(\epsilon)-\frac{692+360\epsilon+692\epsilon^2}{27(1+\epsilon)^3}E(\epsilon)-\frac{4(1-\epsilon)^2}{(1+\epsilon)^2}\int_0^\epsilon\frac{K(\eta)\,d\eta}{1-\eta}\right.$$
$$\left.+\frac{16(1-\epsilon)^2}{(1+\epsilon)^2}\int_0^\epsilon\frac{d\zeta}{1-\zeta^2}\int_0^\zeta\frac{K(\eta)\,d\eta}{1-\eta}\right],$$

where $K(x)$ and $E(x)$ are the complete elliptic integrals of the first and second kind, respectively, of argument x (Abramowitz and Stegun, 1964, p. 589), and

$$\epsilon=(k-2)/(k+2).$$

A. The above Racah Formula 3D–0000 has been reduced by Maximon (1968) to the following simple analytical expressions containing rapidly convergent series expansions:

(1) For k near threshold such that $k-2\lesssim 1$,

$$\sigma=\alpha Z\, r_0^2\frac{2\pi}{3}\left(\frac{k-2}{k}\right)^3\left[1+\frac{1}{2}\epsilon+\frac{23}{40}\epsilon^2+\frac{37}{120}\epsilon^3+\frac{61}{192}\epsilon^4+\cdots\right]$$
$$=\alpha Z^3 r_0^2\frac{2\pi}{3}\left(\frac{k-2}{k}\right)^3\left[1+\frac{1}{2}\epsilon_1+\frac{23}{40}\epsilon_1^2+\frac{11}{60}\epsilon_1^3+\frac{29}{960}\epsilon_1^4+\cdots\right],$$

where the second series is more rapidly convergent, and

$$\epsilon=(k-2)/(k+2),\quad\text{and}\quad\epsilon_1=2\epsilon/[1+(1-\epsilon^2)^{1/2}].$$

The first term in either of the above expansions reduces to the threshold formula previously obtained by Racah [1934, Formula (12)] and by Nishina, Tomonaga, and Sakata [1934, Formula (4)].

(2) For larger photon energies with $k\geq 4$,

$$\sigma=\alpha Z^2 r_0^2\left\{\frac{28}{9}\ln 2k-\frac{218}{27}+\left(\frac{2}{k}\right)^2\left[6\ln 2k-\frac{7}{2}+\frac{2}{3}\ln^3 2k-\ln^2 2k-\frac{\pi^2}{3}\ln 2k+\frac{\pi^2}{6}+2\zeta(3)\right]\right.$$
$$\left.-\left(\frac{2}{k}\right)^4\left[\frac{3}{16}\ln 2k+\frac{1}{8}\right]-\left(\frac{2}{k}\right)^6\left[\frac{29}{9\times 256}\ln 2k-\frac{77}{27\times 512}\right]+\cdots\right\},$$

where

$$\zeta(3)=\sum_{n=1}^{\infty}\frac{1}{n^3}=1.2020569\ldots.$$

The first two terms in the above expansion reduces to the high-energy Formula 3D–0001 given by Racah [1936, Formula (12)], by Bethe and Heitler [1954, Formula (14), p. 260], and by Hough (1948).

(1) *Conditions of Validity*

Table 6.01: A, B.

(2) *References*

Racah (1934), Formula (10) with correction given by Racah [1936, Formula (10), p. 69].

Maximon (1968), Formulas (9), (10), and (12).

(3) *Notes*

a. The Racah formula has been evaluated by Maximon (1968) as a function of the photon energy. Maximon's results are given in Table 6.04 and in Figs. 6.01 and 6.02. Figures 6.01 and 6.02 compare the pair cross sections predicted with Born approximation calculations (3D–0000) and with exact calculations (3D–0006 and 3D–0009) for $Z=82$. General agreement with the exact calculations has been obtained from various experimental results, examples of which are given in the following references: Rosenblum, Shrader, and Warner (1952) (5.3, 10.3, and 17.6 MeV); Dayton (1953) (1.33 and 2.62 MeV); Staub and Winkler (1954) (6.3 MeV); West (1956) (1.17 and 1.33 MeV); Rao, Lakshminarayana, and Jnanananda (1963) (1.12 MeV); Yamazaki and Hollander (1965) (≈1.1 to 2.0 MeV); Titus and Levy (1966) (2.62 MeV); Roche, Avah, and Isabelle (1968) (2.62 MeV); and Garritson and Miller (1968) (≈1.1 to 2.0 MeV)

Formula 3D–0001

[The Heitler–Sauter Formula: Unscreened Point Nucleus for Extreme-Relativistic Energies]

$$\sigma = \alpha Z^2 r_0^2 \left[\frac{28}{9} \ln (2k) - \frac{218}{27}\right]$$

(1) Conditions of Validity

Table 6.01: A, B, D.

(2) References

Heitler (1933).
Heitler (1954), Formula (14), p. 260.

Formula 3D–0003

[The Bethe–Heitler Formula: Screened Point Nucleus for Extreme-Relativistic Energies]

$$\sigma = \alpha Z^2 r_0^2 \left[\frac{28}{9} \ln (183 Z^{-1/3}) - \frac{2}{27}\right]$$

(1) Conditions of Validity

Table 6.01: A, C, D.

(2) References

Heitler (1954), Formula (15), p. 260.

(3) Notes

a. Formula 3D–0003 is obtained with the above complete screening approximation from an analytical integration of Formula 3D–1003B. For intermediate screening, Bethe and Heitler (1954, Table VI, p. 262) give cross-section values for aluminum and lead, which were obtained by a numerical integration of Formula 3D–1003 (Secs. C and D of Formula 3D–1003).

Formula 3D–0005

[The Wheeler–Lamb Formula: Screened Point Nucleus with Atomic Excitation for Extreme-Relativistic Energies]

$$\sigma = \alpha Z r_0^2 (22.6 - 2.08 \ln Z)$$

(1) Conditions of Validity

Table 6.01: A.

(2) References

Wheeler and Lamb (1939), integrated form of Formula (20), as given by Olsen (1968).

(3) Notes

a. For low atomic numbers, Formula 3D–0005 and Fig. 8.01 show that there is a substantial contribution to the pair cross section from processes in which atomic excitation occurs. A detailed study of the incoherent scattering function used in this process and the corresponding pair cross section for helium is given by Knasel (1968).

Formula 3D–0006

[The Øverbø–Mork–Olsen Formula: Unscreened Point Nucleus]

$$\sigma = \int_1^{k-1} \frac{d\sigma}{dE_+} dE_+,$$

where $d\sigma/dE_+$ is given by Formula 3D–1006.

(1) Conditions of Validity

Table 6.01: B

(2) References

Øverbø, Mork, and Olsen (1968).

(3) Notes

a. This formula is evaluated by Øverbø, Mork, and Olsen (1968) in Figs. 6.01 and 6.03. These figures give the dependence, respectively, of the cross section σ and the cross-section ratio σ/σ_R on the photon energy in the region $2\leq k\leq 5$, where σ_R is the unscreened Racah cross section given by Formula 3D–0000 or by the integration of Formula 3D–1000. In the energy region where $6\leq k\leq 30$, Øverbø, Mork, and Olsen (1968) give the following semiempirical formula for lead ($Z=82$):

$$\sigma=\sigma_R-4.02+(16.8/k)\ln(k-0.75)$$

b. Higher-order calculations for the total pair cross section in the threshold region have been carried out previously by Nishina, Tomonaga, and Sakata (1934). However, their calculations have been superseded by the more accurate calculations of Øverbø, Mork, and Olsen (1968). The threshold-region formula given by Nishina, Tomonaga, and Sakata (1934) may be written in the form

$$d\sigma/dE_+=\alpha Z^2r_0^2\tfrac{1}{3}(k-2)\times\frac{(2\pi\alpha Z)^2S(\alpha Z,k)}{[\exp(2\pi\alpha Z/\beta_+)-1][1-\exp(-2\pi\alpha Z/\beta_-)]},$$

where $S(\alpha Z, k)$ was calculated to the first order in αZ only:

$$S(\alpha Z,k)=1+[3(\alpha Z)^2/64(k-2)](\pi^2+8)+\cdots.$$

The formula gives reliable results in the threshold region $k-2\ll 1$ for light elements $\alpha Z\ll 1$. For the condition that $[2(k-2)]^{1/2}\ll\alpha Z\ll 1$, the formula (Nishina, Tomonaga, and Sakata, 1934) for the total cross section is

$$\sigma=\alpha Z^2r_0^2(\pi/12)(k-2)^3(3/\pi)[\tfrac{1}{8}+(1/\pi^2)]\times\{2\pi\alpha Z/[2(k-2)]^{1/2}\}^3\exp\{-2\pi\alpha Z/[2(k-2)]^{1/2}\}$$

and for $\alpha Z\ll[2(k-2)]^{1/2}\ll 1$ the formula is

$$\sigma=\alpha Z^2r_0^2(\pi/12)(k-2)^3.$$

c. More data are needed in the threshold energy region in order to determine the effect of atomic screening on the cross sections predicted by Formula 3D–0006, although the results by Øverbø, Mork, and Olsen (1968) indicate that this effect may be as small as a few percent.

d. The various measurements of the pair cross section are described in the references of Note a for Formula 3D–0000. The results of these measurements show good agreement with the values obtained from the Jaeger–Hulme calculations (1936) which are in agreement with the values predicted by Formula 3D–0006 and by the curves in Figs. 6.01 and 6.03.

Formula 3D–0007

[The Davies–Bethe–Maximon Formula: Unscreened Point Nucleus for Extreme-Relativistic Energies]

$$\sigma=\alpha Z^2r_0^2\left[\frac{28}{9}\ln 2k-\frac{28}{9}f(Z)-\frac{218}{27}\right],$$

where $f(Z)=$ Coulomb correction function, which is discussed by Davies, Bethe, and Maximon (1954) and evaluated in Table 6.05.

(1) Conditions of Validity

Table 6.01: B, D.

(2) References

Davies, Bethe, and Maximon (1954), Formula (44).

Formula 3D–0009

[The Davies–Bethe–Maximon Formula: Screened Point Nucleus for Extreme-Relativistic Energies]

$$\sigma=\alpha Z^2r_0^2k^{-3}\int_1^{k-1}[(E_+^2+E_-^2)\Psi_1+\tfrac{2}{3}E_+E_-\Psi_2]\,dE_+,$$

where Ψ_1 and Ψ_2 are given in Formula 3D–1009.

(a) For the case of complete screening such that $\alpha Z^{1/3}k\gg 1$, Davies, Bethe, and Maximon (1954) give the following simplified formula:

$$\sigma=\alpha Z^2r_0^2\left[\frac{28}{9}\ln(183Z^{-1/3})-\frac{28}{9}f(Z)-\frac{2}{27}\right],$$

where $f(Z)$ = Coulomb correction function, which is discussed by Davies, Bethe, and Maximon (1954) and evaluated in Table 6.05.

(1) Conditions of Validity

Table 6.01: D.

(2) References

Davies, Bethe, and Maximon (1954), Formula (45). The general form for Formula 3D-0009 is given by the integral form of Formula 3D-1009.

(3) Notes

a. Formula 3D-0009 has been evaluated by Sørenssen (1965, 1966) for various elements with the Thomas-Fermi-Moliere form factor and the more accurate Hartree-Fock-Slater atomic form factors. Sørenssen's results show that there is less than 4% differences in the cross sections obtained with the different form factors. For accuracies better than 1%, form factors other than those used by Sørenssen are required, particularly for low-Z elements, as pointed out by Knasel (1968). Sørenssen's results for lead ($Z=82$) with the Thomas-Fermi-Moliere form factor are given in Fig. 6.02 and in Table 6.06. For any other value of Z, the cross section may be evaluated from the formula given below in Part b with the scaling function $S(Z, Z_0)$ given in Table 6.07.

b. The cross-section data for lead can be used to evaluate the pair cross section $\sigma(Z, k)$ for any arbitrary atomic number and photon energy within the accuracy that can be obtained with the Thomas-Fermi-Moliere form-factor approximation. This evaluation can be made by the following scaling formula:

$$\sigma(Z, k) = \alpha Z^2 r_0^2 \{[\sigma(Z_0, k_0)/\alpha Z_0^2 r_0^2] - S(Z, Z_0)\},$$

where $\sigma(Z_0, k_0)$ is the pair cross section which is shown for a reference atomic number Z_0 (in this case, $Z_0=82$) and for k_0 equal to $k(Z/Z_0)^{1/3}$, and where the scaling function $S(Z, Z_0)$ is given as

$$S(Z, Z_0) = (28/27)\{\ln (Z/Z_0) + 3[f(Z) - f(Z_0)]\},$$

with $f(Z)$ defined in Table 6.05. Values for the function $S(Z, Z_0)$ for $Z_0=82$, are given in Table 6.07. In the threshold region, there are no calculations which include both screening effects and Coulomb corrections, and therefore the accuracy of the above scaling formula in this region is uncertain.

A scaling formula of the above type was given first by Bethe and Ashkin [Segre, 1960, p. 340, Eq. (126b)]. However, it should be noted that their equation, which has a misprint, should be given as

$$\frac{\Phi_{\text{pair}}(Z, k)}{\bar{\Phi}(Z)} = \frac{\Phi_{\text{pair}}(Z_0, k(Z/Z_0)^{1/3})}{\bar{\Phi}(Z_0)} - \frac{28}{27}\ln\left(\frac{Z}{Z_0}\right).$$

Formula 3D-1000

[The Bethe-Heitler Formula: Unscreened Point Nucleus]

$$\frac{d\sigma}{dE_+} = \alpha Z^2 r_0^2 \frac{p_+ p_-}{k^3}\left\{-\frac{4}{3} - \frac{2E_+E_-(p_+^2+p_-^2)}{p_+^2 p_-^2} + \left(\frac{E_+L_-}{p_-^3} + \frac{E_-L_+}{p_+^3} - \frac{L_+L_-}{p_+p_-}\right) + L\left[\frac{k^2}{p_+^3 p_-^3}(E_+^2E_-^2 + p_+^2p_-^2)\right.\right.$$

$$\left.\left. - \frac{8}{3}\frac{E_+E_-}{p_+p_-} - \frac{k}{2p_+p_-}\left(\frac{E_+E_- - p_-^2}{p_-^3}L_- + \frac{E_+E_- - p_+^2}{p_+^3}L_+ + \frac{2kE_+E_-}{p_+^2p_-^2}\right)\right]\right\},$$

where $L_+ = 2\ln(E_+ + p_+)$, $L_- = 2\ln(E_- + p_-)$, and $L = 2\ln[(E_+E_- + p_+p_- + 1)/k]$.

(1) Conditions of Validity

Table 6.01: A, B, E.

(2) References

Heitler (1954), Formula (8), p. 258.

(3) Notes

a. Hough (1948) has given simplified formulas which approximately reproduce Formula 3D-1000 in the regions where $k \approx 2$ [(Segre, 1960, Formula (117b)] and where $2 \leq k \leq 15$.

b. Formula 3D-1000 gives a symmetric energy distribution between the electron and positron. This result is erroneous particularly in the region where either β_+ or $\beta_- \ll 1$, because the nucleus repels the positron and attracts the electron. The expected asymmetry in the energy distributions for the electron and positron are brought out in the higher-order calculations of Nishina, Tomonaga, and Sakata (1934), which are also discussed by Heitler (1954, p. 259). These latter calculations have been superseded by the more accurate calculations of Øverbø, Mork, and Olsen (1968), whose results are given in Formula 3D-1006 and in Figs. 6.04, 6.05, 6.06, 6.07, and 6.08.

c. Cross-section values derived from Formula 3D-1000 are given by the dashed lines in Figs. 6.04, 6.05, 6.06, 6.07, and 6.08, for photon energies of 1.07, 1.33, 1.79, 2.55, and 3.32 MeV, respectively.

d. The cross-section formula for 3D-1000 which was given originally by Bethe [1934, Eq. (21), Proc. Roy. Soc. (London)], erroneously contains a plus instead of a minus sign before the expression in the last set of square brackets. This error was corrected in the formula given by Heitler [1954, p. 258, Eq. (8)].

Formula 3D–1001

The Bethe–Heitler Formula: Unscreened Point Nucleus for Extreme-Relativistic Energies]

$$\frac{d\sigma}{dE_+} = 4\alpha Z^2 r_0^2 \frac{E_+^2+E_-^2+\frac{2}{3}E_+E_-}{k^3}\left[\ln\left(\frac{2E_+E_-}{k}\right)-\frac{1}{2}\right].$$

(1) Conditions of Validity

Table 6.01: A, B, D, E.

(2) References

Heitler (1954), Formula (9), p. 258.

Formula 3D–1003

[The Bethe–Heitler Formula: Screened Point Nucleus for Extreme-Relativistic Energies]

$$\frac{d\sigma}{dE_+} = \frac{\alpha Z^2 r_0^2}{k^3}\{(E_+^2+E_-^2)[\Phi_1(\gamma)-\tfrac{4}{3}\ln Z]+\tfrac{2}{3}E_+E_-[\Phi_2(\gamma)-\tfrac{4}{3}\ln Z]\},$$

where the screening functions $\Phi_1(\gamma)$ and $\Phi_2(\gamma)$ are defined as

$$\Phi_1(\gamma) = 4\left\{\int_\delta^1 (q-\delta)^2[1-F(q)]^2\frac{dq}{q^3}\right\}+4+\tfrac{4}{3}\ln Z,$$

$$\Phi_2(\gamma) = 4\int_\delta^1\left[q^3-6\delta^2 q\ln\left(\frac{q}{\delta}\right)+3\delta^2 q-4\delta^3\right][1-F(q)]^2\frac{dq}{q^4}+\tfrac{10}{3}+\tfrac{4}{3}\ln Z,$$

with $\gamma = 100k/(E_+E_-Z^{1/3})$ and $\delta = k/(2E_+E_-)$. $F(q)$ = atomic form factor which is defined in Sec. II and which is evaluated for different screening approximations by Motz, Olsen, and Koch (1964, Formula 1A–102).

A. For exponential screening where $F(q) = [1+(111qZ^{-1/3})^2]^{-1}$, Formula 3D–1003 can be written as follows after the proper substitutions have been made in the inverse bremsstrahlung formula given by Schiff (1951), such that the Schiff formula is multiplied by the phase-space ratio p_+dE_+/k^2dk, and E_1 and E_2 are replaced by $-E_+$ and E_-, respectively:

$$\frac{d\sigma}{dE_+} = \frac{2\alpha Z^2 r_0^2}{k^3}\left\{(E_+^2+E_-^2+\tfrac{2}{3}E_+E_-)\left[\ln M(0)+1-\frac{2}{b}\tan^{-1}b\right]\right.$$
$$\left.-E_+\left[\frac{2}{b^2}\ln(1+b^2)+\frac{4(2-b^2)}{3b^3}\tan^{-1}b-\frac{8}{3b^2}+\frac{2}{9}\right]\right\},$$

where $b = 2E_+E_-Z^{1/3}/111k$, and

$$1/M(0) = (k/2E_+E_-)^2+(Z^{1/3}/111)^2$$

B. For complete screening where $\gamma \ll 1$ with the Thomas–Fermi form factor, Formula 3D–1003 can be written as (Bethe, 1934)

$$\frac{d\sigma}{dE_+} = \frac{4\alpha Z^2 r_0^2}{k^3}[(E_+^2+E_-^2+\tfrac{2}{3}E_+E_-)\ln(183Z^{-1/3})+\tfrac{1}{9}E_+E_-].$$

C. For intermediate screening where $0<\gamma<2$ and for the Thomas–Fermi form factor, the screening functions $\Phi_1(\gamma)$ and $\Phi_2(\gamma)$ in Formula 3D–1003 are given (Bethe, 1934; Segre, 1960, p. 262; Koch and Motz, 1959, Fig. 1) in Fig. 6.09.

The following approximate analytical expression for these screening functions is given by Butcher and Messel (1960):

$$\Phi_1(\gamma) = 20.868-3.242G+0.625G^2,$$

$$\Phi_2(\gamma) = 20.209-1.930G+0.086G^2,$$

for $G\leq 1$ where $G=136k/E_+E_-Z^{1/3}=1.36\gamma$, and for $G>1$,

$$\Phi_1(\gamma)=21.12-4.184\ln(G+0.952),$$
$$\Phi_2(\gamma)=\Phi_1(\gamma).$$

D. For intermediate screening where $2<\gamma<15$ with the Thomas–Fermi form factor, Formula 3D–1003 can be written as (Bethe, 1934)

$$\frac{d\sigma}{dE_+}=\frac{4\alpha Z^2r_0^2}{k^3}(E_+^2+E_-^2+\tfrac{2}{3}E_+E_-)\left[\ln\frac{2E_+E_-}{k}-\frac{1}{2}-c(\gamma)\right],$$

where $c(\gamma)$ is evaluated from the curve in Fig. 6.10.

(1) Conditions of Validity

Table 6.01: A, D, E

(2) References

Bethe (1934).
Segre (1960), Formulas (114) and (115).

(3) Notes

a. The differential pair cross section predicted by Formula 3D–1003 for aluminum is given as a function of the positron energy E_+ in Fig. 6.11 for $k=20$.

Formula 3D–1005

[The Wheeler–Lamb Formula: Screened Point Nucleus with Atomic Excitation]

$$\frac{d\sigma}{dE_+}=\alpha Zr_0^2k^{-3}\{(E_+^2+E_-^2)[\Psi_1(\gamma_1)-\tfrac{8}{3}\ln Z]+\tfrac{2}{3}E_+E_-[\Psi_2(\gamma_1)-\tfrac{8}{3}\ln Z]\},$$

where γ_1 is equal to $100k/E_+E_-Z^{2/3}$, and $\Psi_1(\gamma_1)$ and $\Psi_2(\gamma_1)$ are the screening functions given by Wheeler and Lamb (1939, Fig. 1).

A. For extreme-relativistic energies such that $k\gg(\alpha Z^{1/3})^{-1}$, Wheeler and Lamb (1939) obtain the following formula:

$$\frac{d\sigma}{dE_+}=\alpha Zr_0^2k^{-3}[(E_+^2+E_-^2)(29.1-\tfrac{8}{3}\ln Z)+\tfrac{2}{3}E_+E_-(28.4-\tfrac{8}{3}\ln Z)].$$

(1) Conditions of Validity

Table 6.01: A, E.

(2) References

Wheeler and Lamb (1939, 1956), Fig. 1 and Formula (20).

Formula 3D–1006

[The Øverbø–Mork–Olsen Formula: Unscreened Point Nucleus]

$$\frac{d\sigma}{dE_+}=r_0^2\frac{2}{\alpha k^3}\sum_{\kappa_+\kappa_-M}|A_{\kappa_+\kappa_-M}|^2,$$

where

$$A_{\kappa_+\kappa_-M}=f_{\kappa_+\kappa_-}\sum_{L=L_{\min}}^{L_{\max}}(-1)^{(L-L_{\min})/2}\sum_{n=0}^{L}\frac{(L+n)!}{n!(L-n)!}\left(\frac{1}{2k}\right)^n\frac{\Gamma(a)}{(k+p_++p_-)^a}$$
$$\times\left\{[(E_++1)(E_-+1)]^{1/2}\frac{[(\kappa_+-M)(\kappa_--M)]^{1/2}}{[(2\kappa_+-1)(2\kappa_-+1)]^{1/2}}V(l_-Ll_+'M)R_{\kappa_+\kappa_-}{}^{+}\right.$$
$$\left.-[(E_+-1)(E_--1)]^{1/2}\frac{[(\kappa_++M)(\kappa_-+M)]^{1/2}}{[(2\kappa_++1)(2\kappa_--1)]^{1/2}}V(l_-'Ll_+M)R_{\kappa_+\kappa_-}{}^{-}\right\},$$

with

$$f_{\kappa_+\kappa_-}=\frac{(2p_+)^{\gamma_+-1/2}(2p_-)^{\gamma_--1/2}\exp\left[\frac{1}{2}\pi(y_++y_-)\right]\,|\,\Gamma(\gamma_++iy_+)\,|\,\Gamma(\gamma_-+iy_-)\,|}{\Gamma(2\gamma_++1)\Gamma(2\gamma_-+1)},$$

$$V(l_-Ll_+'M)=(2L+1)[(2l_-+1)/(2l_+'+1)]^{1/2}C_{l_-L}(l_+'0;00)C_{l_-L}(l_+'M;M0),$$

and

$$R_{\kappa_+\kappa_-}{}^{\pm}=\mathrm{Im}\{\exp(-i\tfrac{1}{2}\pi)(\gamma_++\gamma_--L-1)[K_+K_-F_2(a;b_+,b_-;c_+,c_-;x_+,x_-)$$
$$\pm K_+K_-{}^*F_2(a;b_+,b_--1;c_+,c_-;x_+,x_-)\mp K_+{}^*K_-F_2(a;b_+-1,b_-;c_+,c_-;x_+,x_-)$$
$$-K_+{}^*K_-{}^*F_2(a;b_+-1,b_--1;c_+,c_-;x_+,x_-)]\},$$

$$y_\pm=Z\alpha\frac{E_\pm}{p_\pm};\qquad \gamma_\pm=[\kappa_\pm{}^2-(Z\alpha)^2]^{1/2};\qquad l_\pm=\begin{cases}\kappa_\pm & \kappa_\pm>0\\ -\kappa_\pm-1 & \kappa_\pm<0\end{cases};\qquad l_\pm'=\begin{cases}\kappa_\pm-1 & \kappa_\pm>0\\ -\kappa_\pm & \kappa_\pm<0\end{cases},$$

$$a=\gamma_++\gamma_--n,\qquad b_\pm=\gamma_\pm+iy_\pm+1,\qquad c_\pm=2\gamma_\pm+1,\qquad K_\pm=(\gamma_\pm+iy_\pm)\exp(i\eta_\pm),$$

and $\eta_\pm$ is defined by

$$\exp(2i\eta_\pm)=-\frac{\kappa_\pm-(y_\pm/E_\pm)}{\gamma_\pm+iy_\pm};\qquad x_\pm=\frac{2p_\pm}{k+p_++p_-}.$$

$C_{l_-L}(l_+'M;M0)$ is the Clebsch–Gordan coefficient and F_2 the hypergeometric function of two variables (Appell function).

(*1*) *Conditions of Validity*

Table 6.01: B.

(*2*) *References*

Øverbø, Mork, and Olsen (1968).

(*3*) *Notes*

a. This formula is evaluated in the energy region $2\leq k\leq 7$ by Øverbø, Mork, and Olsen (1968) in Figs. 6.04, 6.05, 6.06, 6.07 and 6.08, in which comparisons are made with the symmetrical energy distribution predicted by the first Born Bethe–Heitler Formula 3D–1000. These results show that the asymmetries in the energy distributions persist even up to values of $k=6.50$.

b. More data are needed in order to determine the effect of atomic screening on the cross sections predicted by Formula 3D–1006 in the threshold energy region.

Formula 3D–1007

[The Davies–Bethe–Maximon Formula: Unscreened Point Nucleus for Extreme-Relativistic Energies]

$$\frac{d\sigma}{dE_+}=\frac{4\alpha Z^2r_0^2}{k^3}(E_+{}^2+E_-{}^2+\tfrac{2}{3}E_+E_-)\left(\ln\frac{2E_+E_-}{k}-\frac{1}{2}-f(Z)\right),$$

where $f(Z)=$ Coulomb correction function, which is discussed by Davies, Bethe, and Maximon (1954) and evaluated in Table 6.05.

(*1*) *Conditions of Validity*

Table 6.01: B, D, E, F.

(*2*) *References*

Davies, Bethe, and Maximon (1954), Formula (35).

Formula 3D–1009

[The Davies–Bethe–Maximon Formula: Screened Point Nucleus for Extreme-Relativistic Energies]

$$\frac{d\sigma}{dE_+}=\alpha Z^2r_0^2k^{-3}[(E_+{}^2+E_-{}^2)\Psi_1+\tfrac{2}{3}E_+E_-\Psi_2],$$

where

$$\Psi_1=\Phi_1(\gamma)-\tfrac{4}{3}\ln Z-4f(Z),$$

$$\Psi_2=\Phi_2(\gamma)-\tfrac{4}{3}\ln Z-4f(Z),$$

where for Thomas–Fermi screening, $\Phi_1(\gamma)$ and $\Phi_2(\gamma)$ are given in Formula 3D–1003 and in Fig. 6.09 with γ equal to $100k/(E_+E_-Z^{1/3})$, and the Coulomb correction function $f(Z)$ is given in Table 6.05.

For an arbitrary form factor $F(q)$ (Thomas–Fermi or Hartree–Fock), Ψ_1 and Ψ_2 may be written in the following form (Olsen and Maximon, 1959):

$$\Psi_1=6+4\int_0^1\Gamma(\xi)\,d\xi,$$

$$\Psi_2=6+24\int_0^1\xi(1-\xi)\Gamma(\xi)\,d\xi,$$

where

$$\Gamma(\xi)=\ln(1/\delta)-2-f(Z)+\mathfrak{F}(\delta/\xi),$$

$$\mathfrak{F}\left(\frac{\delta}{\xi}\right)=\int_{\delta/\xi}^{\infty}\{[1-F(q)]^2-1\}\,\frac{q^2-(\delta/\xi)^2}{q^3}\,dq,$$

with $F(q)$ = atomic form factor defined in Sec. II, and

$$\delta=k/2E_+E_-,$$

$$\xi=(1+u^2)^{-1},\qquad u=p_+\theta_+.$$

A. For complete screening where $\gamma\ll1$ with the Thomas–Fermi form factor,

$$\mathfrak{F}(\delta/\xi)=\ln(111\gamma/200\xi),\qquad \Gamma=\ln(111Z^{-1/3}/\xi)-2-f(Z).$$

Then, Formula 3D–1009 can be written as

$$d\sigma/dE_+=(4\alpha Z^2r_0^2/k^3)\{(E_+^2+E_-^2+\tfrac{2}{3}E_+E_-)[\ln(183Z^{-1/3})-f(Z)]+\tfrac{1}{9}E_+E_-\}.$$

B. For intermediate screening where $\gamma\gtrsim1$, the function $-\mathfrak{F}(\delta/\xi)$ is evaluated in the following table (Olsen and Maximon, 1959):

$6Z^{1/3}/121\delta$	0.5	1.0	2.0	4.0	8.0	15.0	20.0
$-\mathfrak{F}(\delta/\xi)$	0.0145	0.0490	0.140	0.331	0.676	1.13	1.37

$6Z^{1/3}/121\delta$	25.0	30.0	40.0	50.0	60.0	80.0	100.0	120.0
$-\mathfrak{F}(\delta/\xi)$	1.56	1.73	2.00	2.22	2.39	2.68	2.90	3.08

The screening functions $\Phi_1(\gamma)$ and $\Phi_2(\gamma)$ are evaluated with the Thomas–Fermi form factor in Fig. 6.09.

C. For intermediate screening where $2<\gamma<15$ with the Thomas–Fermi form factor, Formula 3D–1009 can be written as

$$\frac{d\sigma}{dE_+}=\frac{4\alpha Z^2r_0^2}{k^3}(E_+^2+E_-^2+\tfrac{2}{3}E_+E_-)\left[\ln\frac{2E_+E_-}{k}-\frac{1}{2}-c(\gamma)-f(Z)\right],$$

where $c(\gamma)$ is evaluated from the curve in Fig. 6.10 and is discussed by Bethe (1934).

(1) Conditions of Validity

Table 6.01: D, E, F.

(2) References

Davies, Bethe, and Maximon (1954), Formulas (43) and (42).

(3) Notes

a. A comparison of Formula 3D–1009–A with Formula 3D–1003–B shows that the Coulomb correction can be applied to the Born approximation formula for $d\sigma/dE_+$ by the addition of the term

$$-(4\alpha Z^2r_0^2/k^3)(E_+^2+E_-^2+\tfrac{2}{3}E_+E_-)f(Z),$$

as shown by Davies, Bethe, and Maximon (1954), and Olsen (1955).

b. The differential pair cross section predicted by Formula 3D–1009 for aluminum (solid line) and lead (dashed line) is given as a function of the positron energy E_+ in Fig. 6.11 for $k=1000$.

Formula 3D–1010

[The Jost–Luttinger–Slotnick Formula: Unscreened Point Nucleus]

$$\frac{d\sigma}{d\Omega_r} = \frac{\alpha Z^2 r_0^2}{64\pi^4 k}\{I_1+I_2\},$$

where

$$I_1 = \frac{2}{\eta}\left[\left(\frac{37}{9}-\frac{14}{9}\eta^2\right)E-\left(\frac{11}{9}+\frac{4}{3\eta^2}\right)K\right]+\frac{k^2}{2\eta^3}\left[\left(-\frac{73}{9}+\frac{14}{9}\eta^2\right)E+\left(\frac{29}{9}+\frac{10}{3\eta^2}\right)K\right],$$

$$I_2 = (1-k^2/4\eta^2)(4/\eta)K_1,$$

with

$$\eta = \tfrac{1}{2}(k\cos\theta_r),$$

$$K_1 = \int_1^\eta \frac{d\xi}{\xi}K,$$

and K and E are the complete elliptic integrals of the first and second kind, respectively (Abramowitz and Stegun, 1964, p. 589), of argument $(1-1/\eta^2)^{1/2}$ with η replaced by ξ in the integral for K_1.

(1) Conditions of Validity

Table 6.01: A, B, E.

(2) References

Jost, Luttinger, and Slotnick (1950), Formulas (49), (51), (52), and (53).

(3) Notes

a. The angular distribution of the recoil nucleus predicted by Formula 3D–1010 is given by Jost, Luttinger, and Slotnick (1950, Fig. 4) for selected photon energies of 4.08, 6.12, 10.2, and 16.3 MeV.

Formula 3D–1020

[The Borsellino Formula: Unscreened Point Nucleus]

$$\frac{d\sigma}{dP_p} = 16\alpha Z^2 r_0^2 \frac{FP_p}{(k^2-P_p^2)^2},$$

where

$$P_p = |\,\mathbf{p}_+ + \mathbf{p}_-\,|,$$

$$F = \left[F_1+\frac{W^2}{2k^2}(F_1-\Delta)\right]\operatorname{sech}^{-1}\frac{W}{k}-\left(F_2+\frac{W^2}{6k^2}F_3\right)\frac{P_p}{k}$$

$$= F_1\ln(2k/W)-F_2 \quad \text{for} \quad W\ll k,$$

$$F_1 = (2+1/2W^2-1/16W^4)L-(1+1/4W^2)\Delta,$$

$$F_2 = \tfrac{1}{6}(16+21/4W^2-17/32W^4)L-\tfrac{1}{12}(28+17/4W^2)\Delta,$$

$$F_3 = \tfrac{1}{2}(4-1/16W^4)L-\tfrac{1}{2}(2+1/4W^2)\Delta,$$

$$W = (k^2-P_p^2)^{1/2},$$

$$\Delta = (1-1/W^2)^{1/2},$$

$$L = \cosh^{-1}W.$$

A. The cross-section differential with respect to W, which is functionally related to P_p and is equal to the energy of the electron–positron pair in the center-of-momentum system, of the pair $\mathbf{p}_+ + \mathbf{p}_- = 0$ is given by Borsellino [1953, Eq. (7)] as

$$d\sigma/dW = 16\alpha Z^2 r_0^2 F/W^3$$

(1) Conditions of Validity

Table 6.01: A, B, E.

(2) References

Borsellino (1953), Formulas (4) through (9) as corrected by Hart *et al.* (1959, footnote 15).

(3) Notes

a. Examples of the distributions of the pair momentum P_p and the energy W predicted by the above formulas for selected photon energies are given by Borsellino (1953, Figs. 1 and 2).

Formula 3D–1032

[The Jost–Luttinger–Slotnick Formula: Screened Point Nucleus]

$$\frac{d\sigma}{dq}=\frac{\alpha Z^2 r_0^2[1-F(q)]^2}{8\pi^3 k^2 q^3}\,I(q,k),$$

where

$$I(q,k)=(1-\tfrac{1}{2}q^2)J_1+\left(1-q^2-2qk+\frac{4q^4-4}{3qk}\right)\ln[(y)^{1/2}+(y-1)^{1/2}]+\left(3+\frac{2k}{3q}+\frac{2q^2-4}{3qk}\right)[y(y-1)]^{1/2}$$
$$+\left[-\tfrac{1}{2}(4+q^2)+\tfrac{1}{6}k^2\left(-4+\frac{4}{q^2}\right)\right](1+4/q^2)^{-1/2}\ln\left[\frac{(1+4/q^2)^{1/2}-(1-1/y)^{1/2}}{(1+4/q^2)^{1/2}+(1-1/y)^{1/2}}\right],$$

with

$$y=\tfrac{1}{4}(2qk-q^2),\qquad [k-(k^2-4)^{1/2}]\le q\le[k+(k^2-4)^{1/2}],$$
$$J_1=L_2(-x_1)+L_2(-x_2)+\tfrac{1}{6}\pi^2+\tfrac{1}{2}(\ln\lambda)^2+\tfrac{1}{2}(\ln z)^2-(\ln z)(\ln 2qk),$$

where $L_2(x)$ designates Euler's dilogarithm or the Spence function (Grobner and Hofreiter, 1961, p. 71, Part 2; and Motz, Olsen, and Koch, 1964, Table XIII), and

$$x_1=(z\lambda)^{-1},\qquad x_2=\lambda/z,$$
$$\lambda=\tfrac{1}{4}[q+(q^2+4)^{1/2}]^2,$$
$$z=[(y-1)^{1/2}+y^{1/2}]^2.$$

(a) For $q\ll k$ or $y\approx qk/2$,

$$I(q,k)\approx(1-\tfrac{1}{2}q^2)J_1+\tfrac{1}{3}[1-4y-(2/3y)]\ln z+\tfrac{1}{3}[y^2(1-1/y)^{1/2}]\{11-\tfrac{13}{3}(1-1/y)-2[1-(1/y)]^2\}.$$

If in addition $q\ll 1$,

$$[1-(q^2/2)]J_1\approx-2L_2(1/z)-(\ln z)(\ln 4y)+\tfrac{1}{6}\pi^2+\tfrac{1}{2}(\ln z)^2.$$

(b) For $k\gg 1$ and $qk\approx 2$, Suh and Bethe [1959, Formula (6)] have shown that $I(q,k)$ in the above cross-section formula can be expressed as

$$I(q,k)=32\pi^3k^2q^2\left\{\frac{2}{3}\left(1-\frac{2}{kq}\right)^{1/2}\left(\frac{7}{6}+\frac{25}{6kq}-\frac{2}{(kq)^2}\right)-\left(\frac{2}{kq}-\frac{1-\ln(2kq)}{(kq)^2}+\frac{4}{3(kq)^3}\right)\ln\left[\frac{1+(1-2/kq)^{1/2}}{1-(1-2/kq)^{1/2}}\right]\right.$$
$$\left.-\frac{2}{(kq)^2}\left[L_2\left(\frac{1+(1-2/kq)^{1/2}}{2}\right)-L_2\left(\frac{1-(1-2/kq)^{1/2}}{2}\right)\right]\right\}.$$

(c) For k, $qk\gg 1$ and $q\ll k$, Suh and Bethe [1959, Formula (12)] have shown that $I(q,k)$ in the above cross-section formula can be expressed as

$$I(q,k)=\frac{16\pi^3k^2q^3}{3\xi^2}\left\{1+\frac{(2\xi-1)}{\xi^{1/2}(\xi+2)^{1/2}}\ln[1+\xi+\xi^{1/2}(\xi+2)^{1/2}]\right\}$$

where

$$\xi=(m_r/m_0)T_R.$$

(d) For pair production in the field of a nucleus where $m_r \gg 1$ and $\xi = q^2/2$, Bethe (1934) has shown that

$$I(q,k) = \frac{64\pi^3 k^2 q^2}{3}\left\{\frac{\ln\left[\rho^{1/2}+(\rho+1)^{1/2}\right]}{\rho^{1/2}(\rho+1)^{1/2}} + \frac{1}{q^2}\left(1 - \frac{\ln\left[\rho^{1/2}+(\rho+1)^{1/2}\right]}{\rho^{1/2}(\rho+1)^{1/2}}\right)\right\}$$

where $\rho = q^2/4$.

(1) Conditions of Validity

Table 6.01: A, E.

(2) References

Jost, Luttinger, and Slotnick (1950), Formulas (39) and (43) as corrected by Borsellino (1953, Footnote).

(3) Notes

a. Examples of the momentum distribution predicted by Formula 3D–1032 are given by Jost, Luttinger, and Slotnick (1950, Fig. 3).

b. The relative dependence of $d\sigma/dq$ on q is given by Bethe (1934, Formulas 65, 66, and 69) as

$$\begin{aligned}(d\sigma/dq) &= (a/q)\left[(q-q_{\min})/q\right]^2 && \text{for } q \approx q_{\min}\\ &= (b/q)\left[1-F(q)\right]^2 && \text{for } q_{\min} \ll q \ll 1\\ &= (c/q^3)(\ln q + d) && \text{for } q \gg 1,\end{aligned}$$

where a, b, c, and d are constants and $q_{\min}$ is the minimum momentum transfer.

Formula 3D–1229

[Exact Polarization Formula with Dependence on ($\mathbf{P}_c$, ζ_+): Screened Point Nucleus for Extreme-Relativistic Energies]

$$\frac{d\sigma}{dE_+}(\mathbf{P}_c, \zeta_+) = \tilde{C}\left[\tilde{F}^0 + \mathbf{P}_c \cdot \zeta_+ \tilde{F}^{\zeta+}\right],$$

where $\tilde{C}$, $\tilde{F}^0$, and $\tilde{F}^{\zeta+}$ are given in Part B of Table 6.08, and $\mathbf{P}_c$, and ζ_+ are defined in Sec. II.

(1) Conditions of Validity

Table 6.01: D, E.

(2) References

Olsen and Maximon (1959), Formula (10.8).

Formula 3D–2000

[The Sauter–Gluckstern–Hull Formula: Unscreened Point Nucleus]

$$\begin{aligned}\frac{d^2\sigma}{dE_+ d\Omega_+} = \alpha Z^2 r_0^2 \frac{p_+ p_-}{4\pi k^3}\Bigg\{&-\frac{4\sin^2\theta_+(2E_+^2+1)}{p_+^2 D_+^4} + \frac{(5E_+^2 - 2E_-E_+ + 3)}{p_+^2 D_+^2} + \frac{(p_+^2 - k^2)}{D^2 D_+^2} + \frac{2E_-}{p_+^2 D_+}\\ &+ \frac{L}{p_- p_+}\left[\frac{2E_+\sin^2\theta_+(3k + p_+^2 E_-)}{p_+^2 D_+^4} + \frac{k(E_+^2 - E_+E_- - 1)}{p_+^2 D_+} + \frac{2E_+^2(E_+^2+E_-^2) - (7E_+^2 + 3E_-E_+ + E_-^2) + 1}{p_+^2 D_+^2}\right]\\ &- \left(\frac{\epsilon^D}{p_- D}\right)\left[\frac{2}{D_+^2} - \frac{3k}{D_+} - \frac{k(p_+^2 - k^2)}{D^2 D_+}\right] - \frac{2\epsilon_-}{p_- D_+}\Bigg\},\end{aligned}$$

where

$$D = |\,\mathbf{p}_+ - \mathbf{k}\,| = (p_+^2 + k^2 - 2p_+ k\cos\theta_+)^{1/2},$$

$$L = \ln\left(\frac{E_+E_- + 1 + p_+p_-}{E_+E_- + 1 - p_+p_-}\right), \qquad \epsilon_- = \ln\left(\frac{E_- + p_-}{E_- - p_-}\right),$$

$$\epsilon^D = \ln\left(\frac{D + p_-}{D - p_-}\right), \qquad D_+ = E_+ - p_+\cos\theta_+.$$

(1) Conditions of Validity

Table 6.01: A, B, E.

(2) References

Gluckstern and Hull (1953), Formula 17.1.
Sauter (1934), Formula 11.

(3) Notes

a. The cross sections predicted by Formula 3D–2000 are given in Fig. 6.12 for various values of k, θ_+, and E_+.

b. Formula 3D–2000 is a factor of 2 larger than Formula (17.1) given by Gluckstern and Hull (1953). This factor was erroneously omitted in Formula (17.1) in the process of averaging and summing over the initial and final polarization states of the particles.

c. Olsen [1963, Formula (A2)] has shown that for high energies and for equipartition of energy ($E_+=E_-=k/2$), the average value of θ_+ can be calculated in terms of $u=E_+\theta_+$ from the equation

$$\langle u\rangle=\frac{15\pi}{32}\frac{\ln(k/2)-(2/5)}{\ln(k/2)-(1/2)}\left(1-\frac{12}{5k}\right).$$

d. For large angles and high energies, Hough [1948, Formula (2)] has given a simplified formula for this cross section. Calculations based on the Hough Formula have been made for various cases by Miller (1954) in order to predict the energy and angular distribution of pair electrons produced by a bremsstrahlung photon beam.

Formula 3D–2003

[The Schiff Formula: Screened Point Nucleus for Extreme-Relativistic Energies]

$$\frac{d^2\sigma}{dE_+d\Omega_+}=\frac{2\alpha Z^2r_0^2}{\pi}\frac{E_+^2}{k^3}\left\{-\frac{(E_+-E_-)^2}{(u^2+1)^2}-\frac{16u^2E_+E_-}{(u^2+1)^4}+\left[\frac{(E_+^2+E_-^2)}{(u^2+1)^2}+\frac{4u^2E_+E_-}{(u^2+1)^4}\right]\ln M(u)\right\}$$

where $u=E_+\theta_+$ and

$$\frac{1}{M(u)}=\left(\frac{k}{2E_+E_-}\right)^2+\left(\frac{Z^{1/3}}{111(u^2+1)}\right)^2.$$

(1) Conditions of Validity

Table 6.01: A, D, E, F, H.

(2) References

Schiff (1951), Formula 1.

(3) Notes

a. Formula 3D–2003 is obtained from the inverse bremsstrahlung cross-section formula after the proper substitutions as given in Formula 3D–1003–A.

Formula 3D–2007

[The Olsen–Maximon Formula: Unscreened Point Nucleus for Extreme-Relativistic Energies]

$$d^2\sigma/dE_+d\Omega_+=[d^2\sigma/dE_+d\Omega_+]_{2009},$$

where

$$[d^2\sigma/dE_+d\Omega_+]_{2009}=\text{formula 3D–2009},$$

with

$$\mathfrak{F}(\delta/\xi)=0,$$

and

$$\Gamma=\ln(1/\delta)-2-f(Z).$$

(1) Conditions of Validity

Table 6.01: B, D, E, F.

(2) References

Olsen and Maximon (1959), Formula (10.4) with $\mathfrak{F}(\delta/\xi)=0$.

Formula 3D–2009

[The Olsen–Maximon Formula: Screened Point Nucleus for Extreme-Relativistic Energies]

$$d^2\sigma/dE_+d\Omega_+=(2\alpha Z^2r_0^2E_+^2\xi^2/\pi k^3)[(E_+^2+E_-^2)(3+2\Gamma)+2E_-E_+(1+4u^2\xi^2\Gamma)],$$

where ξ, Γ, and u are defined in Formula 3D–1009.

(1) Conditions of Validity

Table 6.01: D, E, F.

(2) References

Olsen and Maximon (1959), Formula (10.4).

(3) Notes

a. The cross sections predicted by Formula 3D–2009 for $Z=82$ are shown by the dashed lines in Fig. 6.12 for photon energies of k equal to 1000 and 100.

Formula 3D–2011

[The Olsen Formula: Unscreened Point Nucleus for Extreme-Relativistic Energies]

$$\frac{d^2\sigma}{dE_+dw}=\frac{4\alpha Z^2r_0^2}{k^3}\frac{w}{(1+w^2)^2}\left\{2\left(\ln\frac{2E_+E_-}{k}-\frac{E_+}{k}\ln\frac{E_+}{k}-\frac{E_-}{k}\ln\frac{E_-}{k}-\frac{E_+^2+E_-^2}{2k^2}\right)\left(E_+^2+E_-^2+4E_+E_-\frac{w^2}{(1+w^2)^2}\right)\right.$$

$$\left.+8E_+E_-\frac{w^2}{(1+w^2)^2}\left(\frac{E_+E_-(E_+-E_-)}{k^3}\ln\frac{E_-}{E_+}-\frac{E_+^2+E_-^2}{2k^2}-1\right)-\frac{\gamma}{\sinh\gamma}\left[(E_+^2+E_-^2)(1+w^2)+4\left(\frac{E_+E_-}{k}\right)^2\right]\right\},$$

where

$$w=(E_+E_-/k)\theta, \qquad dw=(E_+E_-/k)\,d\Omega/\theta d\Phi,$$

θ = opening angle between electron and positron as defined in Sec. II,

$$d\Omega=\theta d\theta d\Phi,$$

and γ is given by the equation

$$\cosh(\gamma/2)=k[4E_+E_-/(1+w^2)]^{-1/2}.$$

(1) Conditions of Validity

Table 6.01: A, B, D, E, F.

(2) References

Olsen (1963), Formula (7).

(3) Notes

a. Integration of this formula over w with E_+ fixed gives Formula 3D–1001. Similarly, integration over E_+ with γ fixed gives the high-energy, small-angle approximation of the Borsellino Formula 3D–1020, $d\sigma/dW$, as shown by Olsen (1963). For high energies and small angles, $W=\gamma/2$.

Formula 3D–2013

[The Olsen Formula: Screened Point Nucleus for Extreme-Relativistic Energies]

$$\frac{d^2\sigma}{dE_+dw}=\frac{4\alpha Z^2r_0^2}{k^3}\frac{w}{(1+w^2)^2}\left\{2\left(\mu-\frac{E_+}{k}\ln\frac{E_+}{k}-\frac{E_-}{k}\ln\frac{E_-}{k}-\frac{E_+^2+E_-^2}{2k^2}\right)\left[E_+^2+E_-^2+4E_+E_-\frac{w^2}{(1+w^2)^2}\right]\right.$$

$$\left.+8E_+E_-\frac{w^2}{(1+w^2)^2}\left[\frac{E_+E_-(E_+-E_-)}{k^3}\ln\frac{E_-}{E_+}-\frac{E_+^2+E_-^2}{2k^2}-1\right]-\frac{\gamma}{\sinh\gamma}\left[(E_+^2+E_-^2)(1+w^2)+4\left(\frac{E_+E_-}{k}\right)^2\right]\right\},$$

where

$$w=(E_+E_-/k)\theta, \qquad dw=(E_+E_-/k)\,d\Omega/\theta d\Phi,$$

θ = opening angle between electron and positron as defined in Sec. II,

$$d\Omega=\theta d\theta d\Phi,$$

γ is given by the equation

$$\cosh(\gamma/2)=k[4E_+E_-/(1+w^2)]^{-1/2},$$

and

$$\mu=\ln(2E_+E_-/k)+\mathfrak{F}(\delta/\zeta),$$

where the screening function, $\mathfrak{F}(\delta/\zeta)$ [with $\delta=k/2E_+E_-$ and in this case $\zeta=(1+w^2)^{-1}$] is defined and evaluated in Formula 3D–2009 including Parts (a) and (b) for the cases of complete and partial screening.

A. For the case where the electron and positron share equal energy (equipartition of energy) such that $E_+=E_-=k/2$, the formula becomes

$$\frac{d^2\sigma}{dE_+dw}=\frac{4\alpha Z^2r_0^2}{k^3}\frac{w}{(1+w^2)^2}\left\{(\mu+\ln 2)\left[1+\frac{2w^2}{(1+w^2)^2}\right]-\left[\frac{1}{4}+\frac{3w^2}{(1+w^2)^2}\right]-\frac{\gamma}{4\sinh\gamma}(3+2w^2)\right\}.$$

(1) Conditions of Validity

Table 6.01: A, D, E, F.

(2) References

Olsen (1963), Formulas (21) and (22).

(3) Notes

a. Theoretical distributions predicted by Formula 3D–2013(a) show good agreement (Olsen, 1963) with available experimental results for photon energies of 6, 50, and 100 MeV.

b. The mean opening angle between the electron and positron for equipartition of energy is given in terms of w as

$$\langle w\rangle=\frac{15\pi}{32}\frac{\ln k-41/30}{\ln(k/2)-\frac{1}{2}}\left(1-\frac{24}{5k}\right),$$

for no screening with a large-angle correction, and as

$$\langle w\rangle=\frac{15\pi}{32}\frac{\ln(888Z^{1/3})-3/5}{\ln(182Z^{-1/3})-1/24}$$

for complete screening. The most probable value of k for a measured opening angle θ is given as

$$k=3.2/\theta.$$

Experimental data and multiple scattering corrections pertaining to these results are also discussed by Olsen (1963). For further experimental applications, see the works of Khubeis *et al.* (1964); Bertin *et al.* (1966); Castor *et al.* (1966); and Avgerat *et al.* (1966).

Formula 3D–2132

[Born Polarization Formula with Dependence on (P_L, e): Screened Point Nucleus]

$$(d^2\sigma/dE_+d\Omega_+)(P_L,\mathbf{e})=2\bar{C}[\bar{F}^0+P_L\bar{F}^e(1-2(\hat{\mathbf{u}}\cdot\mathbf{e})^2)],$$

where $\bar{C}$, $\bar{F}^0$, and $\bar{F}^e$ are given in Part A of Table 6.09, $\hat{\mathbf{u}}$ is given in Part A of Table 6.10, and P_L and $\mathbf{e}$ are defined in Sec. II.

(1) Conditions of Validity

Table 6.01: A, E.

(2) References

May (1951) and Gluckstern and Hull (1953) for $\bar{F}^e$.

(3) Notes

a. Exponential screening is assumed in the above results, such that $V(r)=-(\alpha Z/r)\exp-(r/\beta)$ with $\beta=111Z^{-1/3}$. The case of no screening is obtained by choosing $\beta^{-1}=0$.

b. For the case of no screening ($\beta^{-1}=0$ in Table 6.09) and for the special cases where $(\hat{\mathbf{u}}\cdot\mathbf{e})=1$ and $(\hat{\mathbf{u}}\cdot\mathbf{e})=0$, Formula 3D–2132 is given by $d\sigma_{II}$ [Eq. (17.2)] and $d\sigma_{III}$ [Eq. (17.3)], respectively, in Gluckstern and Hull (1953). It should be noted that the latter Eq. (17.3) contains a misprint in which the addition sign (+) before the expression in the curly bracket should be replaced by a multiplication sign (×). For these cases, it follows that Formula 3D–2000 which is averaged over the initial photon polarization states, is equal to $\frac{1}{2}(d\sigma_{II}+d\sigma_{III})$

c. The dependence of the cross-section ratio for linearly polarized photons in a plane perpendicular ($\hat{\mathbf{u}}\cdot\mathbf{e}=0$) and parallel ($\hat{\mathbf{u}}\cdot\mathbf{e}=1$) to the emission plane ($\mathbf{k}$, $\mathbf{p}_+$) on the positron energy is given in Fig. 6.13 for values of k equal to 10 and 50, and for different values of $k\theta_+$. The cross sections were evaluated for the case of no screening from Eqs. (17.2) and (17.3) in Gluckstern and Hull (1953).

Formula 3D–2139

[Exact Polarization Formula with Dependence on (P_L, e): Screened Point Nucleus for Extreme-Relativistic Energies]

$(d^2\sigma/dE_+d\Omega_+)(P_L, \mathrm{e}) =$ Formula 3D–2132, with $\bar{C}$, $\bar{F}^0$, and $\bar{F}_e$ given in Part B of Table 6.09.

(1) Conditions of Validity

Table 6.01: D, E, F.

(2) References

Olsen and Maximon (1959), Formula (4.10); Olsen (1968).

Formula 3D–2242

[Born Polarization Formulas with Dependence on ($\mathbf{P}_c$, $\boldsymbol{\zeta}_+$), ($\mathbf{P}_c$, $\zeta_+{}^{\parallel}$), and ($\mathbf{P}_c$, $\zeta_+{}^{\perp}$): Screened Point Nucleus]

A.

$$(d^2\sigma/dE_+d\Omega_+)(\mathbf{P}_c, \boldsymbol{\zeta}_+) = \bar{C}[\bar{F}^0 + (\mathbf{P}_c\cdot\hat{\mathbf{k}})(\mathbf{F}^{\boldsymbol{\zeta}_+,\boldsymbol{\xi}}\cdot\boldsymbol{\zeta}_+)],$$

where

$$\mathbf{F}^{\boldsymbol{\zeta}_+,\boldsymbol{\xi}} = \bar{F}^{\boldsymbol{\zeta}_+\parallel}\hat{\mathbf{p}}_+ + \bar{F}^{\boldsymbol{\zeta}_+\perp}\hat{\mathbf{u}};$$

$$\hat{\mathbf{p}}_+ = \mathbf{p}_+/|\,\mathbf{p}_+\,|, \qquad \hat{\mathbf{u}} = \mathbf{u}/u;$$

$\bar{C}$, $\bar{F}^0$, $\bar{F}^{\boldsymbol{\zeta}_+\parallel}$, and $\bar{F}^{\boldsymbol{\zeta}_+\perp}$ are given in Part A of Table 6.09; and $\mathbf{P}_c$, $\hat{\mathbf{k}}$, $\boldsymbol{\zeta}_+$, $\mathbf{p}_+$, and $\mathbf{u}$ are defined in Sec. II.

B.

$$(d^2\sigma/dE_+d\Omega_+)(\mathbf{P}_c, \zeta_+{}^{\parallel}) = \bar{C}[\bar{F}^0 + (\mathbf{P}_c\cdot\hat{\mathbf{k}})(\boldsymbol{\zeta}_+\cdot\hat{\mathbf{p}}_+)\bar{F}^{\boldsymbol{\zeta}_+\parallel}],$$

where $\bar{C}$, $\bar{F}^0$, and $\bar{F}^{\boldsymbol{\zeta}_+\parallel}$ are given in Part A of Table 6.09; $\mathbf{P}_c$, $\hat{\mathbf{k}}$, and $\boldsymbol{\zeta}_+$ are defined in Sec. II; and $\zeta_+{}^{\parallel} = \boldsymbol{\zeta}_+\cdot\hat{\mathbf{p}}_+$ with $\hat{\mathbf{p}}_+$ given in A above.

C.

$$(d^2\sigma/dE_+d\Omega_+)(\mathbf{P}_c, \zeta_+{}^{\perp}) = \bar{C}[\bar{F}^0 + (\mathbf{P}_c\cdot\hat{\mathbf{k}})(\boldsymbol{\zeta}_+\cdot\hat{\mathbf{u}}\bar{F}^{\boldsymbol{\zeta}_+\perp}],$$

where $\bar{C}$, $\bar{F}^0$, and $\bar{F}^{\boldsymbol{\zeta}_+\perp}$ are given in Part A of Table 6.09; $\mathbf{P}_c$, $\hat{\mathbf{k}}$, $\boldsymbol{\zeta}_+$, and $\mathbf{u}$ are defined in Sec. II; and $\zeta_+{}^{\perp} = \boldsymbol{\zeta}_+\cdot\hat{\mathbf{u}}$.

(1) Conditions of Validity

Table 6.01: A, E.

(2) References

McVoy (1957) for $\bar{F}^{\boldsymbol{\zeta}_+\parallel}$.

Böbel (1957) and Fronsdal and Überall (1958) for $\bar{F}^{\boldsymbol{\zeta}_+\parallel}$ and $\bar{F}^{\boldsymbol{\zeta}_+\perp}$.

(3) Notes

As in Formula 3D–2132.

Formula 3D–2249

[Exact Polarization Formulas with Dependence on ($\mathbf{P}_c$, $\boldsymbol{\zeta}_+$), ($\mathbf{P}_c$, $\zeta_+{}^{\parallel}$), and ($\mathbf{P}_c$, $\zeta_+{}^{\perp}$): Screened Point Nucleus for Extreme-Relativistic Energies]

A.

$$(d^2\sigma/dE_+d\Omega_+)(\mathbf{P}_c, \boldsymbol{\zeta}_+) = \text{Formula 3D–2242–A},$$

with $\bar{C}$, $\bar{F}^0$, $\bar{F}^{\boldsymbol{\zeta}_+\parallel}$, and $\bar{F}^{\boldsymbol{\zeta}_+\perp}$ given in Part B of Table 6.09.

B.

$$(d^2\sigma/dE_+d\Omega_+)(\mathbf{P}_c, \zeta_+{}^{\parallel}) = \text{Formula 3D–2242–B},$$

with $\bar{C}$, $\bar{F}^0$, and $\bar{F}^{\zeta_+\parallel}$ given in Part B of Table 6.09.

C.

$$(d^3\sigma/dE_+d\Omega_+)(\mathbf{P}_e, \zeta_+{}^\perp) = \text{Formula 3D–2242–C},$$

with $\bar{C}$, $\bar{F}^0$, and $\bar{F}^{\zeta_+\perp}$ given in Part B of Table 6.09.

(1) Conditions of Validity

Table 6.01: D, E, F.

(2) References

Olsen and Maximon (1959), Formula (4.10).
Olsen (1968).

Formula 3D–3000

[The Bethe–Heitler Formula: Unscreened Point Nucleus]

$$\frac{d^3\sigma}{dE_+d\Omega_+d\Omega_-} = -\alpha Z^2\left(\frac{r_0}{2\pi}\right)^2\frac{p_+p_-}{k^3q^4}\left[\frac{p_+{}^2\sin^2\theta_+}{D_+{}^2}(4E_-{}^2-q^2)+\frac{p_-{}^2\sin^2\theta_-}{D_-{}^2}(4E_+{}^2-q^2)\right.$$
$$\left.+\frac{2p_+p_-\sin\theta_+\sin\theta_-\cos(\Phi_+-\Phi_-)}{D_-D_+}(4E_+E_-+q^2-2k^2)-2k^2\frac{(p_+{}^2\sin^2\theta_++p_-{}^2\sin^2\theta_-)}{(E_--p_-\cos\theta_-)(E_+-p_+\cos\theta_+)}\right],$$

where q^2 is defined by Eq. (3.03) in Sec. III, and $D_\pm = E_\pm - p_\pm\cos\theta_\pm$.

(1) Conditions of Validity

Table 6.01: A, B, E.

(2) References

Heitler (1954), Formula (6), p. 257.

(3) Notes

a. This formula is symmetrical as between the positron and the electron, as a consequence of the Born approximation which is proportional to the square of the charge. However, the symmetry is destroyed by higher-order calculations, as shown for example by the results of Nishina, Tomonaga, and Sakata (1934), and by the more accurate results of Øverbø, Mork, and Olsen (see Formula 3D–1006).

b. The azimuthal angle Φ_+ given by Heitler (1954) above, is equal to the difference of the azimuthal angles Φ_+ and Φ_- defined in Sec. II.

c. The dependence of the cross section predicted by Formula 3D–3000 on the positron energy is evaluated for the geometries shown in Fig. 6.14, and is shown in Fig. 6.15(a), (b), (c), and (d) for photon energies of $k=10$ and 3.

Formula 3D–3001

[The Bethe–Heitler Formula: Screened Point Nucleus]

$$d^3\sigma/dE_+d\Omega_+d\Omega_- = [d^3\sigma/dE_+d\Omega_+d\Omega_-]_{3000}[1-F(q)]^2,$$

where

$$[d^3\sigma/dE_+d\Omega_+d\Omega_-]_{3000} = \text{Formula 3D–3000}$$

and $F(q)$ is explicitly defined in Formula 3D–1003.

A. For high energies ($k, E_+, E_- \gg 1$) and small angles [$\theta_+ = O(1/E_+)$, $\theta_- = O(1/E_-)$], Olsen and Maximon (1959) have shown that this formula is given by the following expression [see Olsen (1963), Formula (1)]:

$$d^3\sigma/dE_+d\Omega_+d\Omega_- = (2\alpha Z^2r_0{}^2E_+{}^2E_-{}^2/\pi^2k^3q^4)[(E_+{}^2+E_-{}^2)\xi\eta q_\perp{}^2+2E_+E_-(\xi-\eta)^2][1-F(q)]^2,$$

where

$$\xi=(1+u^2)^{-1}, \qquad \eta=(1+v^2)^{-1},$$

$$u=E_+\theta_+, \qquad v=E_-\theta_-,$$

$$\mathbf{q}=\mathbf{k}-\mathbf{p}_+-\mathbf{p}_-,$$

$$\mathbf{q}_\perp=-\mathbf{u}-\mathbf{v}=\text{component of } \mathbf{q} \text{ perpendicular to } \mathbf{k}.$$

(1) Conditions of Validity

Table 6.01: A, E.

(2) References

Heitler (1954), Formula (6), p. 257, multiplied by the screening factor $[1-F(q)]^2$.

Formula 3D–3004

[The Bjorken–Drell–Frautschi Formula: Finite Nucleus for Extreme-Relativistic Energies]

$$\frac{d^3\sigma}{dE_+d\Omega_+d\Omega_-}=-\frac{\alpha Z^2r_0^2}{(2\pi)^2}\frac{E_+E_-}{k^3\bar{q}^4}\frac{2k^2}{(\bar{k}\cdot\bar{p}_-)(\bar{k}\cdot\bar{p}_+)}\left[1-(\bar{k}\cdot\bar{p}_--\bar{p}_+\cdot\bar{p}_-)\frac{m_0}{E_-m_r}\right]^{-1}$$

$$\times\left[G_E^2(S_1+S_2)-\frac{\bar{q}^2}{4(m_r/m_0)^2}\frac{G_M^2}{Z^2}(S_1-S_2)\right],$$

where

$$S_1=(\bar{k}\cdot\bar{p}_+)^2+(\bar{k}\cdot\bar{p}_-)^2+\bar{q}^2(\bar{p}_+\cdot\bar{p}_-),$$

$$S_2=(\bar{q}^2/R^2)[(\bar{p}_+\cdot R)^2+(\bar{p}_-\cdot R)^2],$$

R=four vector with components $\{\mathbf{p}_r, T_r\}$ for nucleus initially at rest,

$\bar{k}$, $\bar{p}_+$, $\bar{p}_-$, $\bar{q}$ are four-component vectors defined in Sec. II, such that

$$\bar{k}\cdot\bar{p}_\pm=\mathbf{k}\cdot\mathbf{p}_\pm-kE_\pm,$$

$$\bar{p}_+\cdot\bar{p}_-=\mathbf{p}_+\cdot\mathbf{p}_--E_+E_-,$$

$$\bar{q}^2=q^2-q_0^2,$$

$$q_0=k-E_+-E_-,$$

and G_E and G_M are the nuclear form factors defined in Sec. II.

A. For small angles such that $\theta_+\ll 1$, recoil effects are negligible and Formula 3D–3004 can be written as

$$d^3\sigma/dE_+d\Omega_+d\Omega_-=[d^3\sigma/dE_+d\Omega_+d\Omega_-]_{3000}G_E^2(\bar{q}),$$

where

$$[d^3\sigma/dE_+d\Omega_+d\Omega_-]_{3000}=\text{Formula 3D–3000.}$$

B. For the special case of symmetric pairs with $E_+=E_-$ and $\theta_+=\theta_-$, this small-angle formula can be written as

$$\frac{d^3\sigma}{dE_+d\Omega_+d\Omega_-}=\frac{4\alpha Z^2r_0^2}{\pi^2}\frac{G_E^2}{k^3\theta_+^6}.$$

C. For nearly symmetric pairs such that $E_+-E_-\ll E_+$, $\theta_+-\theta_-\ll\theta_+$, and $q_\perp=|\mathbf{u}+\mathbf{v}|\ll 1$ (with $\mathbf{u}$ and $\mathbf{v}$ equal to the perpendicular components of $\mathbf{p}_+$ and $\mathbf{p}_-$, respectively), the small-angle formula becomes

$$\frac{d^3\sigma}{dE_+d\Omega_+d\Omega_-}=\frac{\alpha Z^2r_0^2}{\pi^2}\frac{G_E}{k\theta_+^4\bar{q}^4}(q_\perp^2+E_+^2\theta_+^4).$$

D. In the above formulas, m_0 has been neglected compared to k, E_+, and m_r. When m_0 is not neglected, the cross

section may be written in the form

$$\frac{d^3\sigma}{dE_+ d\Omega_+ d\Omega_-} = \frac{\alpha Z^2 r_0^2}{(2\pi)^2} \frac{p_+ p_-}{k^3 \bar{q}^4} \frac{2k^2}{(\bar{p}_+ \cdot \bar{k})(\bar{p}_- \cdot \bar{k})} \frac{m_r p_-^2/m_0}{E_- \bar{p}_- \cdot \bar{p}_r + E_r} [G_E^2(S_1+S_2) - [(G_M/Z)\tfrac{1}{2}\bar{q}(m_0/m_r)]^2(S_1-S_2)],$$

with

$$S_1 = (\bar{p}_+ \cdot \bar{k})^2 + (\bar{p}_- \cdot \bar{k})^2 + \bar{q}^2(\bar{p}_+ \cdot \bar{p}_-) - \left[2\bar{p}_+ \cdot \bar{p}_- + (1-\tfrac{1}{2}\bar{q}^2)\left(\frac{\bar{p}_+ \cdot \bar{k}}{\bar{p}_- \cdot \bar{k}} + \frac{\bar{p}_- \cdot \bar{k}}{\bar{p}_+ \cdot \bar{k}}\right)\right],$$

$$S_2 = (\bar{q}^2/R^2)[(\bar{p}_+ \cdot \bar{R})^2 + (\bar{p}_- \cdot \bar{R})^2] + [(\bar{p}_+ \cdot \bar{k})(\bar{p}_- \cdot \bar{k})]^{-1}$$
$$\times \{2(\bar{p}_+ \cdot \bar{p}_-)(\bar{p}_+ \cdot \bar{k})(\bar{p}_- \cdot \bar{k}) + (2/R^2)[(\bar{p}_+ \cdot \bar{k})(\bar{p}_+ \cdot R) - (\bar{p}_- \cdot \bar{k})(\bar{p}_- \cdot R)]^2 + [(\bar{p}_+ \cdot \bar{k})^2 + (\bar{p}_- \cdot \bar{k})^2]\}$$

(1) Conditions of Validity

Table 6.01: A, B, D, G.

(2) References

Bjorken *et al.* (1958): The Bjorken–Drell–Frautschi Formula 3D–3004 is obtained from the more convenient form given in Blumenthal *et al.* (1966).

Olsen (1968), Formulas (10.16), (10.17), and (10.18) on p. 175 for small-angle approximation.

Drell (1952), Berg and Lindner (1958), and Sarkar (1964) for the formula in Part D above. This formula in the form given was obtained by S. Waldenström (unpublished).

(3) Notes

a. The formula in Part D reduces to the Bjorken–Drell–Frautschi Formula 3D–3004 for $\theta_\pm \gg 1/k$ and $m_0 \ll m_r$, k, E_+, and to the Bethe–Heitler Formula 3D–3000 for $q^2 \ll k m_r/m_0$.

b. Some experimental tests of Formula 3D–3004 are given in Blumenthal *et al.* (1966), Ashbury *et al.* (1967) and Eisenhandler *et al.* (1967).

c. Second-Born corrections and hard-photon radiative corrections to wide-angle, high-energy pair production are given in Brodsky and Gillespie (1968), and Huld (1967), respectively.

Formula 3D–3007

[The Bethe–Maximon Formula: Unscreened Point Nucleus for Extreme-Relativistic Energies]

$$\frac{d^3\sigma}{dE_+ d\Omega_+ d\Omega_-} = \frac{2\alpha^3 Z^4 r_0^2}{(\sinh \pi\alpha Z)^2} \frac{E_+^2 E_-^2}{k^3} \{q^{-4} V^2(x)[k^2(u^2+v^2)\xi\eta - 2E_+E_-(u^2\xi^2+v^2\eta^2) + 2(E_+^2+E_-^2)uv\xi\eta\cos\Phi]$$
$$+ \alpha^2 Z^2 W^2(x)\xi^2\eta^2[k^2(1-(u^2+v^2)\xi\eta) - 2E_+E_-(u^2\xi^2+v^2\eta^2) - 2(E^2+E_-^2)uv\xi\eta\cos\Phi]\},$$

where

$$u = p_+\theta_+, \qquad v = p_-\theta_-,$$
$$\xi = 1/(1+u^2), \qquad \eta = 1/(1+v^2),$$
$$x = 1 - q^2\xi\eta,$$

and V and W are hypergeometric functions (Abramowitz and Stegun, 1964, p. 556), such that

$$V(x) = F(-i\alpha Z, i\alpha Z; 1; x),$$
$$W(x) = (\alpha Z)^{-2}(dV/dx).$$

The functions V and W have been evaluated by Olsen and Maximon (1964, Fig. 3) for copper and lead.

(1) Conditions of Validity

Table 6.01: B, D, E, F.

(2) References

Bethe and Maximon (1954), Formula (7.14).

Formula 3D–3009

[The Bethe–Maximon Formula: Screened Point Nucleus for Extreme-Relativistic Energies]

$$d^3\sigma/dE_+d\Omega_+d\Omega_- = [d^3\sigma/dE_+d\Omega_+d\Omega_-]_{3007}[1-F(q)]^2,$$

where

$$[d^3\sigma/dE_+d\Omega_+d\Omega_-]_{3007} = \text{Formula 3D–3007.}$$

(1) Conditions of Validity

Table 6.01: D, E, F.

(2) References

Bethe and Maximon (1954), Formula (7.14).
Davies, Bethe, and Maximon (1954), p. 790 and Formula (27).

Formula 3D–3119

[Exact Polarization Formula with Dependence on ζ_+: Screened Point Nucleus for Extreme-Relativistic Energies]

$$(d^3\sigma/dE_+d\Omega_+d\Omega_-)(\boldsymbol{\zeta}_+) = 2C[F^0+\mathbf{F}^{\xi}_+\cdot\boldsymbol{\zeta}_+],$$

where C, F^0, and $\mathbf{F}^{\xi}_+$ are given in Part B of Table 6.10, and $\boldsymbol{\zeta}_+$ is defined in Sec. II.

(1) Conditions of Validity

Table 6.01: D, E, F.

(2) References

Olsen and Maximon (1959), Formula (4.10).
Olsen (1968).

Formula 3D–3132

[Born Polarization Formula with Dependence on $(P_L, \mathbf{e})$: Screened Point Nucleus]

$$(d^3\sigma/dE_+d\Omega_+d\Omega_-)(P_L, \mathbf{e}) = 4C[F^0+P_LF^e],$$

where C, F^0, and F^e are given in Part A of Table 6.10, and P_L is defined in Sec. II.

(1) Conditions of Validity

Table 6.01: A, E.

(2) References

May (1951), Gluckstern *et al.* (1951), Gluckstern and Hull (1953), Bobel (1957), Claesson (1957), McVoy (1957), Fronsdal and Überall (1958), and Banerjee (1958).

Formula 3D–3139

[Exact Polarization Formula with Dependence on $(P_L, \mathbf{e})$: Screened Point Nucleus for Extreme-Relativistic Energies]

$$(d^3\sigma/dE_+d\Omega_+d\Omega_-)(P_L, \mathbf{e}) = 4C[F^0+P_LF^e],$$

where C, F^0, and F^e are given in Part B of Table 6.10, and P_L is defined in Sec. II.

(1) *Conditions of Validity*

Table 6.01: D, E, F.

(2) *References*

As in Formula 3D–3119, Maximon and Olsen (1962), for coplanar case.

(3) *Notes*

a. Experimental agreement with the theoretical results predicted by Maximon and Olsen (1962) is obtained by Barbiellini *et al.* (1967).

Formula 3D–3149

[Exact Polarization Formula with Dependence on $\mathbf{P}_c$: Screened Point Nucleus for Extreme-Relativistic Energies]

$$(d^3\sigma/dE_+d\Omega_+d\Omega_-)(\mathbf{P}_c)=4C[F^0+\mathbf{P}_c\cdot\mathbf{F}^\xi],$$

where C, F^0, and $\mathbf{F}^\xi$ are given in Part B of Table 6.10, and $\mathbf{P}_c$ is defined in Sec. II.

(1) *Conditions of Validity*

Table 6.01: D, E, F.

(2) *References*

As in Formula 3D–3119.

Formula 3D–3229

[Exact Polarization Formula with Dependence on (P_L, e, ζ_+): Screened Point Nucleus for Extreme-Relativistic Energies]

$$(d^3\sigma/dE_+d\Omega_+d\Omega_-)(P_L,\mathrm{e},\zeta_+)=2C[F^0+\mathbf{F}^{\zeta_+}\cdot\zeta_++P_L\mathbf{F}^{\zeta_+,e}\cdot\zeta_+],$$

where C, F^0, $\mathbf{F}^{\zeta_+}$, and $\mathbf{F}^{\zeta_+,e}$ are given in Part B of Table 6.10, and P_L is defined in Sec. II.

(1) *Conditions of Validity*

Table 6.01: D, E, F.

(2) *References*

As in Formula 3D–3119.

Formula 3D–3249

[Exact Polarization Formula with Dependence on ($\mathbf{P}_c$, ζ_+): Screened Point Nucleus for Extreme-Relativistic Energies]

$$(d^3\sigma/dE_+d\Omega_+d\Omega_-)(\mathbf{P}_c,\zeta_+)=2C[F^0+\mathbf{P}_c\cdot\mathbf{F}^\xi+\mathbf{F}^{\zeta_+}\cdot\zeta_++P_c(\mathbf{F}^{\zeta_+,\xi}\cdot\zeta_+)],$$

where C, F^0, $\mathbf{F}^\xi$, $\mathbf{F}^{\zeta_+}$, and $\mathbf{F}^{\zeta_+,\xi}$ are given in Part B of Table 6.10, and $\mathbf{P}_c$, $\boldsymbol{\xi}$, and ζ_+ are defined in Sec. II.

(1) *Conditions of Validity*

Table 6.01: D, E, F.

(2) *References*

As in Formula 3D–3119.

Table 6.04. Total pair cross sections evaluated by Maximon (1968) from the Racah Formula 3D–0000.

Photon energy (MeV)	$\sigma/\alpha Z^2 r_0^2$
1.03	9.79×10^{-7}
1.05	3.99×10^{-5}
1.10	7.61×10^{-4}
1.15	2.98×10^{-3}
1.20	7.13×10^{-3}
1.25	1.34×10^{-2}
1.30	2.19×10^{-2}
1.40	4.51×10^{-2}
1.50	7.58×10^{-2}
1.75	1.78×10^{-1}
2.00	3.03×10^{-1}
2.50	5.84×10^{-1}
3.00	8.72×10^{-1}
4.00	1.42
5.00	1.90
6.00	2.33
8.00	3.05
10.0	3.65
15.0	4.78
20.0	5.62
30.0	6.83
40.0	7.70
50.0	8.38
60.0	8.94
80.0	9.82
100.	10.5
150.	11.8
200.	12.7
300.	13.9
400.	14.8
500.	15.5
600.	16.1
800.	17.0
1 000.	17.7
10 000.	24.8
100 000.	32.0

Table 6.05. Evaluation of the Coulomb correction function, $f(Z)$.[a]

Z	$f(Z)$
1	6.40×10^{-5}
4	1.02×10^{-3}
6	2.30×10^{-3}
13	1.07×10^{-2}
20	2.52×10^{-2}
26	4.20×10^{-2}
29	5.19×10^{-2}
32	6.27×10^{-2}
36	7.84×10^{-2}
42	1.05×10^{-1}
47	1.29×10^{-1}
50	1.44×10^{-1}
56	1.76×10^{-1}
73	2.76×10^{-1}
78	3.07×10^{-1}
82	3.32×10^{-1}
92	3.95×10^{-1}

[a] As shown by Eqs. (36) and (38) in Davies, Bethe, and Maximon (1954), $f(Z)=(\alpha Z)^2[\{1+(\alpha Z)^2\}^{-1}+0.202-0.0369\,(\alpha Z)^2+0.0083\,(\alpha Z)^4-0.002\,(\alpha Z)^6]$.

Table 6.06. Total pair cross sections evaluated by Sørenssen (1965) from Formula 3D–0009 with the Thomas–Fermi–Moliére screening approximation for $Z=82$.

Photon energy (MeV)	$\sigma/\alpha Z^2 r_0^2$
10.0	2.67
12.6	3.25
15.9	3.83
20.0	4.41
25.1	4.98
31.6	5.54
39.8	6.07
50.1	6.58
63.1	7.05
79.4	7.49
100	7.89
126	8.25
200	8.86
316	9.33
631	9.82
1.00×10^3	10.0
3.98×10^3	10.4
1.00×10^4	10.5
1.00×10^5	10.5

TABLE 6.07. Evaluation of the scaling function $S(Z, Z_0)$[a] for $Z_0=82$.

Z	$S(Z, Z_0)$
1	−5.60
4	−4.16
6	−3.74
13	−2.91
20	−2.42
26	−2.09
29	−1.95
32	−1.81
36	−1.64
42	−1.40
47	−1.21
50	−1.20
56	−0.880
73	−0.295
78	−0.130
82	0
92	+0.316

[a] As shown in the Notes of Formula 3D-0009, this function is defined as $S(Z, Z_0) = (28/27)[\ln (Z/Z_0) + 3\{f(Z) - f(Z_0)\}]$.

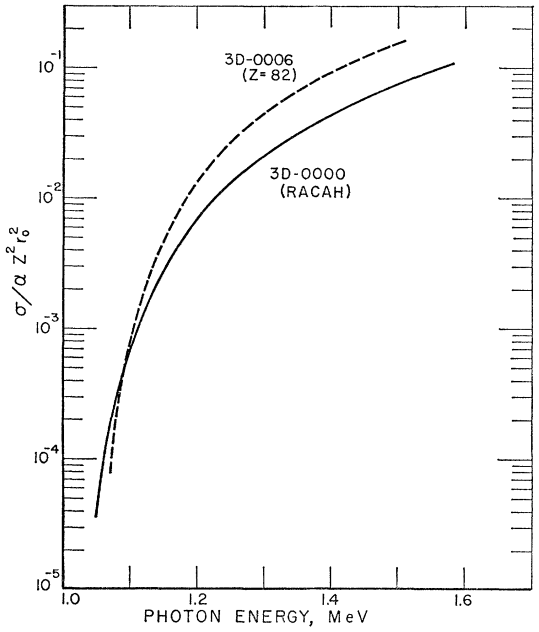

FIG. 6.01. Dependence of the total pair cross section σ (divided by the factor $\alpha Z^2 r_0^2$) on photon energies in the threshold region. The solid line was evaluated by Maximon (1968) from the Born approximation calculations of Racah in Formula 3D-0000, and the dashed line is predicted for $Z=82$ from the exact calculations of Øverbø, Mork, and Olsen, in Formula 3D-0006. Note that the photon energy is given in megaelectron-volt units and is equal to $0.511k$.

TABLE 6.08. Polarization coefficients in the formulas for $d\sigma/dE_+$.

$$\tilde{C} = \alpha Z^2 r_0^2 (1/4k^3)^{a}$$

A. Born approximation results: Not available

B. Exact results for extreme-relativistic energies for Formula 3D-1229 (Olsen and Maximon, 1959):

$$\tilde{F}^0 = (E_+^2 + E_-^2)\Psi_1 + \tfrac{2}{3}E_+E_-\Psi_2$$

$$\tilde{F}^{\zeta}{}_+ = k(E_+ - E_-)\Psi_1 + \tfrac{2}{3}kE_-\Psi_2$$

$$\tilde{\mathbf{F}}^{\zeta}{}_+ = \tilde{F}^{\zeta}{}_+\boldsymbol{\zeta}_+$$

where Ψ_1 and Ψ_2 are the screening functions given in Formula 3D-1009.

[a] This coefficient is the same for Parts A and B.

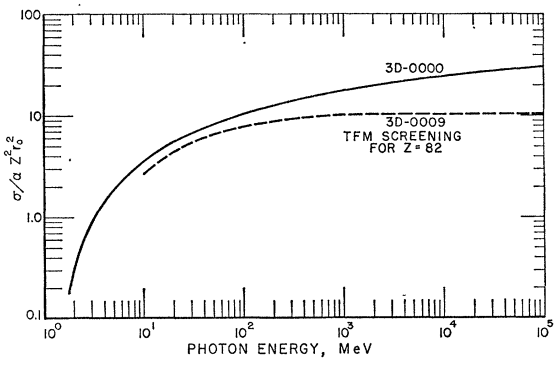

FIG. 6.02. Dependence of the total pair cross section σ (divided by the factor $\alpha Z^2 r_0^2$) on photon energy. The solid line was evaluated by Maximon (1968) from the Born approximation calculations of Racah in Formula 3D-0000, and the dashed line was evaluated by Sørenssen (1965, 1966) with Thomas–Fermi–Moliere screening from the exact calculations of Davies, Bethe, and Maximon (1954) in Formula 3D-0009. Note that the photon energy is given in megaelectron-volt units and is equal to $0.511k$.

TABLE 6.09. Polarization coefficients in the formulas for $d^2\sigma/dE_+d\Omega_+$.

$$\bar{C}=(\alpha Z^2r_0^2/2\pi)\,(p_+/k^3)\,^{a}$$

A. Born approximation results for Formulas 3D–2132 and 3D–2242[b]:

$$\bar{F}^i=-\tfrac{1}{2}A_i[(2p_-/c^2)\,(c-2g^2)\,C_1{}^i+(2p_-g/c)\,C_{11}{}^i$$
$$+(2p_-/d)\,\{(b/c^2)\,(cC_2{}^i-bC_1{}^i)-(1/a)\,(aC_3{}^i-bC_4{}^i)\}$$
$$+(L_1/c^{5/2})[-gcC_2{}^i+\{3gb-2(E_-+D_+)c\}C_1{}^i]$$
$$+(L_1/c^{3/2})[cC_{22}{}^i-bC_{11}{}^i]-(L_2/a^{3/2})\,2(E_-+D_+)\,C_4{}^i$$
$$+(L_2/a^{1/2})\,C_{33}{}^i-C_5{}^iL_3]$$

$$a=4(2kD_++p_-{}^2)$$

$$b=2\beta^{-2}(E_-+D_+)+4D_+[kD_+-(E_+E_-+1)]$$

$$c=(2E_+D_++\beta^{-2})^2-4(D_+{}^2+\beta^{-2})$$

$$d=(2kD_++\beta^{-2})^2+4\beta^{-2}p_-{}^2$$

$$g=\beta^{-2}+2(E_+D_+-1)$$

$$\beta=111Z^{-1/3}$$

$$L_1=2\ln[\{2D_+(E_+E_-+1)+\beta^{-2}E_-+p_-c^{1/2}\}d^{-1/2}]$$

$$L_2=2\ln[\{\beta^{-2}+(\tfrac{1}{2}a^{1/2}+p_-)^2\}d^{-1/2}],\qquad L_3=2\ln(E_-+p_-)$$

Other quantities, such as D_+ and u, that also appear in coefficients below are given in Part A of Table 6.10.

Coefficients in $\bar{F}^i$:

(1) $\bar{F}^0$

$$A_0=1,\ C_1{}^0=4E_+{}^2+\beta^{-2},\ C_{11}{}^0=1$$

$$C_2{}^0=(2/D_+)\,(-4E_+E_--k^2D_+{}^2-\tfrac{1}{2}\beta^{-4})+\beta^{-2}C_{22}{}^0$$

$$C_{22}{}^0=-(2/D_+)\,(p_+{}^2+E_-{}^2+kD_++\beta^{-2})$$

$$C_3{}^0=(4E_-{}^2/D_+{}^2)+\beta^2C_{33}{}^0,\qquad C_{33}{}^0=(1/D_+{}^2)\,(1-2kD_+)$$

$$C_4{}^0=-(2k^2/D_+),\qquad C_5{}^0=-(1/D_+)$$

(2) $\bar{F}^e$

$$A_e=1\qquad C_1{}^e=-C_1{}^0\qquad C_{11}{}^e=-1$$

$$C_2{}^e=-2D_+\{k^2+[4E_+{}^2(E_+E_-+1-kD_+)/u^2]\}$$
$$+\beta^{-2}(C_{22}{}^e+C_{22}{}^0)-C_2{}^0-[\beta^{-4}(E_-+D_+)/u^2]$$

$$C_{22}{}^e=2\{[\tfrac{1}{2}(4E_+{}^2+g+\beta^{-2})\,(E_-+D_+)/u^2]$$
$$-E_--k^2D_+{}^{-1}\}-C_{22}{}^0$$

$$C_3{}^e=-4k^2+[\tfrac{1}{2}a(4E_+{}^2+\beta^{-2})/u^2]-C_3{}^0,$$
$$C_{33}{}^e=(\tfrac{1}{2}a/u^2)-C_{33}{}^0$$

$$C_4{}^e=0,\qquad C_5{}^e=[(E_-+D_+)/u^2]-C_5{}^0$$

(3) $\bar{F}^{\zeta_+\|}$

$$A^{\|}=k/p_+,\qquad C_1{}^{\|}=4E_+(E_+-D_+)-\beta^{-2},\qquad C_{11}{}^{\|}=-1$$

$$C_2{}^{\|}=(2/D_+)[-4E_+E_--2(E_+-E_-)\,D_++kE_+D_+{}^2]+\beta^{-2}C_{22}{}^{\|}$$

$$C_{22}{}^{\|}=(2E_+/D_+)\,(E_+-E_--D_+)$$

$$C_3{}^{\|}=(4E_-/D_+{}^2)\,(E_-+D_+)+\beta^2C_{33}{}^{\|},$$

$$C_{33}{}^{\|}=(1/D_+{}^2)\,(1-2E_+D_+)$$

$$C_4=-2E_+k/D_+,\qquad C_5=0$$

(4) $\bar{F}^{\zeta_+\perp}$

$$A_\perp=k/u^2,\qquad C_1{}^\perp=2u^2+g(p_+{}^2+E_+{}^2-E_+D_+),$$

$$C_{11}{}^\perp=p_+{}^2+E_+{}^2-E_+D_+$$

$$C_2{}^\perp=(2/D_+)[4E_+E_--2D_+(2E_+{}^2E_--E_++E_-)$$
$$-D_+{}^2(2E_+{}^2-E_+E_-+1-kD_+)]+\beta^{-2}C_{22}{}^\perp$$

$$C_{22}{}^\perp=-(2/D_+)\,(u^2+E_+E_--E_-D_+)$$

$$C_3{}^\perp=(1/D_+{}^2)[-4E_-{}^2+4E_-D_+(E_+E_--1)$$
$$+2D_+{}^2(1-E_-{}^2+2E_+E_-)]+\beta^{-2}C_{33}{}^\perp$$

$$C_{33}{}^\perp=(1/D_+{}^2)\,(u^2+E_+D_+-D_+{}^2),$$

$$C_4{}^\perp=(2/D_+)\,(E_+E_-+1-kD_+),\qquad C_5{}^\perp=0$$

B. Exact results for extreme-relativistic energies for Formulas 3D–2139 and 3D–2249 (Olsen and Maximon 1959):

$$\bar{F}^0=2E_+[(E_+{}^2+E_-{}^2)\,(3+2\Gamma)+2E_+E_-(1+4u^2\xi^2\Gamma)]$$

$$\bar{F}^e=-16E_+{}^2E_-u^2\xi^2\Gamma$$

$$\bar{F}^{\zeta_+\|}=2E_+[(E_+{}^2-E_-{}^2)\,(3+2\Gamma)+2kE_-(1+4u^2\xi^2\Gamma)]$$

$$\bar{F}^{\zeta_+\perp}=8E_+E_-k\xi(1-2\xi)\,u\Gamma$$

where

$$u=p_+\theta_+$$

$$\xi=(1+u^2)^{-1}$$

$$\Gamma=\ln(2E_+E_-/k)-2-f(Z)+\mathfrak{F}(k/2E_+E_-\xi),$$

as given in Formula 3D–1009

[a] This coefficient is the same for Parts A and B.

[b] May (1951) and Gluckstern and Hull (1953) for $\bar{F}^e$; McVoy, (1957, 1958) for $\bar{F}^{\zeta_+\|}$; and Böbel (1957) and Fronsdal and Überall (1958) for $\bar{F}^{\zeta_+\|}$ and $\bar{F}^{\zeta_+\perp}$.

TABLE 6.10. Polarization coefficients in the formulas for $d^5\sigma/dE_+d\Omega_+d\Omega_-$.

$$C=\tfrac{1}{2}[\alpha Z^2r_0^2/(2\pi)^2](p_+p_-/k^3)[1-F(q)]^2/q^4$$ [a]

A. Born approximation results for Formula 3D–3132[b]:

$$F^0=(k^2/D_+D_-)(\mathbf{u}+\mathbf{v})^2+\tfrac{1}{2}q^2[(\mathbf{u}/D_+)-(\mathbf{v}/D_-)]^2$$
$$-\tfrac{1}{2}[(2E_+\mathbf{v}/D_-)+(2E_-\mathbf{u}/D_+)]^2$$
$$F^e=-\tfrac{1}{2}q^2\{[(\mathbf{u}/D_+)-(\mathbf{v}/D_-)]^2-2\,|\,[(\mathbf{u}/D_+)-(\mathbf{v}/D_-)]\cdot\mathbf{e}\,|^2\}$$
$$+\tfrac{1}{2}\{[(2E_+\mathbf{v}/D_-)+(2E_-\mathbf{u}/D_+)]^2$$
$$-2\,|\,[(2E_+\mathbf{v}/D_-)+(2E_-\mathbf{u}/D_+)]\cdot\mathbf{e}\,|^2\}$$
$$\mathbf{F}^{\zeta_\pm,\xi}=\boldsymbol{\xi}\cdot\mathbf{k}([\mathbf{E}_\pm\hat{\mathbf{p}}_\pm\mathbf{p}_\pm\cdot(\hat{\mathbf{k}}-\boldsymbol{\beta}_\pm)-\hat{\mathbf{p}}_\pm\times(\mathbf{p}_\pm\times\hat{\mathbf{k}})]$$
$$\times\tfrac{1}{2}\{[(2E_+/D_-)-(2E_-/D_+)]^2-q^2[(1/D_+)-(1/D_-)]^2\}$$
$$\mp[E_\pm\hat{\mathbf{p}}_\pm\mathbf{q}\cdot(\hat{\mathbf{p}}_\pm-\hat{\mathbf{k}}\beta_\pm)-\hat{\mathbf{p}}_\pm\times(\hat{\mathbf{p}}_\pm\times\mathbf{q})]D_\mp^{-1}$$
$$\times\{[(2E_+/D_-)-(2E_-/D_+)]-[(D_+/D_-)-(D_-/D_+)]$$
$$\pm\mathbf{p}_\pm(\mathbf{u}+\mathbf{v})^2D_\mp^{-1}(D_+^{-1}-D_-^{-1}))$$

where

$D_\pm=E_\pm-p_\pm\cos\theta_\pm$

$\hat{\mathbf{u}}=\mathbf{u}/u$

$\mathbf{u}=\mathbf{p}_+-\hat{\mathbf{k}}(\mathbf{p}_+\cdot\hat{\mathbf{k}})=$component of $\mathbf{p}_+$ perpendicular to $\mathbf{k}$

$u=p_+\sin\theta_+$

$\mathbf{v}=\mathbf{p}_--\hat{\mathbf{k}}(\mathbf{p}_-\cdot\hat{\mathbf{k}})=$component of $\mathbf{p}_-$ perpendicular to $\mathbf{k}$

$v=p_-\sin\theta_-$

$\boldsymbol{\beta}_\pm=\mathbf{p}_\pm/E_\pm$

$\mathbf{q}=\hat{\mathbf{k}}-\mathbf{p}_+-\mathbf{p}_-$

B. Exact results[c] for extreme-relativistic energies for Formulas 3D–3119, 3D–3139, 3D–3229, 3D–3149, and 3D–3249 (Olsen and Maximon, 1959; Olsen, 1968):

$$F^0=\tfrac{1}{2}k^2\,|\,\mathbf{J}\,|^2-E_+E_-\,|\,\mathbf{J}_\perp\,|^2$$
$$F^e=E_+E_-\{|\,\mathbf{J}_\perp\,|^2-|\,\mathbf{J}\cdot\mathbf{e}\,|^2-|\,\mathbf{J}\cdot\mathbf{e}^*\,|^2\}$$
$$\mathbf{F}^\xi=-\tfrac{1}{2}(E_+^2+E_-^2)[i\mathbf{J}\times\mathbf{J}^*]$$
$$\mathbf{F}^{\xi_\pm}=\mp\tfrac{1}{2}kE_\mp[i\mathbf{J}\times\mathbf{J}^*]_\perp\mp\tfrac{1}{2}E_+^2-E_-^2)[i\mathbf{J}\times\mathbf{J}^*]_z$$
$$\mathbf{F}^{\zeta_\pm,e}=\pm\tfrac{1}{2}kE_+\{[i\mathbf{J}\times\mathbf{J}^*]_\perp-2\mathrm{Re}([i\mathbf{J}\times\mathbf{J}^*]\cdot\mathbf{e}^*\mathbf{e})\}$$
$$\mathbf{F}^{\zeta_\pm,\xi}=\tfrac{1}{2}k\{(E_\pm-E_\mp)\,|\,\mathbf{J}\,|^2+2E_\mp\,|\,\mathbf{J}_z\,|^2\}\boldsymbol{\xi}\mp kE_\mp\mathrm{Re}\,(\mathbf{J}^*\cdot\boldsymbol{\xi}\mathbf{J}_\perp)$$
$$F_{ij}^{\zeta_+,\zeta_-}=-k\,\mathrm{Re}\,[E_-(\mathbf{J}_\perp)_i(\mathbf{J}_z^*)_j-E_-(\mathbf{J}_\perp)_j(\mathbf{J}_z^*)_i]$$
$$F_{ij}^{\zeta_+,\zeta_-,e}=E_+E_-(\delta_{ij}-2\hat{\mathbf{k}}_i\hat{\mathbf{k}}_j)\{|\,\mathbf{J}_\perp\,|^2-|\,\mathbf{J}\cdot\mathbf{e}\,|^2-|\,\mathbf{J}\cdot\mathbf{e}^*\,|^2\}$$
$$+\tfrac{1}{2}k^2\,|\,J\,|^2\{\delta_{ij}-\hat{\mathbf{k}}_i\hat{\mathbf{k}}_j)-2\,\mathrm{Re}\,(e_ie_j^*)\}$$
$$+kE_+\,\mathrm{Re}\,([(\mathbf{J}_\perp)_j-(\mathbf{J}_z)_j]\{(\mathbf{J}_\perp^*)_i$$
$$-\mathbf{J}^*\cdot\mathbf{e}^*\mathbf{e}_i-\mathbf{J}^*\cdot\mathbf{e}\mathbf{e}_i^*\})+kE_-\,\mathrm{Re}\,([(\mathbf{J})_i-(\mathbf{J}_z)_i]$$
$$\times\{(\mathbf{J}_\perp^*)_j-\mathbf{J}^*\cdot\mathbf{e}\mathbf{e}_j-\mathbf{J}^*\cdot\mathbf{e}\mathbf{e}_j^*\})$$
$$F_{ij}^{\zeta_+,\zeta_-,\xi}=-\tfrac{1}{2}(E_+^2+E_-^2)(\delta_{ij}-2\hat{\mathbf{k}}_i\hat{\mathbf{k}}_j)\boldsymbol{\xi}\cdot[iJ\times J^*]$$

where

$$J_z=\hat{\mathbf{k}}2[(2E_+E_-)^{1/2}/V(1)]$$
$$\times\{(\xi-\eta)V(x)+i\alpha Z\xi\eta^2(\xi+\eta-1)W(x)\}$$
$$\mathbf{J}_\perp=[2(2E_+E_-)^{1/2}/V(1)]$$
$$\times\{(\mathbf{u}\xi+\mathbf{v}\eta)V(x)+i\alpha Z\xi\eta q^2(\mathbf{u}\xi-\mathbf{v}\eta)W(x)\}$$

$$\mathbf{J}=\mathbf{J}_\perp+\mathbf{J}_z$$

$\mathbf{u}=\mathbf{p}_+-\hat{\mathbf{k}}(\mathbf{p}_+\cdot\hat{\mathbf{k}})$ $\quad$ $\mathbf{v}=\mathbf{p}_--\hat{\mathbf{k}}(\mathbf{p}_-\cdot\hat{\mathbf{k}})$

$u=p_+\theta_+$ $\quad$ $v=p_-\theta_-$

$\xi=(1+u^2)^{-1}$, $\quad$ $\eta=(1+v^2)^{-1}$

$V(1)=[\sinh(\pi\alpha Z)]/(\pi\alpha Z)$

[a] This coefficient is the same for Parts A and B. $\mathbf{F}^\xi$, $\mathbf{F}^{\zeta_\pm}$, $\mathbf{F}^{\zeta_\pm,e}$, $F_{ij}^{\zeta_+,\zeta_-}$, $F_{ij}^{\zeta_+,\zeta_-,e}$, and $F_{ij}^{\zeta_+,\zeta_-,\xi}$ are not available in Born calculations.

[b] Wick (1951); May (1951); Gluckstern *et al.* (1951); Gluckstern and Hull (1953); Böbel (1957); Claesson (1957); McVoy (1957); Fronsdal and Überall (1958); and Banerjee (1958).

[c] These coefficients for the exact calculations are obtained from Eq. (4.10) in Olsen and Maximon (1959). Some errors in the signs in that equation have been corrected here.

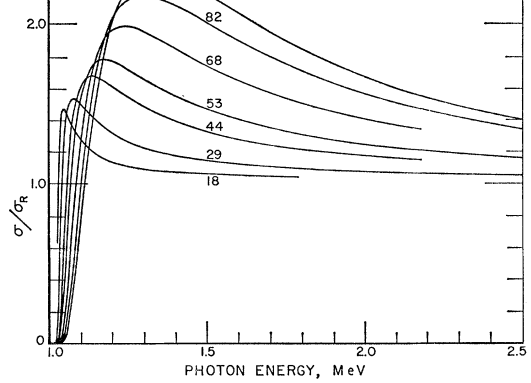

FIG. 6.03. Dependence of the total pair cross section for the unscreened point nucleus on the photon energies in the threshold region and on the atomic numbers which are attached to the various curves. The exact cross section σ is obtained from the calculations of Øverbø, Mork, and Olsen (1968), and the Born cross section σ_R is given by the Racah Formula 3D–0000 which is evaluated in Table 6.04 and in Figs. 6.01 and 6.02. Note that the photon energy is given in megaelectron-volt units and is equal to $0.511k$.

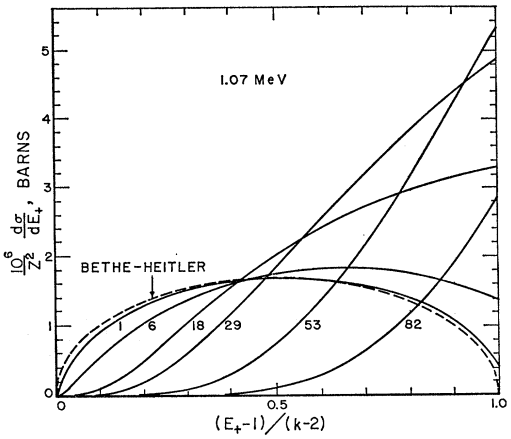

FIG. 6.04. Dependence of the differential pair cross section $d\sigma/dE_+$ on the positron energy E_+ for an incident photon energy of 1.07 MeV. The dashed curve gives the Born approximation cross sections for an unscreened point nucleus derived from the Bethe–Heitler Formula 3D-1000. The solid curves give the exact cross sections for an unscreened point nucleus derived from the Øverbø–Mork–Olsen Formula 3D–1006 for the various atomic numbers attached to each curve.

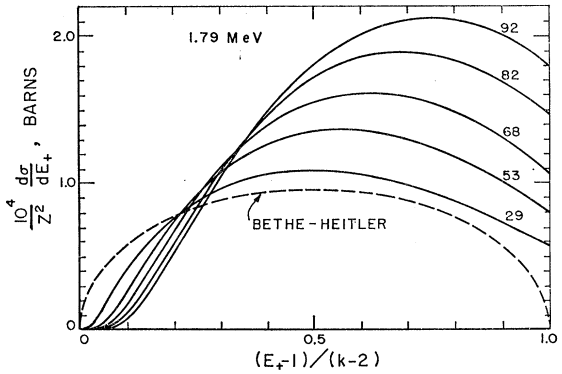

FIG. 6.06. Dependence of the differential pair cross section $d\sigma/dE_+$ on the positron energy E_+ for an incident photon energy of 1.79 MeV. The meaning of the different curves is explained in Fig. 6.04.

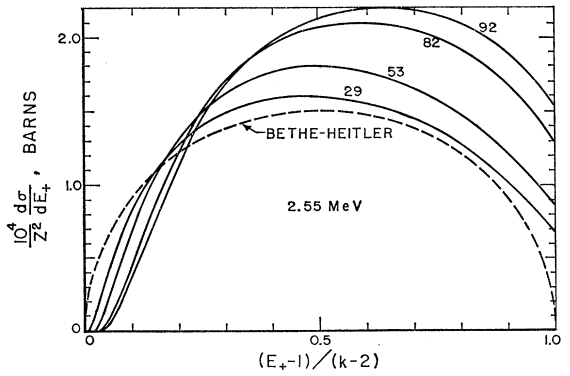

FIG. 6.07. Dependence of the differential pair cross section $d\sigma/dE_+$ on the positron energy E_+ for an incident photon energy of 2.55 MeV. The meaning of the different curves is explained in Fig. 6.04.

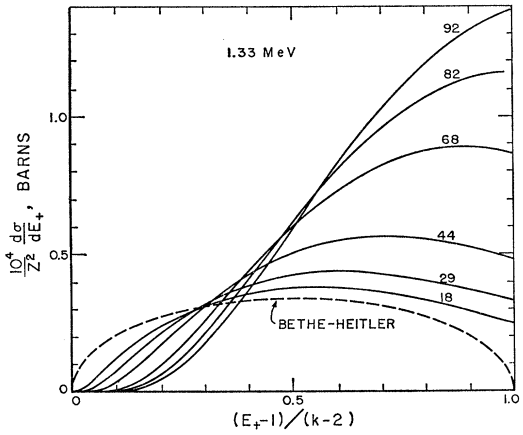

FIG. 6.05. Dependence of the differential pair cross section $d\sigma/dE_+$ on the positron energy E_+ for an incident photon energy of 1.33 MeV. The meaning of the different curves is explained in Fig. 6.04.

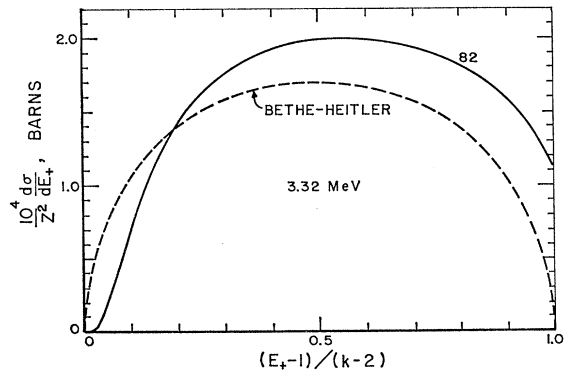

FIG. 6.08. Dependence of the differential pair cross section $d\sigma/dE_+$ on the positron energy E_+ for an incident photon energy of 3.32 MeV. The meaning of the different curves is explained in Fig. 6.04.

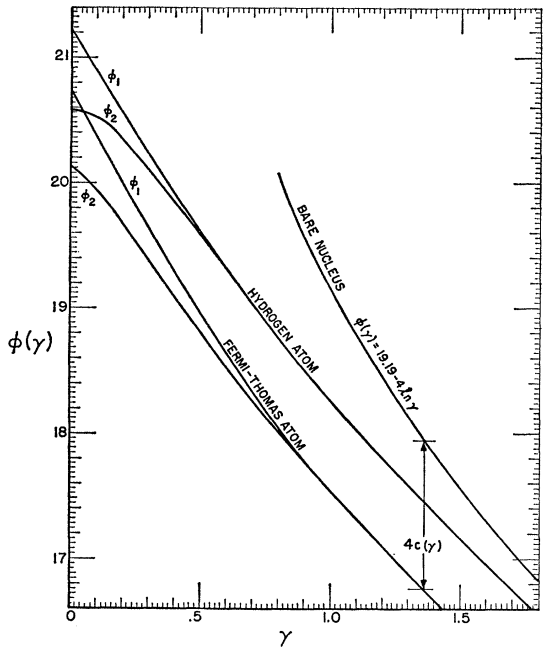

FIG. 6.09. Screening factors $\Phi_1(\gamma)$ and $\Phi_2(\gamma)$ for the Bethe–Heitler Formula 3*D*-1003, where $\gamma = 100\, k/(E_+E_-Z^{1/3})$. The curve for the "hydrogen atom" was calculated by Wheeler and Lamb (1939) with exact wave functions. The curves for the Thomas–Fermi atom and the bare nucleus differ by the factor $4c(\gamma)$, where $c(\gamma)$ is evaluated in Fig. 6.10.

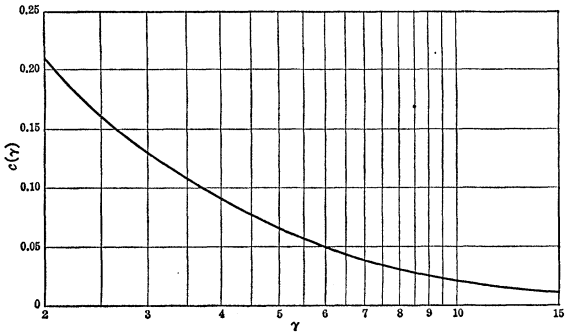

FIG. 6.10. Screening factor $c(\gamma)$ for the Bethe–Heitler Formula 3D–1003.

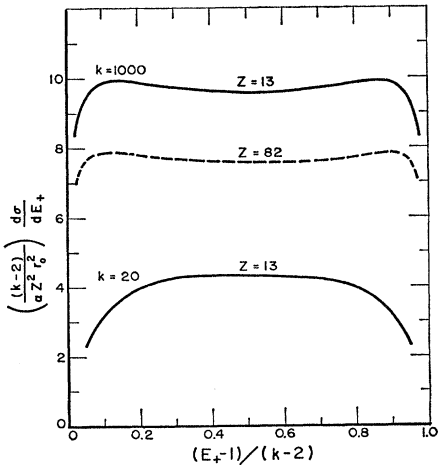

FIG. 6.11. Dependence of the differential pair cross section $d\sigma/dE_+$ on the positron energy E_+ for aluminum ($Z=13$, solid lines) and lead ($Z=82$, dashed line). The curves for $k=1000$ are calculated from the Davies–Bethe–Maximon Formula 3D–1009, and the curve for $k=20$ is derived from the Bethe–Heitler Formula 3D–1003.

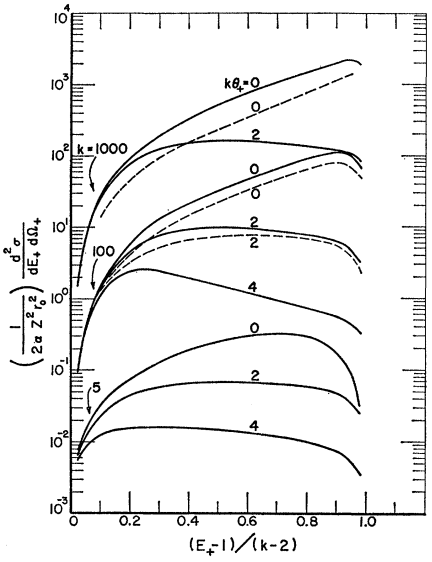

FIG. 6.12. Dependence of the differential pair cross section $d^2\sigma/dE_+d\Omega_+$ on the positron energy E_+ for incident photon energies of k equal to 1000, 100, and 5. The cross sections are calculated for different values of the parameter $k\theta_+$ shown by the numbers over the curves. The solid lines were calculated with the unscreened, Born approximation Formula 3D–2000, and the dashed lines were calculated for $Z=82$ with the screened, exact Formula 3D–2009.

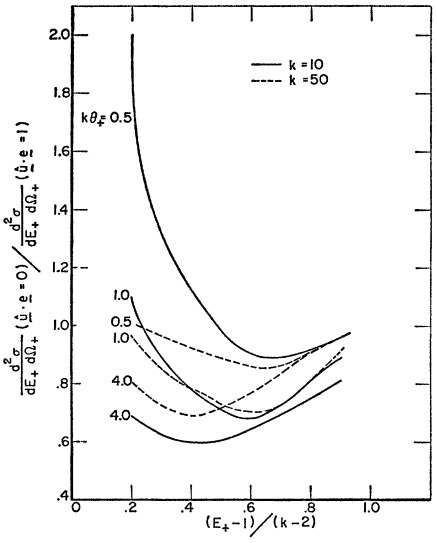

FIG. 6.13. Dependence of the differential pair cross section ratio

$$(d^2\sigma/dE_+d\Omega_+)(\hat{\mathbf{u}}\cdot\mathbf{e}=0)/(d^2\sigma/dE_+d\Omega_+)(\hat{\mathbf{u}}\cdot\mathbf{e}=1)$$

on the positron energy for linearly polarized photons in a plane perpendicular ($\hat{\mathbf{u}}\cdot\mathbf{e}=0$) and parallel ($\hat{\mathbf{u}}\cdot\mathbf{e}=1$) to the emission plane ($\mathbf{k}$, $\mathbf{p}_+$). The cross sections $(d^2\sigma/dE_+d\Omega_+)(\hat{\mathbf{u}}\cdot\mathbf{e}=0)$ and $(d^2\sigma/dE_+d\Omega_+)(\hat{\mathbf{u}}\cdot\mathbf{e}=1)$, were evaluated from Formulas (17.3) and (17.2), respectively, in Gluckstern and Hull (1953).

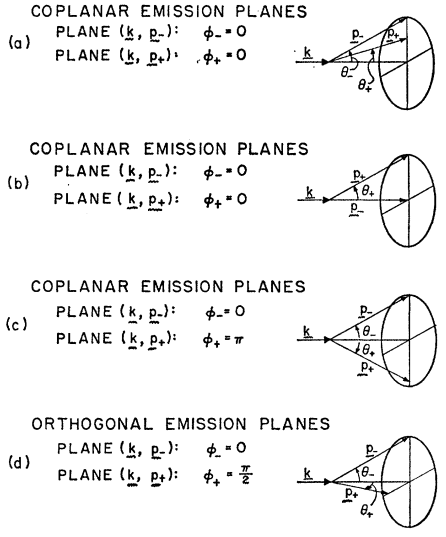

FIG. 6.14. Definitions of the geometries for the vectors, $\mathbf{k}$, $\mathbf{p}_+$, and $\mathbf{p}_-$, which are used in the evaluation of the differential pair cross section given by Formula 3D–3000 in Figure 6.15.

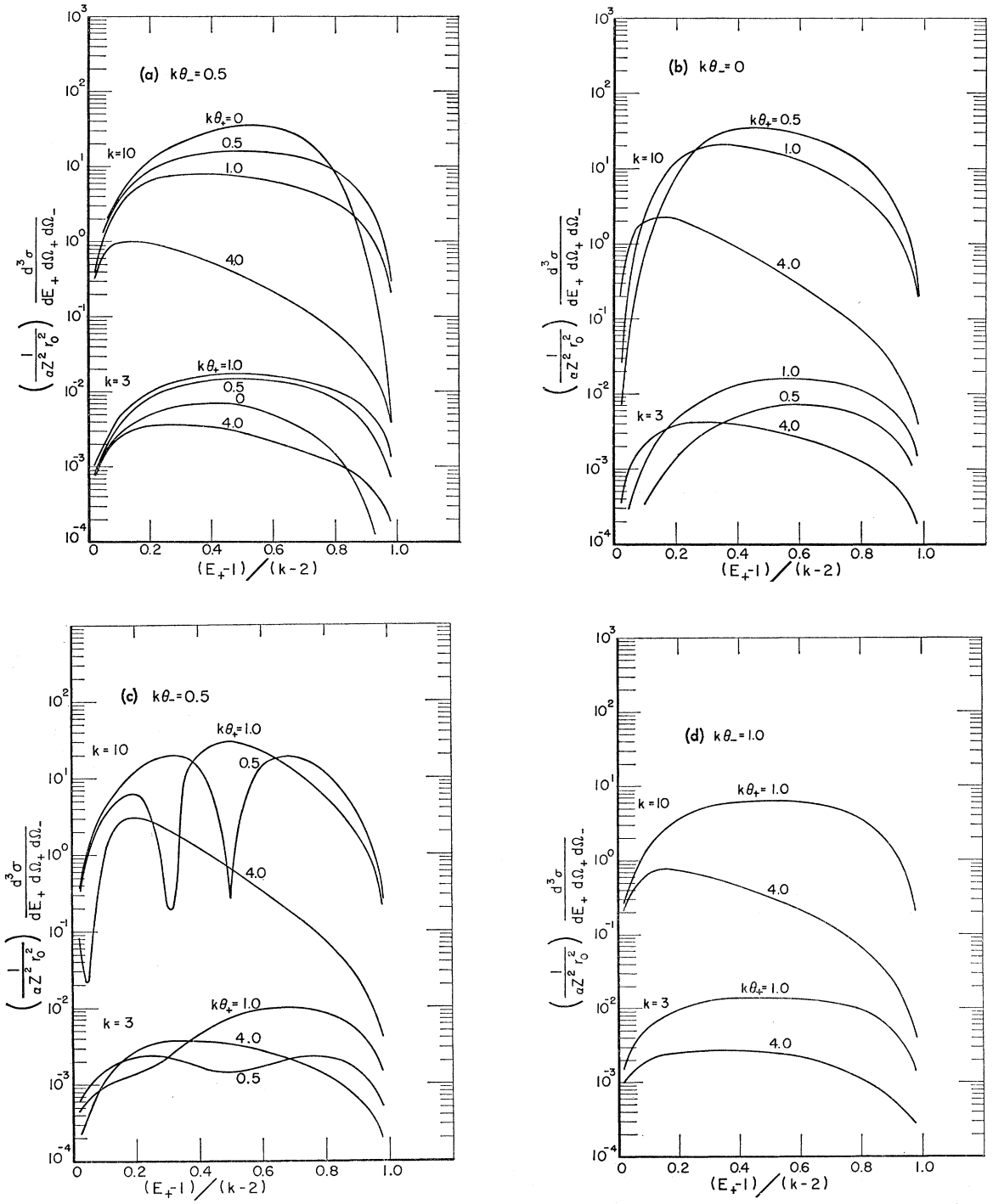

FIG. 6.15. Dependence of the differential pair cross section given by Formula 3D–3000 on the positron energy for photon energies of k equal to 10 and 3. The cross sections are evaluated for an electron emission angle such that $k\theta_-=0.5$, 0, 0.5, and 1.0 in parts (a)–(d), respectively, and for positron emission angles specified in terms of $k\theta_+$ by the numbers on the curves. The geometry for the azimuthal angles in (a) is given in Fig. 6.14(a), for (b) in Fig. 6.14(b), for (c) in Fig. 6.14(c), and for (d) in Fig. 6.14(d).

Table 7.01. Cross-section formulas without polarization dependence for pair production in an electron field

Pair cross section in electron field	Photon energy region				
	$4 \leq k \leq 4.002$	$4 < k < 16$	$k > 16$	$k > 100$	$k > 10^4$
σ	4B–0000 Votruba	4B–0001 Mork	4B–0002 Borsellino–Ghizetti	4B–0003 Borsellino	4B–0004 Bethe–Heitler
$d\sigma/dq$				4B–1003 Suh–Bethe	
$d^3\sigma/dE_+ d\Omega_+ d\Omega_-$		4B–3001 Votruba–Mork	4B–3002 Borsellino		

VII. CROSS-SECTION FORMULAS FOR PAIR PRODUCTION IN AN ELECTRON FIELD

Electron–positron pair production in the field of an electron is called triplet production. This process involves two additional effects which do not occur in the field of an atom. These are (1) the exchange effects involving the two electrons and (2) the effects in which the quantum is absorbed by the target electron (designated as the γ–e interaction in the terminology of Feynman diagrams). Because of these effects, the cross-section calculations are complicated and most of the available results (Ghizzetti, 1947; Borsellino, 1947; Votruba, 1948; Rohrlich, 1955; Suh, 1959; Kopylov, 1964; and Mork, 1967) contain various approximations, as discussed, for example, in the summary by Joseph and Rohrlich (1958).

Borsellino (1947) calculated the triplet cross section by neglecting the exchange and γ–e interactions. In this same approximation, Borsellino (1947) and Ghizzetti (1947) derived a high-energy formula for the triplet cross section. On the other hand, Votruba (1948) calculated the differential triplet cross section with the inclusion of the exchange and γ–e interactions. However, Votruba's total cross section contains many approximations and is not reliable except near threshold. Likewise, Rohrlich and Joseph (1955) obtain a cross section which is not reliable because it is based on Votruba's approximate expressions as shown by Suh and Bethe (1959).

Mork (1967) has carried out accurate calculations for the triplet cross section and has verified the accuracy and limitations of the previous calculations. For example, for the total triplet cross section, Mork has shown that (a) the Votruba results (Formula 4B–0000) are valid near threshold and (b) the Borsellino results (Formula 4B–0004) are valid at high energies ($k > 16$) where the exchange and γ–e interactions are negligible. These latter effects give a 4% decrease of the cross section at 6.0 MeV, and 6% at 5 MeV. At extremely high photon energies, the triplet cross section approaches the Bethe–Heitler cross section such that at 100 MeV, the exact cross section is approximately 10% lower than the Bethe–Heitler value.

A summary of the various formulas that are available for the total and differential triplet cross sections are given in Table 7.01. These formulas are classified according to the different energy regions in which their validity has been confirmed by Mork's results.

Formula 4B–0000

[The Votruba Formula for Triplet Production Near Threshold]

$$\sigma = \alpha r_0^2 (\pi \sqrt{3}/4 \times 3^5)(k-4)^2.$$

(1) Conditions of Validity

Threshold photon energies: $4 \leq k \leq 4.002$.

(2) References

Votruba (1948).

(3) Notes

a. The validity of Formula 4B–0000 in the threshold energy region has been verified by the calculations of Mork (1967).

b. Few experimental results are available near the threshold region (for example, see Frei *et al.* 1965), and more data are needed for quantitative comparisons with the Votruba Formula.

Formula 4B–0001

[The Mork Formula for Triplet Production at Intermediate Energies]

$$\sigma=(\Delta_{BH}+\Delta_B+\Delta_{BG})(1-\Delta_M),$$

where Δ_M is the Mork correction term (Mork, 1967, Fig. 4) which is given in Fig. 7.02. The quantity, $(\Delta_{BH}+\Delta_B+\Delta_{BG})$, has been evaluated by Borsellino (1947) and Ghizzetti (1947) for this intermediate energy region, $4<k<16$, and their results are given in Table 7.02.

(1) Conditions of Validity

Intermediate photon energies: $4<k<16$.

(2) References

Mork (1967).

(3) Notes

a. The energy dependence of the cross section predicted by Formula 4B–0001 for $4<k<16$ is shown in Fig. 7.01.

b. A comparison of the cross sections predicted by Formula 4B–0001 with various experimental results is given in Fig. 8 of Mork (1967).

Formula 4B–0002

[The Borsellino–Ghizzetti Formula for Triplet Production at High Energies]

$$\sigma=\Delta_{BH}+\Delta_B+\Delta_{BG},$$

where Δ_{BH} and Δ_B are given in the Borsellino Formula 4B–0003, and for high photon energies $(k>16)$

$$\Delta_{BG}=\alpha r_0^2\frac{1}{k^2}\left[\frac{8}{3}(\ln 2k)^3-\left(4-\frac{1}{k}\right)(\ln 2k)^2-\frac{1}{18}\left(168+\frac{106}{k}+\frac{49}{k^2}\right)\ln 2k-11.8-\frac{16.8}{k}-\frac{0.27}{k^2}\right].$$

(1) Conditions of Validity

High photon energies: $k>16$.

(2) References

Borsellino (1947) and Ghizzetti (1947).

(3) Notes

a. The energy dependence of the cross section predicted by Formula 4B–0002 for $k>16$ is shown in Fig. 7.01.

Formula 4B–0003

[The Borsellino Formula for Triplet Production at Very High Energies]

$$\sigma=\Delta_{BH}+\Delta_B,$$

where

$$\Delta_{BH}=\alpha r_0^2\left[\tfrac{28}{9}\ln(2k)-\tfrac{218}{27}\right]=\text{Bethe–Heitler Formula 4B–0004},$$

$$\Delta_B=-\alpha r_0^2k^{-1}\left[\tfrac{4}{3}(\ln 2k)^3-3(\ln 2k)^2+6.84\ln 2k-21.51\right].$$

(1) Conditions of Validity

Very high photon energies: $k>100$.

(2) References

Borsellino (1947).

(3) Notes

a. Borsellino's results (1947) contain a misprint in which the sign in the last term for Δ_B above is incorrectly given as $+21.51$ rather than -21.51.

b. The energy dependence of the cross section predicted by Formula 4B–0003 for $k>100$ is shown in Fig. 7.01.

c. Experimental results in this energy region are given in Sondhu *et al.* (1962).

Formula 4B–0004

[The Bethe–Heitler Formula for Triplet Production at Extremely High Energies]

$$\sigma=\alpha r_0^2\left[\tfrac{28}{9}\ln(2k)-\tfrac{218}{27}\right]$$

(1) Conditions of Validity

Extremely high photon energies: $k>10^4$.

(2) References

Heitler (1954), Formula (14), p. 260.

(3) Notes

a. The energy dependence of the cross section predicted by Formula 4B–0004 for $k>10^4$ is shown in Fig. 7.01.

Formula 4B–1003

[The Suh–Bethe Recoil Formula for Triplet Production at Very High Energies]

$$d\sigma/dq=\alpha r_0^2\,\tfrac{2}{3}[q/(T_r+1)T_r^2]\{1+[(2T_r-1)/q]\ln(T_r+1+q)\},$$

where the momentum transfer **q** is defined in Sec. II, with q^2 given by Eq. (3.03) in Sec. III.

(1) Conditions of Validity

Very high photon energies: $k>100$.
Intermediate q values: $q\ll k$, $kq\gg 1$.

(2) References

Suh and Bethe (1959), Formula (16).

(3) Notes

a. The triplet recoil momentum distributions which are derived by Mork (1967) are given in Fig. 7.03 for values of k equal to 1000, 100, 50, and 20. The curves for k equal to 1000 and 100 are given by the Suh–Bethe Formula 4B–1003.

b. The momentum distributions predicted by Formula 4B–1003 have shown agreement with available experimental results (Hart *et al.* 1959; Gates *et al.* 1962), except in the region of large recoil momentum where the theoretical values are larger than the experimental values. Other experimental results are given in Sondhu *et al.* (1962).

Formula 4B–3001

[The Votruba–Mork Formula for Triplet Production in the Laboratory System]

$$\frac{d^3\sigma}{dE_+d\Omega_+d\Omega_-}=\frac{\alpha r_0^2}{4\pi\,|\,\kappa_0\,|}\frac{p_+p_-}{E_r}\frac{1}{1-(\beta_-\cdot\beta_r/\beta_-^2)}(X_U+X_V+X_W),$$

where

$$X_U=U+S_1U+S_2U+S_3U+S_2S_1U+S_3S_1U+S_3S_2U+S_3S_2S_1U;$$

S_1, S_2, and S_3 denote the following substitutions

S_1: $\bar{k}\leftrightarrow-\bar{k}$, $\bar{p}_0\leftrightarrow\bar{p}_r$, $\bar{p}_-\leftrightarrow-\bar{p}_+$,

S_2: $\bar{p}_0\leftrightarrow-\bar{p}_+$,

S_3: $\bar{p}_r\leftrightarrow\bar{p}_-$,

where, as defined in Sec. II, $\bar{p}_0$ is the initial four momentum of the target electron, $\bar{p}_r$ is the four momentum of the recoiling target electron, and $\bar{p}_+$ and $\bar{p}_-$ are the four-momentum vectors of the positron–electron pair. The expres-

sions for X_V and X_W are identical to X_U with V and W substituted for U, respectively. U, V, and W are given by

$$U=\tfrac{1}{2}(1+\tau_1)^{-2}\{\kappa_3^{-2}[-\kappa_3(\kappa_1\tau_2+\kappa_0\sigma_3)+\tau_1\kappa_3-\tau_2\sigma_1-\tau_3\sigma_3+\kappa_1\tau_2+\kappa_0\sigma_3-\kappa_2\kappa_3+\kappa_2+\tau_1+2\kappa_3-\sigma_2+2]$$
$$+(\kappa_2\kappa_3)^{-1}[\sigma_2(\kappa_1(\tau_2+\tau_3)-\sigma_1\tau_2-\sigma_3\tau_3)+\kappa_2(\sigma_1\tau_2+\sigma_3\tau_3-2\tau_3\sigma_1)+\sigma_2(\tau_1-\sigma_2+2\kappa_2)-\kappa_0\kappa_1-\tau_1\kappa_2+2\sigma_2-\kappa_2]\},$$

$$V=\tfrac{1}{4}(1+\tau_1)^{-1}(1-\sigma_2)^{-1}\{(\kappa_0\kappa_3)^{-1}[2(\kappa_0-\kappa_3-2\tau_3)+\kappa_0(\kappa_1+\tau_1+\sigma_1-\sigma_2+\sigma_3)+\kappa_3(-\kappa_2-\tau_1+\tau_2+\sigma_2-\sigma_3)$$
$$+\tau_3(-\kappa_1-\kappa_2+2\sigma_2-2\tau_1)+\kappa_0(\sigma_1(\sigma_2-\tau_2)-2\sigma_3(\kappa_3+\tau_3))+\kappa_3(\tau_1\tau_2+\sigma_1\tau_2+2\sigma_3\tau_3)+\tau_3(2(\tau_2\sigma_1+\sigma_3\tau_3)-\kappa_1\tau_2+\kappa_2\sigma_1)]\}$$
$$-\text{the same expression with the substitution } \bar{p}_+\rightleftarrows\bar{p}_-,$$

$$W=\tfrac{1}{8}(1+\tau_1)^{-1}(\sigma_1-1)^{-1}\{2\kappa_2^{-2}[2\kappa_1\kappa_2\tau_3+\kappa_2(-\kappa_0-\kappa_1+\kappa_3-\tau_1+\tau_3+\sigma_1)+2\tau_3(\sigma_3-\kappa_1)+\kappa_0+\kappa_1-2\kappa_2-\kappa_3-\tau_1$$
$$-\tau_2+\tau_3+\sigma_1+\sigma_2-\sigma_3-2]+(\kappa_2\kappa_0)^{-1}\{2[\sigma_3(\kappa_2\tau_3+\kappa_3\tau_2-\kappa_0(\sigma_2+\tau_3)+2\tau_2\tau_3)+\tau_3(\kappa_2\tau_1-\kappa_1\tau_2)]$$
$$+2\kappa_0(\kappa_1-\kappa_3+\tau_1+\tau_2-\tau_3-\tfrac{1}{2}\sigma_1-\sigma_2+\sigma_3)+\kappa_1(2\kappa_3-\tau_3+\sigma_2)+\kappa_2(2\tau_3+\sigma_1-2\tau_1-2\tau_2)$$
$$+\kappa_3(\tau_1-\sigma_3)-2\tau_2(\tau_1+\tau_2-\tau_3-\sigma_1-\sigma_2+\sigma_3)+2\kappa_1-\kappa_3+\kappa_0-\kappa_2-4\tau_2\}$$
$$+(\kappa_2\kappa_3)^{-1}\{2[\sigma_3(\kappa_3\tau_2-\kappa_3\tau_3-\kappa_2\tau_3-\kappa_0\sigma_2+2\sigma_2\tau_3)+\tau_3(\sigma_1\kappa_2-\kappa_1\sigma_2)]+\kappa_0(2\kappa_1+2\kappa_3-\sigma_1-\sigma_3)+\kappa_1(2\kappa_3+\tau_2+\tau_3)$$
$$+\kappa_2(\tau_1-2\tau_3-2\sigma_1-2\sigma_2)+\kappa_3(\tau_1+2(\tau_2-\tau_3-\sigma_1-\sigma_2+\sigma_3))+2\sigma_2(-\tau_1-\tau_2+\tau_3+\sigma_1+\sigma_2-\sigma_3)$$
$$+(-2\kappa_0-2\kappa_1+\kappa_2+\kappa_3-4\sigma_2)\}+(\kappa_0\kappa_3)^{-1}[4\sigma_3(\kappa_3+\tau_3)(\kappa_0-\tau_3)+2\tau_3(\tau_1+\tau_2-\tau_3-\sigma_1-\sigma_2+\sigma_3)$$
$$+\kappa_0(-2\tau_2+2\tau_3-2\kappa_2-3\sigma_3)+\kappa_1(2\kappa_2-\tau_2+2\tau_3+\sigma_2)+\kappa_2(2\kappa_3+\tau_1+2\tau_3-\sigma_1)+\kappa_3(-2\tau_3-2\sigma_2+3\sigma_3)$$
$$+2\kappa_1-2\kappa_2+3\kappa_3-3\kappa_0+4\tau_3]\}.$$

Here

$$\kappa_0=\bar{p}_0\cdot\bar{k},\quad \tau_1=\bar{p}_0\cdot\bar{p}_r,\quad \sigma_1=\bar{p}_+\cdot\bar{p}_r,$$
$$\kappa_1=\bar{p}_r\cdot\bar{k},\quad \tau_2=\bar{p}_0\cdot\bar{p}_-,\quad \sigma_2=\bar{p}_+\cdot\bar{p}_-,$$
$$\kappa_2=\bar{p}_-\cdot\bar{k},\quad \tau_3=\bar{p}_0\cdot\bar{p}_+,\quad \sigma_3=\bar{p}_r\cdot\bar{p}_-,$$
$$\kappa_3=\bar{p}_+\cdot\bar{k}.$$

Only five of these quantities are independent. The energy–momentum conservation laws give five relations:

$$\kappa_3=\kappa_0-\kappa_1-\kappa_2,\quad \tau_3=\kappa_0-1-\tau_1-\tau_2,$$
$$\sigma_3=\kappa_0+1-\sigma_1-\sigma_2,\quad \sigma_1=\kappa_0-\kappa_2-\tau_2,$$
$$\sigma_2=\kappa_0-\kappa_1-\tau_1.$$

(1) Conditions of Validity

Threshold and intermediate photon energies: $4<k<16$.

(2) References

Mork (1965).

Formula 4B–3002

[The Borsellino Formula for Triplet Production in the Laboratory System]

$$\frac{d^3\sigma}{dE_+d\Omega_+d\Omega_-}=\frac{\alpha r_0^2}{(2\pi)^2}\frac{p_+p_-}{k^3\bar{q}^4}\frac{2k^2}{(\bar{p}_+\cdot\bar{k})(\bar{p}_-\cdot\bar{k})}\frac{p_-^2}{E_-\bar{p}_-\cdot\bar{p}_r+E_r}[S_1(1-\tfrac{1}{4}\bar{q}^2)+S_2(1+\tfrac{1}{4}\bar{q}^2)],$$

where S_1 and S_2 have the same meaning as in Formula 3D–3004, and D and $\bar{p}_+$, $\bar{p}_-$, $\bar{p}_r$, $\bar{k}$, and $\bar{q}$ are the four-component vectors defined in Sec. II of this paper.

(1) Conditions of Validity

High photon energies: $k>16$.

(2) References

Borsellino (1947).

Table 7.02. The Borsellino–Ghizzetti cross sections[a] for intermediate photon energies in the region where $4<k<20$.

k	$\sigma/\alpha r_0^2$	k	$\sigma/\alpha r_0^2$
4	0	12.4	0.989
4.4	0.004	12.8	1.049
4.8	0.017	13.2	1.108
5.2	0.038	13.6	1.167
5.6	0.067	14	1.226
6	0.102	14.4	1.285
6.4	0.142	14.8	1.343
6.8	0.186	15.2	1.401
7.2	0.234	15.6	1.458
7.6	0.285	16	1.514
8	0.338	16.4	1.570
8.4	0.393	16.8	1.626
8.8	0.450	17.2	1.681
9.2	0.509	17.6	1.735
9.6	0.568	18	1.789
10	0.627	18.4	1.842
10.4	0.687	18.8	1.895
10.8	0.747	19.2	1.947
11.2	0.808	19.6	1.999
11.6	0.868	20	2.050
12	0.929	...	...

[a] These cross sections were evaluated by Borsellino (1947) and Ghizzetti (1947). The cross section σ in this table is equal to the quantity $(\Delta_{BH}+\Delta_B+\Delta_{BG})$ which is given in Formula 4B–0001.

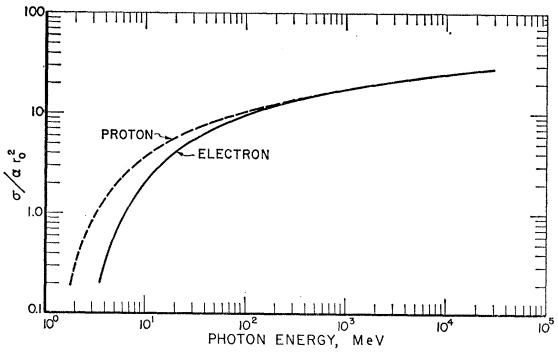

Fig. 7.01. Cross section σ for pair production in an electron field (solid line) and proton field (dashed line). For the electron field, the cross-section curve is given by Formulas 4B–0001, 4B–0002, and 4B–0003, in the photon energy regions from approximately 2.04 to 8 MeV, 8 to 50 MeV, and 50 to 10^4 MeV and above, respectively. For the proton field, the cross-section curve is given by the Racah Formula 3D–0000. Note that the photon energy is given in megaelectron-volt units and is equal to $0.511k$.

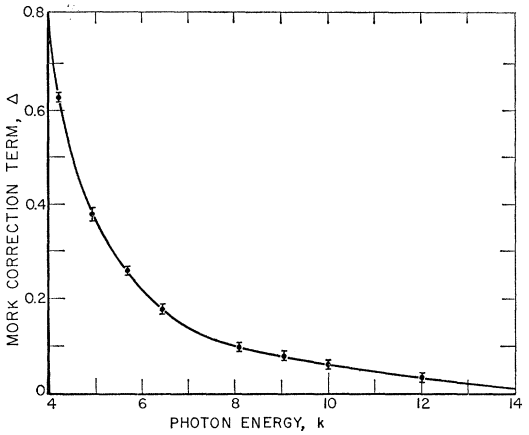

Fig. 7.02. Correction term Δ which is given by Mork (1967) in the triplet-cross-section Formula 4B–0001 for the intermediate energy region where $4<k<16$. Note that the photon energy k is given in m_0c^2 units.

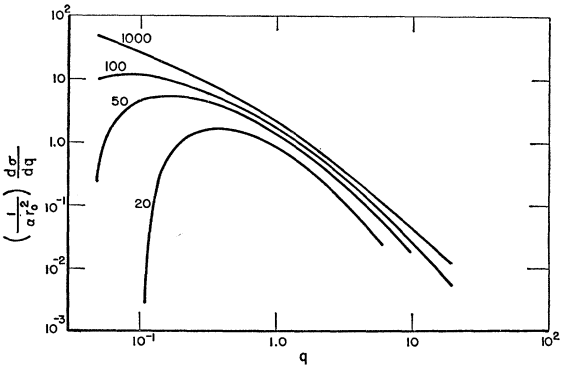

Fig. 7.03. Dependence of the triplet differential cross section $d\sigma/dq$ on the momentum q of the recoiling electron for values of the photon energy k equal to 1000, 100, 50, and 20, as given by Mork (1967).

TABLE 8.01. Selection of pair formulas from Table 6.02(a) for different regions of the incident photon energy.

Pair cross section	Formulas $k \leq 6$	$6 \leq k \leq 30$	$k \geq 30$	Comments
σ	3D-0006	Interpolate between curves given by 3D-0006 and 3D-0009	3D-0009	Experimental results are listed in Notes for Formula 3D-0000
$d\sigma/dE_+$	3D-1006	3D-1000	3D-1009	Accuracy uncertain for $6 \leq k \leq 30$
$d^2\sigma/dE_+d\Omega_+$	3D-2000	3D-2000	3D-2009 ($\theta_\pm \leq 1/E_+$)	Accuracy uncertain for 3D-2000 with $Z \geq 10$, and for 3D-2009 at large angles ($\theta_\pm \gg 1/E_\pm$)
$d^3\sigma/dE_+d\Omega_+d\Omega_-$	3D-3000	3D-3000	3D-3009 ($\theta_\pm \leq 1/E_\pm$), 3D-3004 ($\theta_\pm \gg 1/E_\pm$)	Accuracy uncertain for 3D-3000 with $Z \geq 10$, and for 3D-3009 at large angles ($\theta_\pm \gg 1/E_\pm$)

VIII. DISCUSSION OF PAIR CROSS-SECTION FORMULAS

The various cross-section formulas for pair production by photons are summarized in Tables 6.02(a), 6.02(b), 6.03, and 7.01. In Tables 6.02(a), 6.02(b), and 7.01, the formulas are classified according to the different approximations used in the calculations, and the conditions of validity for these approximations are quantitatively summarized in Table 6.01. In Table 6.03, the formulas are classified according to their dependence on different polarization variables, and the approximations are identified under the conditions of validity for each formula.

The fact that different formulas exist for each form (total or differential) of the pair cross section indicates that there is no single formula that is valid for every set of conditions. At best, such a single formula would not be analytical and would be difficult, if not impractical, to evaluate. Therefore, it is necessary to select a formula from the above tables according to the physical conditions that are imposed in a given experimental situation. If the conditions of validity are satisfied, the accuracy of a given formula is expected to be better than a few percent; otherwise, the accuracy cannot be specified unless comparisons have been made with experimental results.

The formulas in Table 6.02(a) apply to the process of pair production in an atomic field without atomic excitation (designated as coherent or elastic pair production). These formulas are classified in two main categories, according to whether the calculations are "First Born" or "Exact" as described in Sec. IV. The subdivisions in each category indicate whether the calculations contain screening or high-energy approximations, or nuclear-size effects. Guidelines for the selection of the pair formulas in Table 6.02(a) are given in Table 8.01 for different regions of the incident photon energy and the atomic number of the target. The most accurate formulas are derived with the "exact" calculations; however, for particle energies that are not very large compared to the electron rest energy, these formulas have a limited application because (a) they are only available for the total and differential cross sections σ and $d\sigma/dE_+$, (b) they are not given in closed form, and (c) they do not include screening corrections. As shown in Table 6.02(a), exact calculations are not available for the differential cross sections $d\sigma/d\Omega_r$, $d\sigma/dP_p$, $d\sigma/dq$, and $d^2\sigma/dE_+dw$, and as pointed out in Table 8.01, the accuracy of the cross sections predicted by these formulas is uncertain in the photon energy regions where the Born condition,

$$[\alpha Z/(1-4/k^2)^{1/2}] \ll 1,$$

is not satisfied.

The formulas in Table 6.02(b) apply to the process of pair production in an atomic field with atomic excitation (designated as incoherent or inelastic pair production). For this process, only the Wheeler-Lamb (1939, 1956) calculations are available, and they provide Born approximation formulas for the total and differential cross sections σ and $d\sigma/dE_+$, respectively. The accuracy of the cross sections predicted by these formulas depends on the atomic number and the atomic incoherent scattering function for the target atom. For low atomic numbers, the Born condition is satisfied (except near threshold), but it is more difficult to formulate accurate expressions for the incoherent scattering function (Knasel, 1968), and for high atomic numbers, the reverse conditions are true.

The relative contributions of the inelastic and elastic pair processes described above must be evaluated in order to determine the total number of pairs that are produced experimentally. For this evaluation, the total pair cross section is given by the sum of the elastic and inelastic cross sections, σ(elastic) and σ(inelastic), and the formulas for these cross sections are listed in Tables

6.02(a) and 6.02(b), respectively. The cross-section ratio σ(inelastic)/σ(elastic), which is predicted by Formulas 3D–0005 and 3D–0009, is given in Fig. 8.01 for photon energies in the region between 10^2 and 10^4 MeV. The results in Fig. 8.01 indicate that this ratio is negligible (<0.02) for the high-Z (lead) target and is large (>0.5) for the low-Z (helium) target. Because the relative contribution of the inelastic pair process increases as the atomic number decreases, it is important to obtain more accurate data for the low-Z inelastic pair cross sections such as provided by Knasel (1968). On the other hand, the experimental data (references in Note a, Formula 3D–0000) that are available for the total elastic cross section show good agreement with the predictions of the exact Formula 3D–0006 for high-Z targets and for photon energies below 10 MeV.

The accuracy of the polarization formulas in Table 6.03 is uncertain because there are no experimental data on polarization effects that can be compared with the theoretical predictions. However, based on comparisons of experimental and theoretical total cross sections, the cross sections predicted by the exact formulas, 3D–2139, 3D–2249, 3D–3139, 3D–3229, 3D–3149, and 3D–3249, are expected to have better than 1% accuracy if the conditions of validity for the formulas are satisfied.

For pair production in an electron field, the cross section formulas are specified in Table 7.01 for different regions of the incident photon energy. As discussed by Mork (1967), the cross sections predicted by these formulas show good agreement with the available experimental results (references to these results are given in the notes of the formulas in Sec. VII). The accuracy of the Votruba Formula 4B–0000 is uncertain in the threshold region ($k\approx 4$). Otherwise, the triplet formulas in Table 7.01 are expected to give cross sections with an accuracy of the order of the fine structure constant ($\alpha=1/137$) provided that the specified conditions of validity are satisfied.

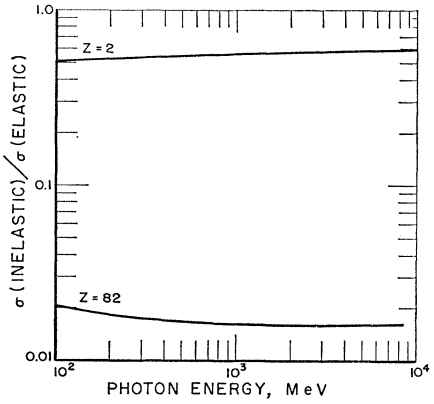

Fig. 8.01. Comparison of the cross-section ratio σ(inelastic)/σ(elastic) for helium ($Z=2$) and lead ($Z=82$). The cross section σ(inelastic) refers to pair production in an atomic field with atomic excitation, and is evaluated by Formula 3D–0005 for $Z=82$ and by Knasel (1968) for $Z=2$. The cross section σ(elastic) refers to pair production in an atomic field without atomic excitation, and is evaluated by Formula 3D–0009 for $Z=82$ and 2. Note that the photon energy is given in mega-electron-volt units and is equal to $0.511k$.

The experimental data that are presently available on pair production in an atomic field pertain mostly to the *total* pair cross section. Unfortunately, most of these data which are partially summarized in Note a of Formula 3D–0000 give relative values for the cross section, and comparisons with theory are made with various normalizing constants. There are few direct measurements of the absolute total cross section (for example, see West, 1956; Rao *et al.*, 1963; Titus and Levy, 1966; Garritson and Miller, 1968). These absolute measurements have been carried out with monoenergetic photons in the energy region from approximately 1.1 to 3.0 MeV, and the experimental results show good agreement (within accuracies of 10% to 20%) with the cross sections that are predicted by the exact Formula 3D–0006 (Jaeger and Hulme, 1936; Øverbø, Mork, and Olsen, 1968) and summarized in Figs. 6.01 and 6.03. Additional experimental results recently obtained by Piowaty and Miller (1969) in the threshold energy region from 1.1 to 1.5 MeV also show good agreement with the cross sections predicted by Formula 3D–0006 for lead. In this energy region below 3 MeV, the results show that for high-Z targets, the experimental cross sections and the exact theoretical cross sections given by Formula 3D–0006 may be factors of 2 larger than the Born approximation cross sections predicted by the Racah Formula 3D–0000. For low-Z targets, the experimental cross sections include contributions both from the elastic and the inelastic pair-production cross sections discussed above and in Fig. 8.01.

In addition to the experimental data on total cross sections discussed above, there are very few absolute measurements of the various differential pair cross sections summarized in Table 6.02. Experimental data on differential cross sections are valuable not only because they provide more detailed information on the pair process, but also because they provide more sensitive tests of the theory. Among the few experimental studies in this category are the measurements by Plimpton and Hammer (1963) of the positron energy spectrum produced in high-Z targets at an emission angle of 90° with the photon beam from a 75-MeV synchrotron.* Also in this category are the large-angle pair measurements (Blumenthal *et al.*, 1966; Ashbury *et al.*, 1967; Eisenhandler *et al.*, 1967) which were carried out in the billion-electron-volt region with carbon targets in order to test the predictions of the

* The experimental results in these measurements show an order-of-magnitude disagreement with the predictions of the Born approximation theory. Although this disagreement may be attributed in part to the breakdown of the Born approximation, a contributing factor may arise from the experimental difficulties in determining absolute cross sections with bremsstrahlung photon beams which have a continuous energy distribution. More studies are required to resolve this uncertainty, including measurements with monoenergetic photon beams and exact calculations of the differential cross section for large-angle pair production.

Bjorken–Drell–Frautschi Formula 3D–3004 and the validity of quantum electrodynamics at high energies.*

The above summary indicates that the present experimental results on pair production are not sufficiently comprehensive to establish the accuracy of the pair formulas listed in Table 6.02. For the total cross section below 3 MeV and above 15 MeV, the data show that within the experimental uncertainties, the most accurate cross sections are obtained from the exact Formulas 3D–0006 and 3D–0009, respectively, as shown in Table 8.01. Because of the success obtained with the exact calculations for the total cross section, it is expected that the most accurate differential pair cross section may likewise be obtained from the exact differential Formula 3D–1006 for the energy region below 3 MeV, and Formulas 3D–1009, 3D–2009, and 3D–3009 for the energy region above 15 MeV and for small angles. However, for the other cases shown in Table 8.01, there are considerable uncertainties. To remove these uncertainties, there is a need for (a) more experimental data with good accuracy on the total pair cross sections in the intermediate energy region, $6 \leq k \leq 30$, where only interpolation procedures and semiempirical formulas exist, (b) experimental data on the various differential pair cross sections in the energy region where $k < 30$, (c) absolute pair cross section measurements in the energy region where $k > 30$, and (d) studies of the total and differential pair cross sections for targets with low atomic numbers in order to determine the relative contributions of the elastic and inelastic pair-production processes which are examined in Fig. 8.01.

ACKNOWLEDGMENTS

We wish to thank Miss Kathleen Farrell for programming various cross-section formulas and providing the data for Figs. 6.11, 6.12, 6.13, and 6.15(a)–(d), Dr. A. Harvey for making available the computer facilities at Queens College, and Dr. Roald Schrack for providing Figs. 3.03(a) and (b). Also, we wish to thank Dr. K. Mork and Mr. S. Waldenström for a critical examination of Formulas 3D–1006, 3D–3004, and 4B-3001.

REFERENCES

C. D. Anderson, Phys. Rev. **41,** 405 (1932).
C. D. Anderson, Phys. Rev. **43,** 491 (1933); **44,** 406 (1933).
M. Abramowitz and I. A. Stegun, *Handbook of Mathematical Functions* (National Bureau of Standards Applied Mathematics Series 55, Washington, D. C., 1964).
J. Augerat, J. Castor, and P. Y. Bertin, Compt. Rend. **262,** 835 (1966).
J. G. Ashbury, W. K. Bertram, U. Becker, P. Joos, M. Rohde, A. J. S. Smith, S. Friedlander, C. L. Jordan, and C. C. Ting, Phys. Rev. Letters **18,** 65 (1967).
H. A. Bethe, Proc. Cambridge Phil. Soc. **30,** 524 (1934); H. A. Bethe and W. Heitler, Proc. Roy. Soc. (London) **A146,** 83 (1934).
A. Borsellino, Nuovo Cimento **4,** 112 (1947); Rev. Univ. Nac. Tucumán **A6,** 7 (1947).
T. H. Berlin and L. Madansky, Phys. Rev. **78,** 623 (1950).
A. Borsellino, Phys. Rev. **89,** 1023 (1953).
H. Bethe and J. Ashkin, *Experimental Nuclear Physics* (John Wiley and Sons, Inc., New York, 1953), Vol. I, p. 325.
H. A. Bethe and L. C. Maximon, Phys. Rev. **93,** 768 (1954).
G. Böbel, Nuovo Cimento **6,** 1241 (1957).
H. Banerjee, Phys. Rev. **111,** 532 (1958).
R. A. Berg and C. N. Lindner, Phys. Rev. **112,** 2072 (1958); Nucl. Phys. **26,** 262 (1961).
J. D. Bjorken, S. D. Drell, and S. C. Frautschi, Phys. Rev. **112,** 1409 (1958).
J. C. Butcher and H. Messel, Nucl. Phys. **20,** 15 (1960).
R. B. Blumenthal, D. C. Ehn, W. C. Faissler, P. M. Joseph, L. J. Lanzerotti, F. M. Pipkin, and D. G. Stairs, Phys. Rev. **144,** 1199 (1966).
P. Y. Bertin, J. Castor, J. Augerat, J. Gardès, and L. Avon, Nucl. Instr. Methods **42,** 38 (1966).
C. Barbiellini, T. Letardi, R. Visentin, and F. Grianti, Nuovo Cimento **51A,** 1124 (1967).
S. J. Brodsky and J. R. Gillespie, Phys. Rev. **173,** 1011 (1968).
A. Claesson, Arkiv Fysik **12,** 569 (1957).
J. Castor, J. Augerat, and J. Berthot, Compt. Rend. **262,** 646 (1966).
P. A. M. Dirac, Proc. Roy. Soc. (London) **117,** 610 (1928); **118,** 351 (1928).
P. A. M. Dirac, Proc. Roy. Soc. (London) **126,** 360 (1930).
S. D. Drell, Phys. Rev. **87,** 753 (1952).
I. E. Dayton, Phys. Rev. **89,** 544 (1953).
H. Davies, H. A. Bethe, and L. C. Maximon, Phys. Rev. **93,** 788 (1954).
E. Eisenhandler, J. Feigenbaum, N. Mistry, P. Mostek, D. Rust, A. Silverman, C. Sinclair, and R. Talman, Phys. Rev. Letters **18,** 425 (1967).
W. H. Furry, Phys. Rev. **46,** 391 (1934).
C. Fronsdal and H. Überall, Nuovo Cimento **8,** 163 (1958); Phys. Rev. **111,** 580 (1958).
C. J. Frei, H. H. Staub, and H. Stüssi, Helv. Phys. Acta **38,** 262 (1965).
A. G. Ghizzetti, Rev. Univ. Nac. Tucuman A. **6,** 37 (1947).
R. L. Gluckstern, M. H. Hull, Jr., and G. Breit, Science **114,** 480 (1951); Phys. Rev. **90,** 1026 (1953).
R. L. Gluckstern and M. H. Hull, Jr., Phys. Rev. **90,** 1030 (1953).
G. White Grodstein, *X-Ray Attenuation Coefficients from 10 kev to 100 Mev* [National Bureau of Standards Circular 583 (1957), U.S. Department of Commerce, Washington, D.C.].
W. Gröbner and N. Hofreiter, *Integraltafel* (Springer–Verlag, Berlin, 1961), 3rd ed.
D. C. Gates, R. W. Kenney, and W. P. Swanson, Phys. Rev. **125,** 1310 (1962).
G. R. Garritson and W. C. Miller, Bull. Am. Phys. Soc. **13,** 716 (1968), (Abstract KE 5).
W. Heitler and F. Sauter, Nature **132,** 892 (1933).
P. V. C. Hough, Phys. Rev. **73,** 266 (1948).
P. V. C. Hough, Phys. Rev. **74,** 80 (1948).
W. Heitler, *The Quantum Theory of Radiation* (Oxford University Press, London, 1954), 3rd ed.
E. L. Hart, G. Cocconi, V. T. Cocconi, and J. M. Sellen, Phys. Rev. **115,** 678 (1959).
R. Hagedorn, *Relativistic Kinematics* (W. A. Benjamin, Inc., New York, 1963).
B. Huld, Phys. Letters **24B,** 185 (1967).
J. C. Jaeger and H. R. Hulme, Proc. Roy. Soc. (London) **153,** 443 (1936).
R. Jost, J. M. Luttinger, and M. Slotnick, Phys. Rev. **80,** 189 (1950).
J. M. Jauch and F. Rohrlich, *The Theory of Photons and Electrons* (Addison-Wesley Publ. Co., Inc., Cambridge, Mass., 1955).
J. Joseph and F. Rohrlich, Rev. Mod. Phys. **30,** 354 (1958).
H. A. Kramers, Phil. Mag. **46,** 836 (1923).
H. W. Koch and J. W. Motz, Rev. Mod. Phys. **31,** 920 (1959).
G. I. Kopylov, L. A. Kulyukina, and I. V. Polubarinov, Sov. Phys.—JETP **19,** 1158 (1964) [Zh. Eksp. Teor. Fiz. **46,** 1715 (1964)].
I. Khubeis, H. Schopper, and C. Weddingen, Nucl. Phys. **50,** 286 (1964).
H. Kolbenstvedt and H. Olsen, Nuovo Cimento **40,** 13 (1965).
T. M. Knasel, Phys. Rev. **171,** 1643 (1968).
M. M. May, Phys. Rev. **84,** 265 (1951).

* Although the early results of Blumenthal *et al.* (1966) indicate a breakdown in the predictions of quantum electrodynamics in the 1–5-BeV energy region, the more recent results of Ashbury *et al.* (1967) and Eisenhandler *et al.* (1967) contradict the early findings and strongly confirm the validity of quantum electrodynamics in this energy region.

R. C. Miller, Phys. Rev. **95,** 796 (1954).
K. W. McVoy, Phys. Rev. **106,** 828 (1957); K. W. McVoy and F. J. Dyson, *ibid.* **106,** 1360 (1957); K. W. McVoy, *ibid.* **111,** 1333 (1958).
L. C. Maximon and H. Olsen, Phys. Rev. **126,** 310 (1962).
J. W. Motz, H. Olsen, and H. W. Koch, Rev. Mod. Phys. **36,** 881 (1964).
K. J. Mork, Arkiv for det Fysiske Seminar i Trondheim, No. 7 (1965).
K. J. Mork, Phys. Rev. **160,** 1065 (1967).
L. C. Maximon, J. Res. Natl. Bur. Std. **72B,** 79 (1968).
Y. Nishina and S. Tomonaga, Proc. Phys.-Math. Soc. Japan **15,** 298 (1933).
Y. Nishina, S. Tomonaga, and S. Sakata, Sci. Pap. Inst. Phys. Chem. Res. Suppl. (Tokyo) **24,** (1934), No. 17.
J. R. Oppenheimer and M. S. Plesset, Phys. Rev. **44,** 53 (1933).
H. Olsen, Phys. Rev. **99,** 1335 (1955).
H. Olsen and L. C. Maximon, Phys. Rev. **114,** 887 (1959).
H. Olsen and L. C. Maximon, Nuovo Cimento **24,** 186 (1962).
Haakon Olsen, Phys. Rev. **131,** 406 (1963).
H. Olsen and L. C. Maximon, Phys. Rev. Letters **13,** 112 (1964).
H. Olsen, *Applications of Quantum Electrodynamics, Springer Tracts in Modern Physics* (Springer-Verlag, Heidelberg, Germany, 1968), Vol. 44.
I. Øverbø, K. Mork, and H. Olsen, Phys. Rev. **175,** 1978 (1968).
W. Pauli, *Handbuch der Physik* (Springer Verlag, Berlin 1933), Vol. 24, Pt. 1, p. 246.
J. D. Plimpton and C. L. Hammer, Nuovo Cimento **30,** 1349 (1963). J. M. Piowaty and W. C. Miller (unpublished), University of Notre Dame, South Bend, Ind., 1969.
G. Racah, Nuovo Cimento **11,** 477 (1934).
G. Racah, Nuovo Cimento **13,** 66 (1936).
E. S. Rosenblum, E. F. Shrader, and R. M. Warner, Jr., Phys. Rev. **88,** 612 (1952).
F. Rohrlich and J. Joseph, Phys. Rev. **100,** 1241 (1955).
J. Rama Rao, V. Lakshminarayana, and S. Jnanananda, Proc. Phys. Soc. (London) **81,** 949 (1963).
G. Roche, L. Avan, and D. Isabelle, Nuovo Cimento **57B,** 125 (1968).
F. Sauter, Ann. Physik **20,** 404 (1934).
A. Sommerfeld and A. W. Maue, Ann. Physik **22,** 629 (1935).
L. I. Schiff, Phys. Rev. **83,** 252 (1951).
H. Staub and H. Winkler, Helv. Phys. Acta **27,** 223 (1954).
K. S. Suh and H. A. Bethe, Phys. Rev. **115,** 672 (1959).
E. Segre, *Experimental Nuclear Physics,* (John Wiley & Sons, New York, 1960), Vol. 1, Pt. II.
H. S. Sondhu, E. H. Webb, R. C. Mohanty, and R. R. Roy, Phys. Rev. **125,** 1017 (1962).
S. Sarkar, Nuovo Cimento **34,** 141 (1964).
A. Sørenssen, Nuovo Cimento **38,** 745 (1965); **41,** 543 (1966).
F. Titus and A. J. Levy, Nucl. Phys. **80,** 588 (1966).
V. Votruba, Phys. Rev. **73,** 1468 (1948); Acad. Tchèque Sci. Bull. Intern. **49,** 19 (1948).
J. A. Wheeler and W. E. Lamb, Jr., Phys. Rev. **55,** 858 (1939).
G. C. Wick, Phys. Rev. **81,** 467 (1951); M. May and G. C. Wick, *ibid.* **81,** 628 (1951).
J. A. Wheeler and W. E. Lamb, Jr., Phys. Rev. **101,** 1836 (1956).
H. I. West, Jr., Phys. Rev. **101,** 915 (1956).
C. N. Yang, Phys. Rev. **77,** 722 (1950).
T. Yamazaki and J. M. Hollander, Phys. Rev. **140,** B630 (1965).